Drill-hole Spacing Optimzation in Grade-Control

by

Caio César Cardoso Gomes

A thesis submitted in partial fulfillment of the requirements for the degree of

Master of Science

in

Mining Engineering

Department of Civil and Environmental Engineering
University of Alberta

Abstract

Final estimates at the grade-control (GC) stage of mining are built to maximize the correct classification of mineable blocks. The costs include drilling, mining, and processing. When considering dedicated GC drilling, Drill-hole spacing (DHS) optimization for profit balances the cost of estimation uncertainty and the cost of the drilling. The drilling amount is optimal when drilling less would incur large estimation costs and drilling more would incur large drilling costs.

To support DHS optimization in GC, a DHS framework for regularly-spaced drill-holes is developed and evaluated. Aiming at increasing profit and going beyond regularly-spaced drilling, a second DHS methodology is designed, where DHS from two phases are optimized. An automated workflow is developed that delivers the location of the final optimal GC samples in addition to optimal DHS decisions.

The methodology of DHS optimization for profit is investigated by considering geology, mining selectivity, spatial continuity, ore price, and other factors. Each factor is varied one at a time, and optimal DHS decisions and profit changes are recorded and summarized. Finally, the DHS frameworks are demonstrated on real data from a copper-molybdenum deposit.

The research establishes a conceptual foundation and practical details for developing DHS optimization for final estimates in mining operations with dedicated drilling systems. The nested DHS framework can lead to improved results, but greater flexibility at the time of mining is required.

Dedication

This work is dedicated to B, J and L (Love). To mom (Gratitude). To D, J and J (go for your dreams).

"Walk on the strength of your own light and no darkness shall ever reach you."

- Lao Tzu

Acknowledgments

I profoundly thank Professor Clayton for accepting, supporting, and supervising my research with great distinction. I thank Professor Jeff for co-supervision and invaluable contribution to the development of this work. The learning journey has been incredibly rich.

I thank my CCG colleagues for the great collaboration. I thank Paulo and Rafael for being good friends during the program.

I thank Prof. Joao Felipe, Marcelo and Prof. Lydia for kindly having served as professional references so this MSc. program could become a reality for me.

I am the product of the effort of countless people in my lifetime and before it. Here are some personal acknowledgments:

I thank my treasured wife and most precious daughters for ALL.

I deeply thank my Mom and Dad for everything. Mom, for all she did so I could grow healthy, learn values and skills, have memorable experiences, and become a decent adult. I thank Daniel for being a genuine older brother. I thank my sister Julia and brothers Judah and Gustavo.

To all the many friends and good fellows I have had so far. To the people who (intentionally or not) taught me important lessons along the way, good and hard ones. You know who you are. Thanks!

Table of Contents

List of Tables

List of Figures

List of Symbols

Symbol	Description
cm^3	Cubic centimeter
c_d	Cost per drill-hole
C_{ij}	Total cost from realization i and spacing j
FP_{ij}	Final profit from realization i and spacing j
FP_j	Average final profit for spacing j across all l realizations
g	Grade
gr	Gram
h	Lag distance
i	Indexer for summation
l	Number of realizations
l_{area}	side's length of a squared GC area
lb	Pound
m	Meter
$m_{[]}$	Cost of mined material
n_{dh}	Number of drill-holes
ppm	Parts per million
Q	Quantity of mined material
r	Metallurgical recovery
R_{ij}	Revenue from realization i and spacing j
s	Ore selling price
Sph	Spherical structure
t	Metric ton
ρ	Correlation coefficient
^{o}	Degrees
\$	Dollar
μ	Mean
%	Percent
ρ_s	Rank correlation coefficient
σ	Standard deviation
σ^2	Variance

Symbol	Description
γ	Variogram

List of Abbreviations

Abbreviation	Description
2D	Two-dimensional
APV	Average profit variation
BH	Blast-hole
CDF	Cumulative distribution function
COG	Cut-off grade
CS	Coarse spacings
Cu	Copper
CV	Coefficient of variation
DHS	Drill-hole spacing
DL	Dig-limits
EM	Exponential model
FP	Final profit
FS	Fine spacings
GC	Grade-control
GSLIB	Geostatistical software library
HTPG	Hierarchical truncated pluri-Gaussian
LVA	Locally varying anisotropy
MPS	Multiple point statistics
Mo	Molybdenum
NN	Nearest neighbor
OK	Ordinary kriging
O-W	Ore-waste
RC	Reverse circulation
RMSE	Root mean squared-error
SGS	Sequential Gaussian simulation
SMU	Smallest mining unit
SoR	Slope of regression
TEE	Total estimation errors

Chapter 1

Introduction

1.1 The relevance of drill-hole spacing in the mining industry

The information provided by drill-hole sampling in the mining industry represents the most reliable and abundant data source. Reinforced in the National Standards of Disclosure for Mineral Projects (NI 43-101), the description of the procedures and extent of drilling are key and mandatory items for disclosure given that it "materially impacts the accuracy and reliability of mineral resources results" (CSA, 2011). While the NI 43-101's description is directed at pubic disclosure, the consequences of drilling on accuracy and reliability are also true for the production stage. Drilling often comes at high cost. Extensive drilling provides excellent information about the mineral deposit. Drilling less will reduce cost but will compromise mine planning, leading to diminished ore recovery in mining or excessive dilution through misclassification of ore and waste. As Boucher, Dimitrakopoulos, and Vargas-Guzman (2005) put it, drilling is a major cost for any mining operation, which, depending on the assessment of spacing, has the potential to either enhance profitability or diminish returns. Therefore, informed decisions about optimal DHS are an essential task in geostatistics that adds value to mining projects. The optimal DHS is sensitive to many factors, including:

1. inherent geologic characteristics of the deposit,
2. mining and operational parameters/constraints from the mining project,
3. economic parameters,
4. the purpose of the mineral resource estimation to be done from that drilling information, and
5. the most suitable metric to be optimized.

Optimal processes maximize financial gains and minimize costs. The optimal DHS in mining is dependent on the purpose of the model to be built, which will guide the optimization.

1.2 DHS in the stages of mining projects

There are three main purposes when calculating a mineral resource estimate:

1. Exploration: Long-term life-of-mine estimation based on sparse drilling data. Usually the goal is to quantify global characteristics of the deposit such as tonnage, metal content, and general patterns of the grade distribution and variability. This kind of estimation is performed to guide exploratory phases, support economic feasibility and life-of-mine planning studies.

2. Classification and Disclosure: Estimations are done as the mineral project develops from exploration towards feasibility and operational phases. Specific guidelines must be followed, and detailed presentation and validation reports accompany the estimated resource. The mineral resource is classified to allow public disclosure.

3. Production: The final stage of mineral resource estimation takes place when sampling is done prior to blasting and mining of benches or stopes. The main goal is to have local accuracy of grades. The drilling information is abundant and closely spaced, commonly considering data from previous stages of drilling as well.

Regarding long-term models, an estimate cannot be, at the same type, locally precise (conditionally unbiased) and globally accurate, that is predict actual tonnage and grade recovered by mining (Isaaks, 2005). As listed above, the three most common estimation goals call for different strategies of drilling, and the 'optimal choice' depends on the intent of the model. J. Deutsch and Deutsch (2015) stated the greater suitability of long-term models (or interim estimates) to have close predictions of ore content while short-term models (or final estimates) are mostly built to minimize misclassification errors and conditional bias. In summary, long-term models aim at global resources, while short-term grade-control (GC) models aim at local precision. For example, a model aimed at classification and disclosure considers uncertainties of metal content and ore tonnage, a GC model built for production purposes should aim to maximize net value.

Data spacing has a direct relationship with model uncertainty: as data spacing decreases, so does uncertainty. Studies show that the relationship has a strong dependence on the variogram function (Pinto, 2016). Establishing a target uncertainty for minimizing an operation's risk (Usero et al., 2019) is useful but does not guarantee optimal outcomes in terms of economic value and amount drilled. In that sense, Barnett et al. (2018) propose principles to guide the assessment of optimal drilling spacing, where the connection with uncertainty is explained.

This research focuses on GC estimation. The final one before mining. As such, no factor is more relevant than maximizing profit. Final models may be assessed through the slope of regression (SoR) metric of true values against estimated grades (Kentwell, 2022). The profit achieved usually comes mostly from correctly determining if material is below or above the cut-off threshold. The percentage of misclassified blocks is a metric here called total estimation errors (TEE), as shown on Figure 1.1. The figure shows how both metrics of estimation performance are determined. While high values of SoR indicate good adherence of local estimated grades, low TEE suggests greater blocks being correctly assigned.

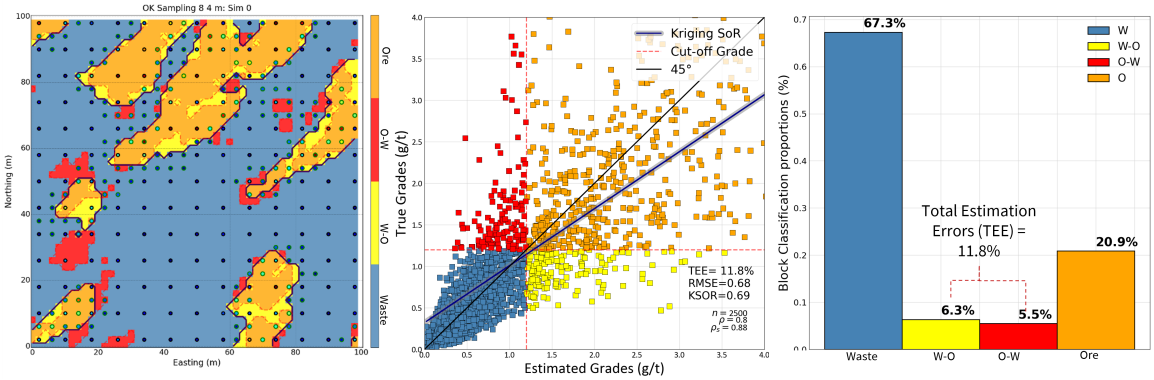

Figure 1.1: Example of estimated final model (on the left), the SoR between true and estimated values (on the middle) and the Total Estimation Errors (TEE – on the right side).

Notably, establishing an optimal DHS for profit is a form of Value of Information (VoI) analysis. The addition of more drilling information is beneficial to profit until adding more information causes decreasing profit. That is, profit is maximized when the VoI of additional drill-holes is maximum. After the turning point, the small revenue increase brought by the additional drilling is smaller than its cost.

1.3 The VoI concept

VoI is a concept from decision and risk analysis that answers the fundamental question if the value derived from a decision exceeds the cost of implementing it (Harding, 2021). This concept has become popular and has been applied in multiple businesses. In the mining industry, VoI has been utilized for additional guidance in DHS both in the exploration stage and for final estimates.

VoI is increasingly being used to support decision-making during exploration drilling for subsurface resources. Recent works are proposing VoI methodologies to address the optimization of value regarding the sequence and placement of exploratory drills (Caers et al., 2022; Hall et al., 2022). VoI, in this research, is the financial profit derived from mining and processing the material in any part of a mine. The decision of the optimal amount of drilling data is determined when it maximizes profit. It considers all parameters affecting the value, including costs (from drilling, mining, and processing), ore selling price, mining selectivity, and revenues (primarily due to properly identified ore and its metal recovery). DHS optimization aimed at profit can be understood as a VoI analysis, where the optimized DHS adds the greatest value in terms of profit.

1.4 DHS optimization previous works

In Afonseca and Silva (2022), many previous DHS studies are reviewed and classified based on their scheme to assess uncertainty and on the targeted metric to be optimized. Two main classes of methods for optimizing drill hole spacing are proposed and named 'Model Uncertainty', which makes

use of estimation for determining grades, and 'Raw Uncertainty', which uses stochastic simulation (Deutsch & Journel, 1997) to generate probability distributions of grade. The distinction of methods is closely related to capturing either local uncertainty or global uncertainty, respectively.

Afonseca and Silva (2022) state that the exercise of DHS optimization is not unique since it requires a variable to be optimized against and that best spacing may vary across different choices of decision variables. Furthermore, the suitability of simulation-based DHS studies for exploratory stages and kriging-based methods for grade-control cases is considered, given that the first will emphasize global accuracies while the latter enhances local uncertainties and misclassified blocks. The case study from Afonseca and Silva (2022) defines the broadest sample spacing across three different estimation methods: ordinary kriging (OK), Local Uniform Conditioning (LUC) and sequential Gaussian simulation (SGS). Their results are checked for misclassification errors and suitability for classifying resources. The issue of maximizing value is not approached.

The idea of multi-staged drilling studies or, at least, optimizing the final drill-hole positions is also relevant to the thesis. This has been considered in Koppe et al. (2011). They tackle not only the spacing problem but also the concept of drill-hole placement. Decision on where to place final samples to maximize economic value is done through a DHS optimization aimed at short-term context. Usual regular spacing is compared against irregular spacing where additional drill-holes are placed in high-uncertainty areas. Contextualization of the problem and the way to define uncertainty significantly affect the optimal solution. Uncertainty, for example, is determined as the Inter-Quartile-Range (IQR). Another factor raised was the absence of any mineable limits implementation on the process. On a similar line, Silva and Boisvert (2013) developed a drilling optimizer method that maximizes the amount of classified ore tonnage while also accounting for kriging variance (as a metric for uncertainty) and grades in the form of penalty term in its objective function. Results on a 3-D case study provide a trade-off between the potential gain in mineral resources tonnage and reduction in uncertainty by adding more drilling against the cost of adding them (Silva & Boisvert, 2014). Santibanez-Leal, Ortiz, and Silva (2020) also explore variable sampling spacing for GC context to select optimal location. In this study, final adaptive sampling is placed based on a combination of conditional entropy and maximizing extraction for ore-waste discrimination.

The paper from Vargas (2017) offers a worth-seeking workflow. The drill hole spacing optimization was sequentially approached through a function where the optimal solution is found when the cost of additional drilling equals the cost associated with misclassified blocks (both ore estimated as waste and waste estimated as ore). Vargas (2017) uses SGS and indicator simulation (SIS) to generate six true scenarios. The mix used is explained to vary the continuity style since SGS would be more spatially erratic while SIS grades would be more connected. This is similar to aspects of the research developed below: how different geology types will affect drill-hole spacing optimizations. Finally, Vargas (2017) discuss how extreme grade blocks significantly increase lost value and how that should be limited. The lack of dig lines implementation is pointed out as an aspect of

improvement. Harding (2021) uses the VoI concept to set up a link between geologic, economic, and engineering uncertainties and apply it to an optimal drilling spacing analysis. It presents the non-linear negative relationship between geologic uncertainty and value, and how understanding this interaction is important for optimizal of DHS. Diminishing uncertainty improves value until a certain threshold, where typically, the cost of reducing uncertainty generates diminishing returns. That turning point is the optimal solution, and finding it depends on the variables considered and mining specificities.

Spatial continuity, DHS and model uncertainty

Dimensionless analysis is desirable to generalize research results to a broader number of situations. The work from Pinto and Deutsch (2014) surveys the relationship between variogram range, data spacing, and model uncertainty. They investigate and discuss that, although model uncertainty and data spacing have a clear non-linear relationship, they are positively correlated and many particularities of that relationship are scrutinized, especially relating to the variogram range. The expected derivative of uncertainty quantifies how much uncertainty is actually reduced as spacings do as well. For values of spacing smaller than 1/4 of the variogram range, it is seen to be a region of diminishing returns in resolving uncertainty. And that for spacings above 1 to 2 times the variogram range, the uncertainty tends to stabilize. Those findings provide rules regarding the relationship between the spatial continuity of the geological phenomenon being modeled and the optimal drilling amount.

Journel (2018) debates the limitations of representing geological models based on histograms and variograms. The effect of estimating sparse data, even at GC stage, might be models that possess significant uncertainty on grades as well as on global patterns of spatial configuration. Journel (2018) provides an interesting 'eye-opener' example, where different geology types are drawn from the same conditioning data. The two-point-based variograms of those exhaustive geology types exhibit very similar spatial continuity structures, despite their clear distinct spatial patterns.

Mineral deposits have inherently two components acting on its distribution of grades - geological controls and partial randomness (Journel & Huijbregts, 1976). Depending on the DHS, sampling different geologic conditions may lead to datasets with similar variograms or histograms, although the underlying mineral deposit could be contrasting. It is usually assumed that denser sampling can potentially distinguish similar geological configurations, or reduce the randomness effect. The research topic of this thesis includes assessing how different geology types and spatial continuities influence optimal DHS decisions.

1.5 Research motivation

Despite that DHS studies are common in the mining industry, there is no standardization of techniques, particularly for GC. The aim of this research is to set a framework of DHS optimization for final mineral estimates, while motivating the utilization of profit as the most relevant target metric in a GC context. Furthermore, a specific DHS methodology is developed for enhanced profitability in an automated format that also goes beyond regular grids in drilling. Practical examples and techniques are proposed to facilitate overall content assimilation.

1.6 Thesis outline

The conceptual foundation of the research direction and steps are as follows:

1. Build a comprehensive coded standard workflow for DHS optimization aimed at GC estimation.
2. Develop a computational DHS and placement technique to enhance profitability in GC context.
3. Assess how different factors such as geology, spatial continuity and mining selectivity impact DHS optimization for profit.
4. Apply the developed DHS optimization workflows on a real dataset, gather results, and evaluate them.

The thesis structure follows these topics. Chapter 2 presents a standard DHS framework for profit optimization. Chapter 3 proposes a new DHS methodology that uses the strategy of only placing final samples along the borders of estimated ore-waste boundaries in order to increase profitability. Chapter 4 shows a sensitivity analysis employing a wide range of mining, economic and geologic elements varied systematically one at a time and checking how DHS optimizations for profit are affected by the changes. In Chapter 5, a real dataset from a copper-molybdenum deposit is utilized to demonstrate both DHS methodologies (from Chapters 2 and 3).

Chapter 2

A Framework for Drill-Hole Spacing: Optimization for Profit

2.1 Introduction

The determination of an optimal DHS has a variety of solutions. It is highly dependent on several factors, such as:

1. the mining stage (exploratory, reserves conversion, or grade-control, for instance);
2. varying values of operational, economic, and financial parameters;
3. which metric to be optimized (maximize profit, reduce error/uncertainty, grade accuracy, global accuracy).

The most commonly used metrics are uncertainty-related (Afonseca & Silva, 2022; Silva & Boisvert, 2014; Usero et al., 2019) or financial (Boucher et al., 2005; Koppe et al., 2011; Ortiz, Magri, & Líbano, 2012; Vargas, 2017). This chapter's proposed methodology of DHS optimization directly addresses the problem of determining the DHS that provides the best financial solution (i.e., maximizes profit). For that, ore models must be translated into financial results, which is done by a transfer function (TF). The TF should comprise all the operational and geological elements involved in drilling, mining, and processing and transform them into financial values. The misclassification of blocks (ore-as-waste and waste-as-ore) is converted to financial values. The motivation for having a profit-driven approach is that instead of searching for some uncertainty metric and quality threshold in estimated products, rather encapsulate all factors in a single equation in terms of economic value, since it is what matters for decision-making in the mining business, especially for final estimates. Moreover, it can be verified that reducing the uncertainty of estimated products is positively correlated to final profit only until a certain threshold, after which reducing errors leads to money loss.

The results of a DHS optimization for profit are specific to the selection of mining attributes for costs, cut-off grade, ore price, mining selectivity, and geological features like spatial continuity and deposit grades. Hence, one of the key aspects of DHS studies for maximizing profit should be to carefully incorporate every critical constraint of the ore process into the transfer function for determining profit.

2.2 The DHS framework for maximizing profit

The proposed methodology applies to sampled data from any mineral deposit, aiming at optimal DHS decision for the GC stage. The code can be adapted to accommodate variations from specific mineral deposits, such as underground mining projects, non-linear variables, or multiple elements of interest. The method assesses how the ultimate sampling and estimation of a deposit's bench should be undertaken before being blasted and mined so that it can be the most profitable possible. It has been designed for univariate cases and regular DHS grids. The DHS methodology is summarized in a bullet-point list of main steps (numeration based on Figure 2.1), as follows:

- Step 1 - Define input values: Attribute value to the required attributes for posterior profit calculations. Some of the most relevant attributes include smallest mining unit (SMU) sizes, cut-off grade(s), ore selling price, plant recovery, and distinct costs (ore/waste mining, processing).
- Step 2 - Simulate a range of high-resolution exhaustive truths conditioned by the input data: data values, locations, and spatial continuity model. A reasonable number of simulations is suggested for more stable DHS results. The minimum varies depending on the area's size and available data. The bigger the data and area size, the smaller the number of simulations needed for stability.
- Step 3 - Determine the range of spacing values to be tested. Sample every simulated product in many different regular spacings.
- Step 4 - Estimate and re-block the simulated truths to the estimated block size. Compare each estimated product with its underlying simulated reference and label miss-classified blocks: Waste estimated as ore (W-O) and ore estimated as waste (O-W).
- Step 5 - Apply dig-limits (mining design) selectivity to the estimated ore-waste boundaries, transforming them into mineable limits given the mining constraints and scale.
- Steps 6 and 7 - Customize the transfer function accounting for important financial constraints on the process. Calculate profits, revenues, and costs per DHS scenario estimation across the entire series of simulations.

Figure 2.1 illustrates the proposed steps of the DHS methodology for maximizing profit.

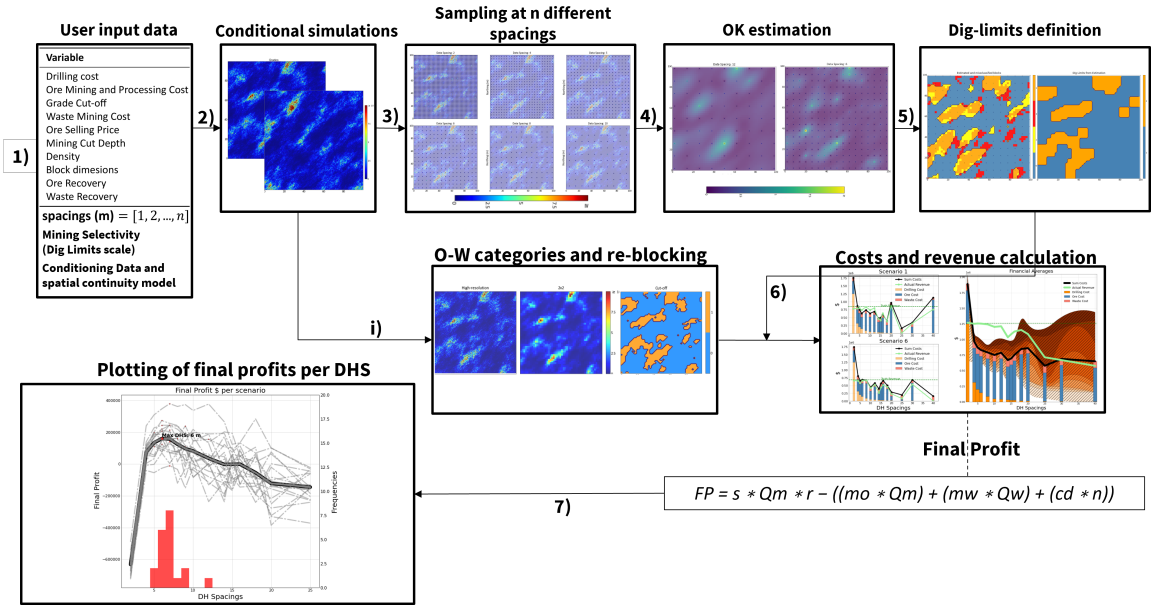

Figure 2.1: Diagram of the DHS optimization workflow, which starts by receiving user inputs.

The diagram from Figure 2.1 displays the sequence of steps involved in the regular DHS optimization for profit. Each step is now more detailedly described following the same numeration from Section 3.2 and Figure 2.1.

2.2.1 Step 1 - input values

There is a minimum set of financial and operational parameter values to be defined so that a typical DHS optimization for profit in a mining operation can be processed and produce reasonable results. They are listed in Table 2.1:

Table 2.1: Table showing required parameters' values and a suggested unit as input for a DHS assessment for profit.

Parameters required	**Units**
Operational costs and values	
- Drilling cost	$/drill-hole
- Ore mining and processing cost	$/t
- Mining cut depth	meters
- SMU dimensions	mxmxm
- Waste mining cost	$/t
- Average density	g/cm^3
- Ore recovery	%
Economic values	
- Cut-off grade	%
- Selling price	$/lb

Table 2.1 contains basic parameters for running a DHS optimization for profit. Depending on the project and the level of information available, more parameters can be added. If reliable, the

more representative financial specificities are considered, the more robust tends to be the DHS optimization. The specificities are later incorporated into the TF so the optimization of profit results simultaneously accounts for all of them.

2.2.2 Step 2 - simulation of exhaustive truths

High-resolution simulations (that is, small-size grid cells) conditioned by the input data, represent possible truths of the assessed mineral deposit (Figure 2.3). The simulations honor the data values at their locations, the spatial continuity model, and the input data statistics (Goovaerts, 1997), thus being considered adequate as one of the many possible unknown *'true'* scenarios of the area under investigation. Therefore, the DHS analysis benefits from as many simulated truths as possible to capture the uncertainty. Multiple realizations provide the proper uncertainty assessment required to support a technical planning decision (Deutsch, 2018), like the choice of an optimal DHS. The choice of a reasonable number of realizations should balance the size of the model and the stability of the final results. Average final profit curves should vary smoothly on a trend, not highly fluctuating across DHS (Figure 2.7b).

In relation to resolution, simulation cell-sizes should mostly match the minimal sampling volume of the mineral project. Very high-resolution simulations potentially lead to more local variability in the reference model grades, which could be propagated to the re-sampled data if not up-scaled. After being generated, the high-resolution simulations need to be up-scaled to match the estimations' grid size to establish misclassification errors. In summary, high-resolution simulation is used for re-sampling, and up-scaled simulation is used for comparison with estimated models.

2.2.3 Step 3 - sampling and spacings

The sampling spacing scenarios are selections of data values directly from the simulated *'truths'*, considering no sampling errors at a regular pre-defined grid (Figure 2.4). The DHS options should be wide-ranged, from the shortest realistically executable spacing up to the widest, considering that deposit's specific GC context. The *spacings* array is specified by the users. A few extreme spacings on both ends are suggested so that the decrease in profit in both directions of spacing is clear. Also, using relatively small lags between the most likely drilling spacings is a good idea so that the profit function can find optimal spacings values in detail. The resolution of the simulated realizations matters for sampling because the simulation cell size will constrain the sampling size. If the simulated cell resolution is, for example, 0.05m, the practitioner should decide if that volume reflects the actual drilling volume or not. Simulation should be either up-scaled to the size of sampling dimensions or realizations should be executed on grid-cells that already reflect the sampling support.

2.2.4 Step 4 - Estimation and misclassification errors

The DHS workflow is independent of which geostatistical method is used for estimation. In the example application, as it is the usual GC standard practice in the mining industry, Ordinary Kriging (OK) (Isaaks & Srivastava, 1989; Matheron, 1963) is employed. OK is widely used for final estimates due to its suitability for grade local accuracy, especially if conditional bias is minimized (Isaaks, 2005; Verly, 2005). However, there are GC solutions based on stochastically-simulated grade uncertainty models associated with economic classification functions (Dimitrakopoulos & Godoy, 2014). Each DHS sampled data from every simulated truth is estimated by OK, composing a scenario. (Figure 2.2).

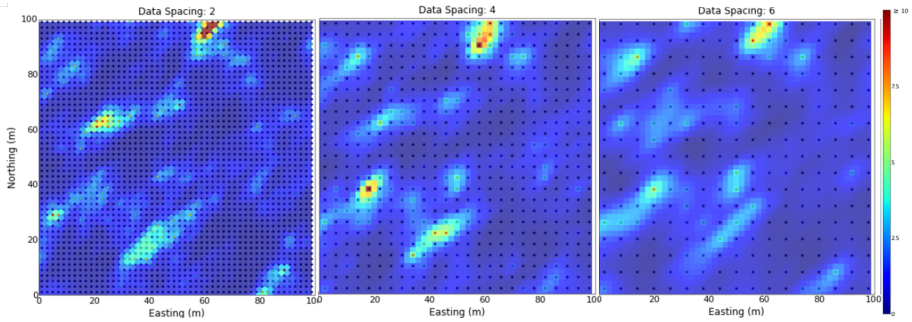

Figure 2.2: Estimated maps of DHS: 2, 4, and 6m from realization #0.

The estimated block models from each DHS are checked against its respective re-blocked *'truth'* to label block-by-block error class and quantify its misclassification errors. Blocks can be either correctly classified or misclassified into two classes:

- W-O also named as **dilution**;
- O-W also commonly named as **ore-loss**.

The definition of ore and waste relies on a cut-off value. Misclassification errors determine profit in the TF and are a global performance measure. They can be used to track the relationship between profit and estimation quality.

2.2.5 Step 5 - Mineable limits definition

Mines have selectivity and mining constraints based on equipment, topography, mining methods, and time. The ore-waste limits from final estimation products must be transformed into optimized mineable delimitations (Figure 2.6). For this, `IGC_DL` (Vasylchuk & Deutsch, 2018) is used, which seeks to optimize the classification of surface mining material subject to excavating constraints. The maximization of limits respecting mining constraints is supposed to achieve up to 98% of the maximum attainable total expected profit. The optimized classified map of mining destinations is built through a floating selection frame, where equipment selectivity constraints are incorporated by

the dimensions of the rectangular frame (Vasylchuk & Deutsch, 2018). The floating frame operates on an expected profit model from the GC area.

2.2.6 Steps 6 and 7 - The transfer function and profit calculations

One of the main distinctions between DHS workflows relies on what function the decision of maximization is made upon. For the methodology presented here, final profit (FP) represents the item to be maximized. How FP is determined represents a workflow core element. The formula for calculating the final profit per scenario is:

$$FP = s * Q_m * r - ((m_o * Q_m) + (m_w * Q_w) + (c_d * n)), \tag{2.1}$$

where FP = final profit(\$), s = ore selling price (\$/lb), r = metallurgical recovery (%), m_o = cost of mining ore (\$/t), Q_m = quantity of mined ore (t), m_w = cost of mining waste (\$/t), Q_w = Quantity of mined waste (t), c_d = cost per drill-hole (\$/dh) and n = number of drill-holes.

FP is the revenue minus the summation of all costs involved in drilling, mining, and processing for each scenario. The units for each variable vary depending on the deposit specifications, although one should be alert to input values in concordant units across all data. The calculations assume that each of the estimation scenarios will be mined entirely.

The TF is a customizable tool; detailed customization of constraints in a given operation is critical for realistically successful DHS studies for profit. The FPs, grouped by DHS, are averaged and plotted in different ways to communicate results (view Figure 2.7), including uncertainty (example in Figures 2.8 and 2.9).

2.3 Example of DHS optimization for profit

2.3.1 Implementation

The example considers unconditional SGS (Deutsch & Journel, 1997) realizations transformed into log-normal distributions. Dependency analysis is done after reaching the maximum FP with the intention of better understanding how each parameter affects the DHS results. The parameters to run the DHS optimization are given in Table 2.2:

Table 2.2: Summary of cost variables required for the DHS analysis and the values chosen for the case study.

Variable	Value	Units
Drilling cost	400	$/drill-hole
Ore mining and processing cost	12	$/t
Cut-off grade	1.2	g/t
Waste mining cost	1	$/t
Ore selling price	11	$/g
Mining cut depth	5	meters
Density	3	g/cm^3
Block dimensions	2x2x5	m,m,m
Ore recovery	100	%
Dilution recovery	50	%

The proposed DHS analysis for maximizing profit is tested in a square area of 100mx100m with grid cell sizes of 0.1mx0.1m. The area size should represent a typical mining bench surveyed for GC sampling. The 0.1m dimension represents an approximate reasonable sampling support for surface-dedicated drilling systems like RC or core-drills (Abzalov, 2016).

A total of 20 two-dimensional unconditional Gaussian simulations are created (Step 2 from workflow in Figure 2.1) to generate possible high-resolution *'truths'* in the area. The number of realizations is based on the model's number of cells (reflecting processing times) balanced with steady FP results. The number of realizations should be small enough to be processed in a reasonable time while big enough to produce stable results. No geological data is used as input. The realizations are transformed to log-normal distributions of mean $\mu = 1$ and variance $\sigma^2 = 2$.

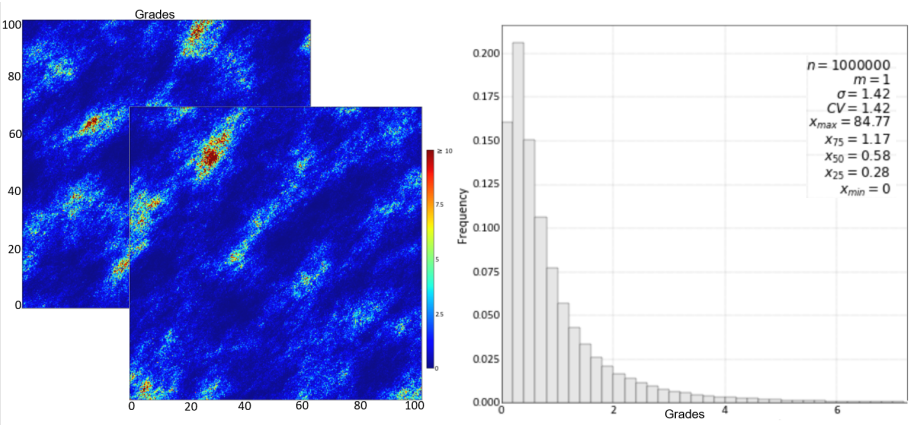

Figure 2.3: Log-normalized high-resolution simulated realizations' map (left) and histogram (right) of one of the unconditional realizations.

The simulated realizations (Figure 2.3) have a spatial continuity of 25m, nugget effect of 20% and an anisotropy ratio of 2:1, where the maximum direction is parallel to 45°.

The array of sampling spacings to be tested in the DHS study is:

$$\textbf{spacings (m)} = [2, 3, 4, 5, 6, 7, 8, 9, 10, 11, 12, 14, 15, 16, 18, 20]. \tag{2.2}$$

In Step 3, regular sampling data is extracted from each of the simulations for all values within Equation 2.2, leading to 320 scenarios (20 realizations x 16 sampling spacings).

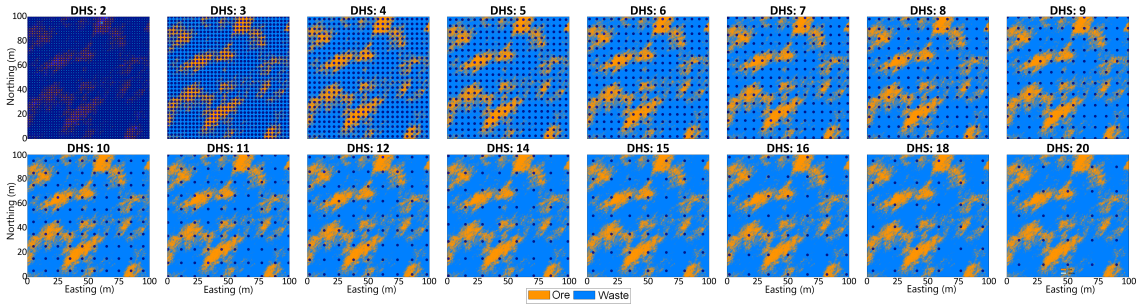

Figure 2.4: Drill-hole sampling spacings visualization across one of the realizations labeled as ore and waste.

Next, OK is used to estimate each sampling dataset, assuming the same spatial continuity model from the simulation. The same variographic model from the simulation is used for estimating data at all spacings, standardizing estimates across DHS. Thus, not allowing variography to influence DHS results at this stage.

An illustration of the process that simulations and estimations undergo is provided in Figure 2.5.

(a) Simulated truth being up-scaled and labeled as ore and waste.

(b) Estimation at DHS: 6m being labeled by cut-off grade and misclassification of estimated cells..

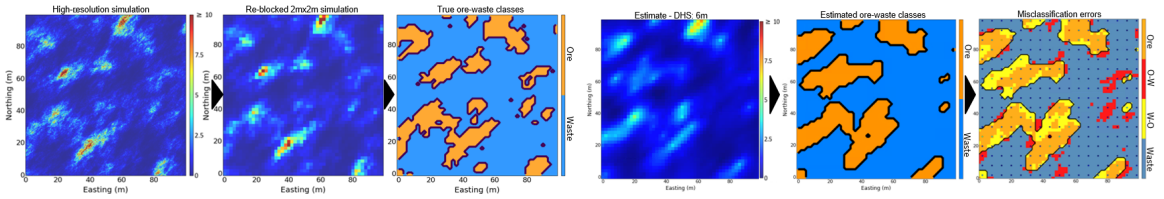

Figure 2.5: Processes of re-blocking, classifying as ore and waste, and assigning misclassification errors between estimations and simulations - example from realization 1.

The estimations are processed for assigning misclassified blocks, found through comparison with reference re-blocked simulations (Section 2.2.4). Subsequently, dig limits are calculated to maximize expected profit, given the excavating constraints established for the case. The transformation of an estimated ore-waste boundary into mineable limits is exhibited in Figure 2.6.

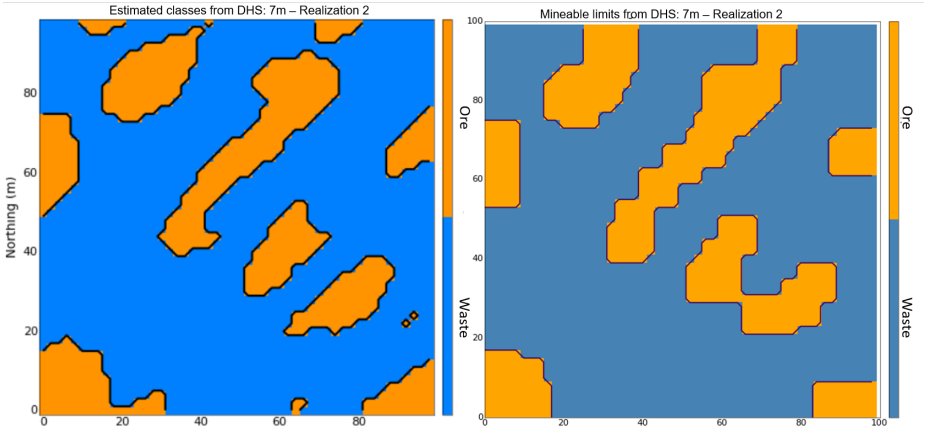

Figure 2.6: Estimation at DHS:7m being processed into mineable limits (Section 2.2.5).

In steps 6 and 7, revenues (R), costs (C), and FP are quantified for every DHS per scenario, following notation from Equation 2.1, where $i = 1, ..., l$ realizations and $j = 2m, ..., 20m (spacings$ options):

$$\text{Revenue: } R_{ij} = s * Q_{mij} * r, \tag{2.3}$$

$$\text{Total costs: } C_{ij} = ((m_o * Q_{mij}) + (m_w * Q_{wij}) + (c_d * n_j)), \tag{2.4}$$

$$\text{leading to } FP_{ij} = R_{i_j} - C_{i_j} \tag{2.5}$$

Calculations of FP for each DHS are averaged amid all realizations, and maximum profit DHS option is found:

$$FP_j = \frac{\sum_{i=1}^{l} FP_{ij}}{l} \tag{2.6}$$

2.3.2 Results

Optimal DHS, profit, and costs

The DHS study's final results are attained after passing all 320 scenarios through FP Equation 2.1, and averaged by each DHS. Figure 2.7 reveals the financial results by spacing in terms of revenue and costs (Figure 2.7a) and the final profits (Figure 2.7b). Cost composition, which includes drilling, ore, and waste costs, is detailed in Figure 2.7a. The difference between revenue and costs culminates in the gray line from sub-figure 2.7b.

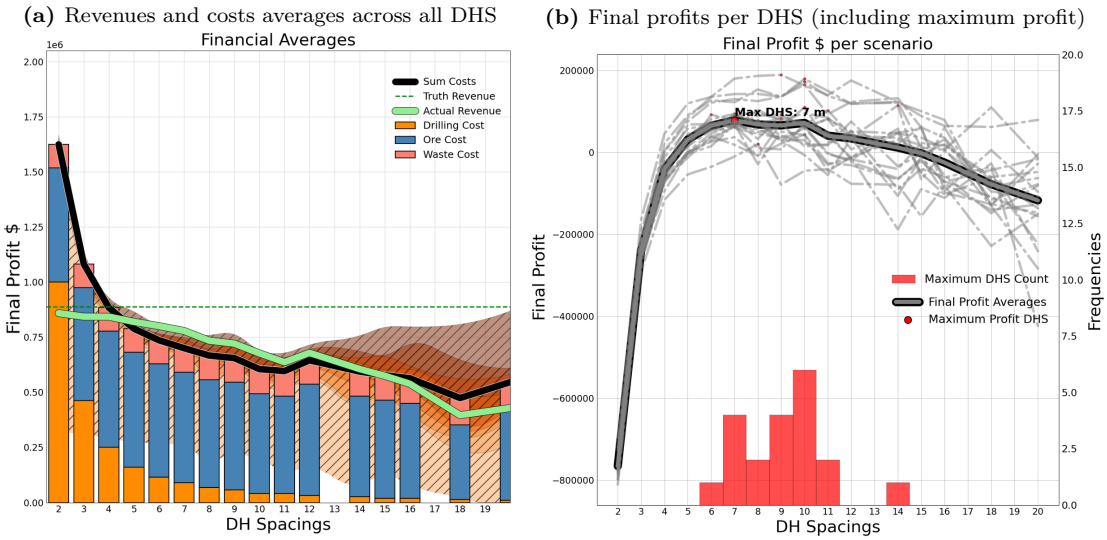

Figure 2.7: Plots of results along each DHS: (a) averages of revenues and costs, (b) final profits (including the maximum profit DHS).

Drilling costs rise exponentially due to it being linearly related to drilling amount, which in turn is a power function of DHS. Drilling costs shape the exponential rise of total costs, as shown by the orange bars in Figure 2.7a. Hence, the exponential rise of costs as DHS reduces determines profitability results for each DHS. The optimal DHS occurs when the greatest positive difference happens between green (revenue) and black lines (sum costs). This difference is positive between 5 and 12m spacings in the example. In Figure 2.7b, the final profit curves communicate the most profitable DHS at the averaged results (thick gray line), while the dashed lines represent each realization. The average FP line exhibits a flat portion among higher values, which suggests that a single DHS does not critically determine the best FP. The most profitable DHS is 7m. However, surrounding DHSs perform similarly, such as 6m, 8m, 9m, and 10m. This reinforces the importance of assessing optimal DHS upon multiple simulated realizations to accomplish representative results.

Relationship between DHS and estimation errors

TEE and root-mean-squared-error (RMSE) are selected metrics for expressing estimation uncertainty. Figure 2.8 displays the linear positive relationship between estimation uncertainty and DHS. As DHS reduces, estimation uncertainty follows.

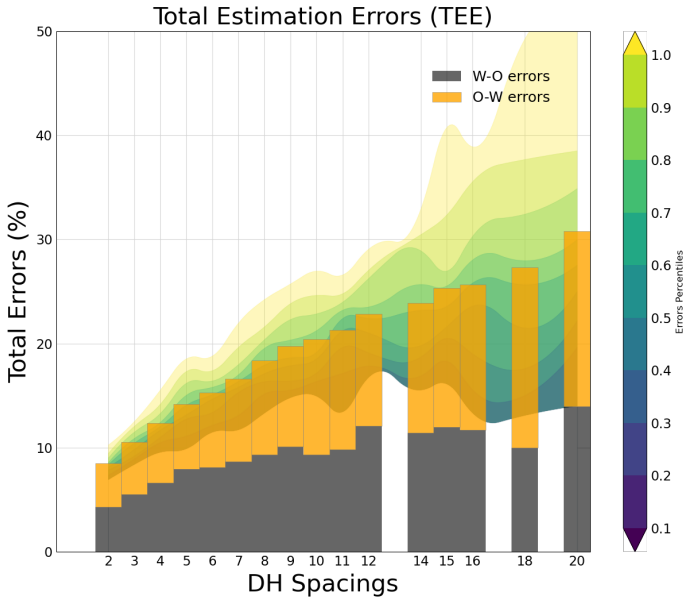

Figure 2.8: TEE per DHS is plotted as stacked bars: W-O (dilution) is gray and O-W (ore-loss) orange. The spread of TEE values across the 20 realizations are shown as shaded areas, colored by percentiles.

Across the range of DHS, TEE goes from 30% of TEE at the widest DHS to less than 10% of TEE at the shortest, while the optimal DHS of 7m has around 17% TEE. Diminishing errors in estimation are only desirable until a certain level when the goal is to optimize financial gains. Setting a specific threshold of uncertainty for quality reasons (e.g., 15% of TEE) may not guarantee the optimal profitability of DHS. The uncertainty level leading to optimal profitability is likely variable across different cases.

Profit and estimation errors

Unlike DHS, profit relates to estimation errors in a parabolic manner, as shown by Figure 2.9. The average FP results' shape amidst both estimation error metrics is highly similar.

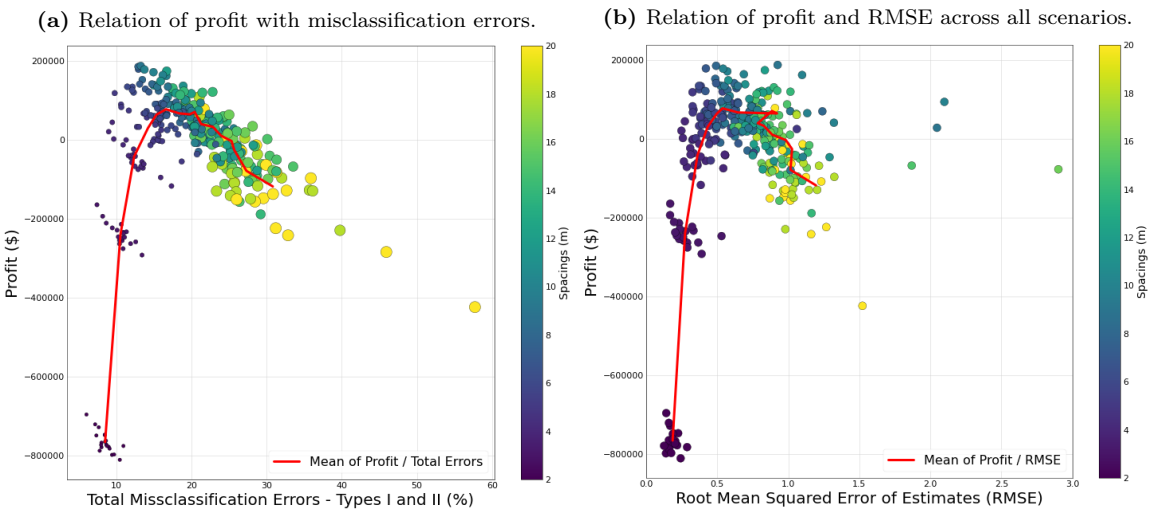

Figure 2.9: (a) Final profit against total estimation errors and (b) RMSE of estimated grades plotted against FP for all estimated scenarios.

Both metrics, TEE and RMSE, deliver the same relation with profit. The decrease in uncertainty is financially attractive only until a peak and subsequent turning point. For TEE, the profit peak occurs around 17%, and for RMSE, around 0.5, at the same DHS. The slope of profit decrease when further reducing errors beyond the maximum value is much steeper than before it, as the data insinuates.

2.3.3 Dependencies analysis

Dependency analysis yields a better understanding of how each parameter affects the example's results. A variation on each parameter at a time is done in two ways: (i) 50% increase and (ii) 50% decrease in its value. The analysis can inform each parameter's impact on the process' outcomes and how sensitive the final results are to each. The inputs and results are provided in Table 2.3.

Table 2.3: Dependencies assessment table: values changed in each dependency and its results.

Dependencies	**Dependencies values and its results**		
	-50% Value	**Base-case**	**+50% Value**
Drilling cost ($/unit)	200	400	600
- Maximum DHS (m)	6	7	10
- Final profit (k $)	121.4	71.6	53.3
Cut-off grade	0.7	1.2	1.7
- Maximum DHS (m)	8	7	10
- Final profit (k $)	533.4	71.6	-160.3
Dilution penalty (% recovery)	0	50	100
- Maximum DHS (m)	7	7	10
- Final profit (k $)	58.2	71.6	97.9
Coefficient of variation	0.7	1.4	2.1
- Maximum DHS (m)	10	7	7
- Final profit (k $)	-52.0	71.6	163.5
Variogram range (m)	12	25	37
- Maximum DHS (m)	6	7	8
- Final profit (k $)	63.5	71.6	215.9
Mining selectivity (mxm)	6x6	4x4	2x2
- Maximum DHS (m)	6	7	7
- Final profit (k $)	58.2	71.6	97.9
Nugget effect (%)	0.1	0.2	0.3
- Maximum DHS (m)	7	7	7
- Final profit (k $)	126.6	71.6	-160.3

The dependencies can be divided into the ones related to the mineral deposit characteristics (CV, nugget effect, and variogram range) and those related to mining operation specificities (drilling cost, mining selectivity, cut-off grade, and waste recovery). Figure 2.10 informs the results as tornado charts.

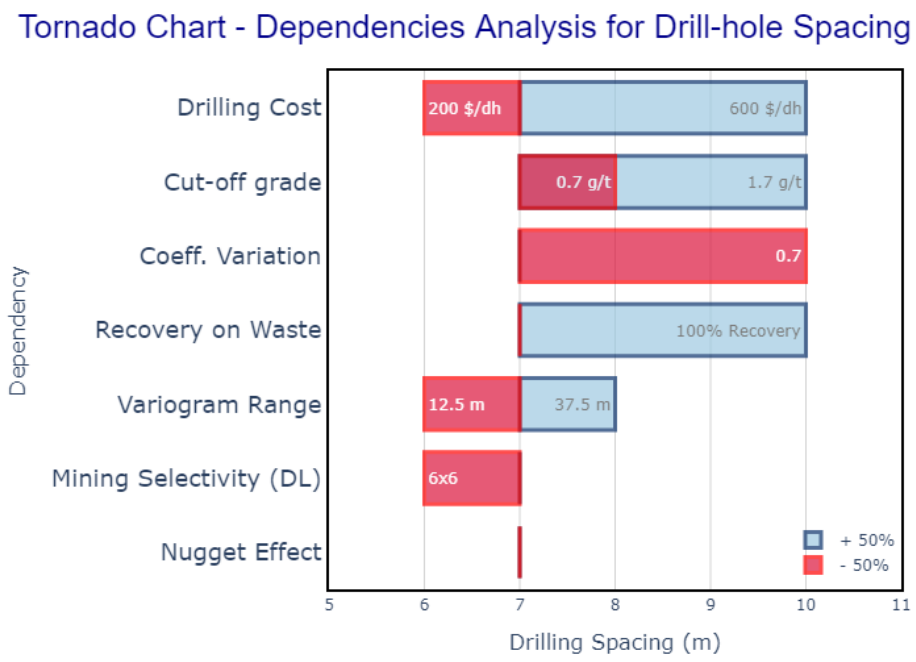

(a) Optimal DHS tornado chart.

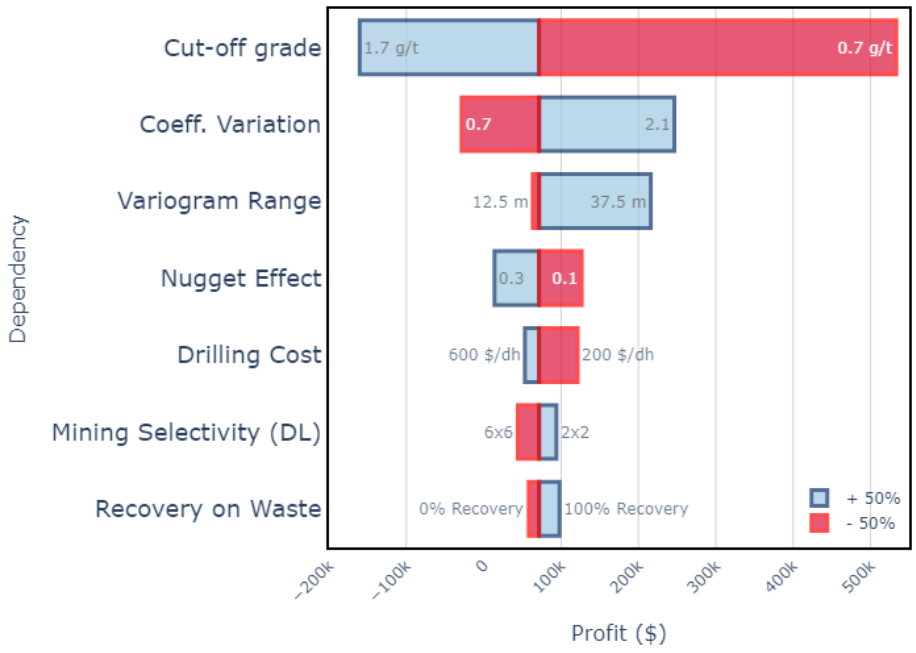

(b) Maximum profit tornado chart.

Figure 2.10: Tornado charts containing the maximums achieved per dependency variation. 50% increases are represented by light-blue bars, and 50% decrease by red bars.

The ranked dependencies convey the most influential ones on the final results. The main remarks on the dependencies study are:

1. Deposit-related dependencies:

a. CV: An ore of less variability (low CV) allows less drilling. Regarding profit, it is also very influential because it alters the distribution of grades of the entire dataset, hence changing profit substantially.

b. Nugget effect: Higher nugget effect harms profitability, although it does not impact optimal DHS in the example.

c. Variogram range: more spatially continuous ore allows less drilling (wider DHS) and increases profit significantly. Shorter-ranged ore calls for shorter DHS and reduces profit.

2. Operational dependencies:

a. Drilling cost: Most influential parameter on changing optimal DHS. A greater drilling cost led to a wider optimal DHS.

b. Cut-off grade: a feature that depends on operational and economic factors. Most influential parameter for profit changes and second most for optimal DHS due to implicating a consequent change in ore selling price as well. Economic factors can greatly influence a financial optimization like the DHS for profit.

c. Mining selectivity: The variations applied were insufficient to generate relevant changes.

d. Recovery on waste: When dilution has poor recovery, profits are diminished, but DHS is unaffected. When dilution recovers as ore, optimal DHS gets significantly wider, and profits naturally increase.

2.4 Discussions

Using a more robust metal recovery function could impact DHS optimization overall outcomes. Metal recovery results from complex interactions between metallurgical processes and ore's geological properties. Even though metal recovery is not only dependable on feed grade alone, a customized grade-recovery curve to determine recovery rates given data grades could improve the accuracy of such a DHS analysis. No grade recovery function was applied for the example's simplicity.

Assuming the same variogram model (identical from the simulations) across all DHS on estimations in the practical example for simplicity might have produced varying DHS optimal results. In practice, different DHS would produce, at least, slightly different models of spatial continuity. For wider DHS options, variogram values are expected to increase, since pairs of data are theoretically moving towards becoming independent from one another (Clark et al., 1979). Therefore, wider DHS are likely to generate less continuous variogram models, which would affect DHS optimization results. In subsequent examples throughout this Thesis, autofitting variogram models for each sampled DHS could be employed.

The regular DHS workflow for optimizing profit has been presented, explained, and applied to a synthetic data example. Relationships between main variables have been described, and the

dependency analysis revealed insight into DHS outcomes.

Chapter 3

A Nested Methodology for GC Sampling Targeted at Ore-Waste Boundaries

3.1 Introduction

Regular drilling is effective for mining operations while also being practical to plan and execute. Usually, mining operations undergo multiple drilling campaigns between long-term models and the actual mining of benches/stopes. Resource models are updated between drilling phases. Subsequent drilling phases might benefit from updated ore positioning for deciding how and where to place drill-holes. When optimizing profit for final estimates, the optimal DHS solution is the one that maximizes the proper destination of ore and waste without adding excessive costs with drilling. Thus, maximizing the correct destination of blocks with the least amount of drilling is optimal.

A new DHS method is created to assist in finding the optimal DHS solution for placing final drill-holes by using the updated model from the previous drilling phase and focusing on its ore-waste (O-W) boundaries. The O-W boundaries are considered the area of greatest relevance in determining value for a final estimate since it controls the proper classification of blocks. Reducing the uncertainty in O-W areas is a reasonable strategy to adopt. Resource model uncertainty may arise from unsampled areas and geological contacts but are also linked to high spatial variability (Chiles & Delfiner, 2012). The proposed method optimizes the DHS and decides the location of final samples in an automated manner, focusing on increasing sampling density around O-W borders. It is designed for dedicated drilling systems and optimizes two phases of drilling (thus the term 'nested').

The O-W targeted drilling workflow is grounded on two main ideas that are considered strategic for increasing profitability:

1. To maximize the correct destination of mineable blocks, and

2. To benefit from the previous estimated model to place final GC drill-holes more effectively.

As such, the correct O-W classification relies on having precise grade estimates near the cut-off grade range. A way to achieve that is through denser sampling patterns near the O-W boundaries. The final sampling on this new workflow is then limited to the surroundings of previously estimated O-W boundaries. That procedure, however, demands that the O-W boundaries are reliable for the strategy to succeed. Otherwise, placing GC samples along poor O-W boundaries will not increase profit. Therefore, the new DHS optimizes two drilling phases concomitantly. Although both phases

are regularly spaced, the latter is limited to O-W boundaries, resulting in a final combined DHS, which is irregularly spaced.

Lastly, the nested DHS methodology is employed in the same synthetic example from Chapter 2, so comparisons of FP are valid between DHS methods. The concepts and mechanisms for the methodology are described, along with illustrations of the process.

3.2 Methodology

The O-W targeted DHS process is about finding the best DHS and determining the best placement of FS to maximize profit. It is based on the same regular DHS methodology but with modifications on the sampling and estimation stages. The definition of a set of DHS options for a first coarse sampling (CS) and the second fine sampling (FS) are required. The steps of the O-W nested DHS framework are listed (highlighted in **bold** are the exclusive steps from the nested DHS methodology):

- Step 1 - Define input values.
- Step 2 - Generate a range of high-resolution conditional SGS realizations to serve as references of the true underlying deposit.
- **Step 3** - Re-sample simulated grades in every CS option, estimate them, and define their O-W boundaries.
- **Step 4** - Buffer the O-W boundaries, sample the simulation restricted to the O-W buffers, combine a final dataset merging CS and FS re-samplings and generate final estimations of the GC area.
- Step 5 - Transform final estimated maps into mineable dig-limits.
- Step 6 - Assign misclassification labels to the mineable blocks by comparing estimated and simulated grades.
- Steps 7 and 8 - Customize the transfer function and calculate profits, revenues, and costs per DHS scenario estimation across the entire series of simulations. Average and plot final results of profit.

The O-W targeted DHS framework is shown as a diagram in Figure 3.1, containing its main steps and a detailed zoom on the O-W targeting procedures.

(a) Diagram O-W targeted DHS Optimization workflow with all involved steps.

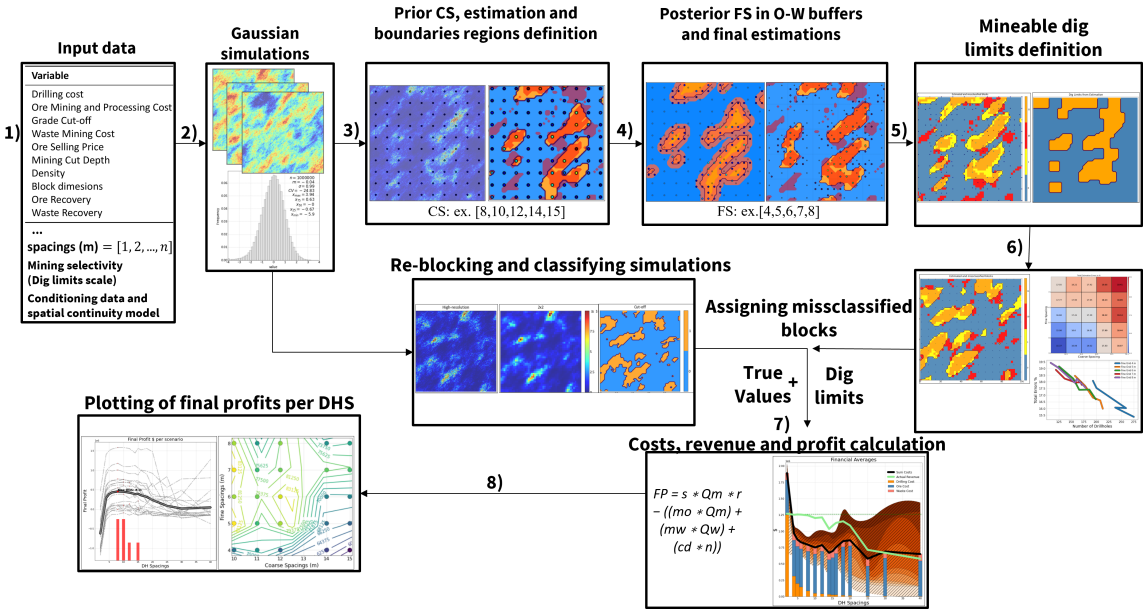

(b) Detailed view of key difference in DHS 2: Determining O-W areas for placing final samples.

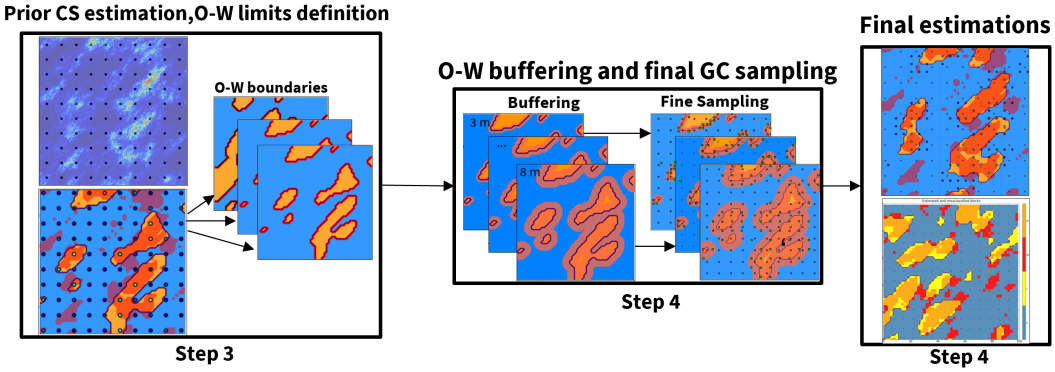

Figure 3.1: Diagram of nested DHS steps and detail on targeting O-W boundaries.

The main processes of the two-phased DHS methodology are highlighted in Figure 3.1b, which are:

- the determination and buffering of the O-W boundaries,
- the FS procedure within the O-W boundaries and the merging of CS and FS final re-sampled data.

The technical considerations related to exclusive steps from the O-W targeted DHS method are described next. The common steps between both DHS frameworks are described in Section 2.2, thus are not repeated here.

3.2.1 Buffering ore-waste boundaries

The generation of O-W buffers to accommodate final sampling is made by offsetting all of its vertices until a certain specified distance. An illustration of this process is displayed in Figure 3.2 next.

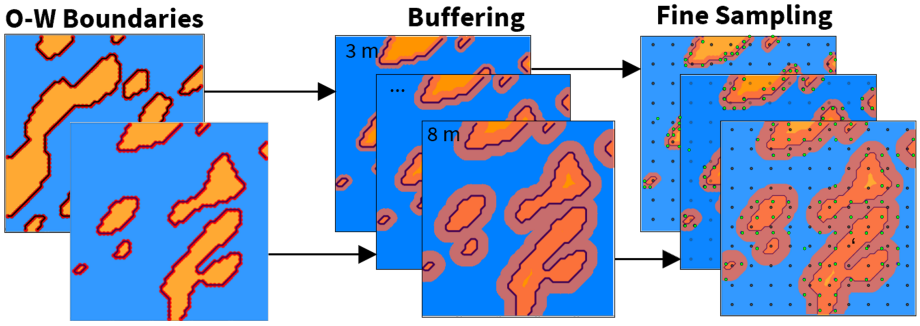

Figure 3.2: Process for buffering O-W zones and fine-sampling within its limits.

To build the O-W region, all the O-W vertices of the prior estimation must be collected and used as input data for an isotropic nearest neighbor (NN) estimation (Rossi & Deutsch, 2013) on the high-resolution grid of simulation. The range of the NN estimation coincides with the buffering distance chosen. The high-resolution grid becomes flagged within the buffering distance from any O-W vertices used as input. The buffering happens in both directions, towards ore and waste, and its distance must allow final samples to be placed preferentially on both sides of the O-W zones. Therefore, the buffered distances should have at least the FS length to accommodate minimally one sample on each side of all estimated borders on the GC area. Buffer distance might vary depending on the modeler's intent and the mineral deposit's characteristics.

3.2.2 The FS procedure

The next step is to place final samples within the O-W zones and clean redundant final samples according to a tolerance threshold in meters. When combining drilling phases (CS and FS) and testing all combinations, it is important to have the drilling grids aligned regarding origin coordinates. After aligning grids, a post-processing step is required to perform cleaning: removing overlapping samples and short-distanced pairs between pre-existing coarse and fine grids. The tolerance $\boldsymbol{t}$ threshold should be smaller than the FS to allow the sampling pattern to become denser on the O-W regions than outside of it (Figure 3.3).

Adding as many spacings as possible is recommended to establish good options across CS and FS. FS should be smaller than CS yet wide enough to avoid excessive costs. The fraction between CS and FS dimensions matters for the effectiveness of the combined drilling pattern. Prior and final drilling spacings do not necessarily need to be divisible by the same number or have stable remainders to be effective. Irregular patterns of combined drilling spacings can also be effective by avoiding unnecessary samples, as the following example shows.

3.3 Example of application

The DHS methodology targeted at O-W boundaries is applied to example from Section 2.3. The set of unconditional realizations, transfer function (Equation 2.1), and parameters are equal to the Chapter 2 example, allowing relative and absolute comparisons between the results. The goal is to assess whether the O-W DHS methodology can overcome regular DHS in terms of final profitability.

The difference in parameters between the two methodologies is the spacings array. The CS and FS distances to be tested for establishing which combination returns the maximum profit are specified by the following arrays:

$$\textbf{CS (m)} = [8, 10, 12, 14, 16]. \tag{3.1}$$

and

$$\textbf{FS (m)} = [3, 4, 5, 6, 7, 8]. \tag{3.2}$$

Following the steps from Figure 3.1a, the application example is conducted through the same procedures. Figure 3.3 gives an illustrative example of the FS procedure restricted to the O-W zones. Varying FS densities are exhibited for a CS: 10m, where the distance buffered also increases together with FS to accommodate larger sampling spacings.

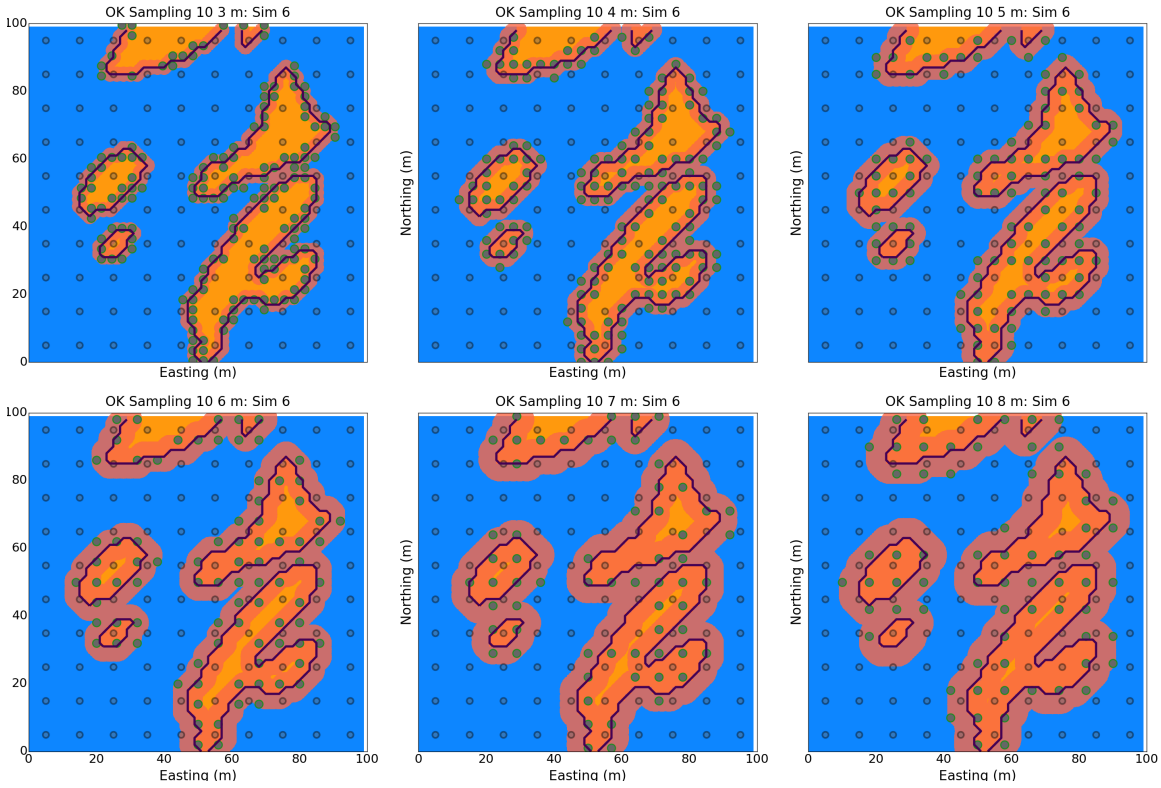

Figure 3.3: The fine sampling procedure for CS: 10m in realization #6.

Figure 3.4 illustrates the process of merging each estimated map with the underlying simulated

truth to verify estimation performance, which in turn posteriorly influences the resultant FP. The top row shows a high-resolution simulation being up-scaled and then classified as ore and waste.

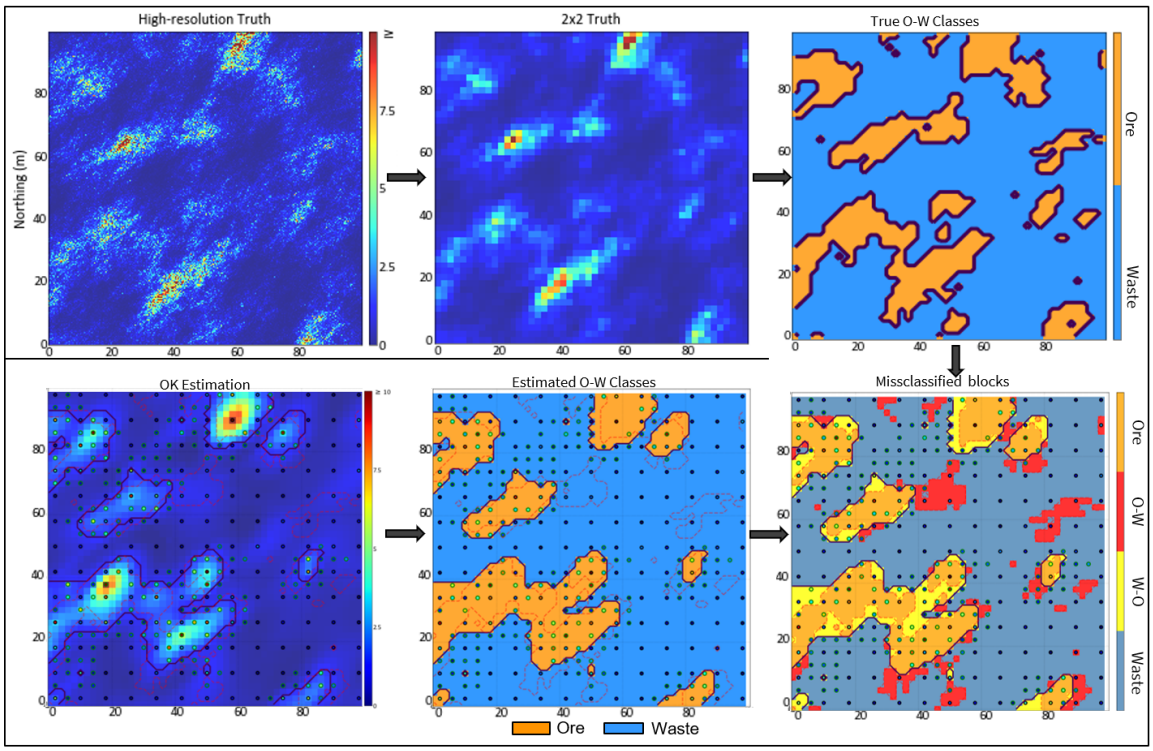

Figure 3.4: Process for establishing misclassification errors: (Top row) Up-scaling and assigning O-W classes to simulation, (bottom row) Assigning O-W classes to estimation and verifying against simulation to establishing misclassifications.

The bottom row of Figue 3.4 shows the progress from a final estimation map (overlaid by the final combined dataset) to generating O-W classes, and finally leading to misclassification classes by cross-checking it with the simulated reference.

3.3.1 Results

The number of drill-holes, combined DHS, TEE, and FP are examined. There are 30 combinations of DHS possible (5 of CS x 6 of FS). Results are, therefore, grouped by DHS combinations and averaged across all 20 simulated scenarios. Figure 3.5 exhibits TEE results relative to the combined DHS:

(a) Waste-as-ore estimation errors matrix: dilution

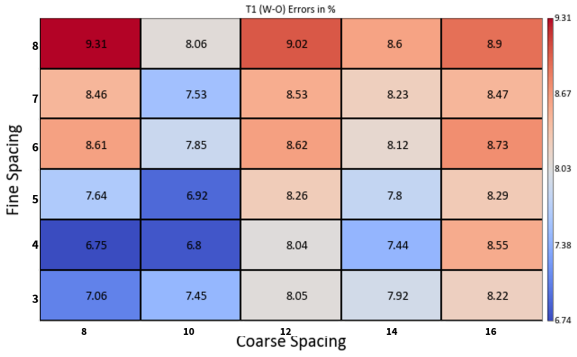

(b) Ore-as-waste estimation errors matrix: ore-loss

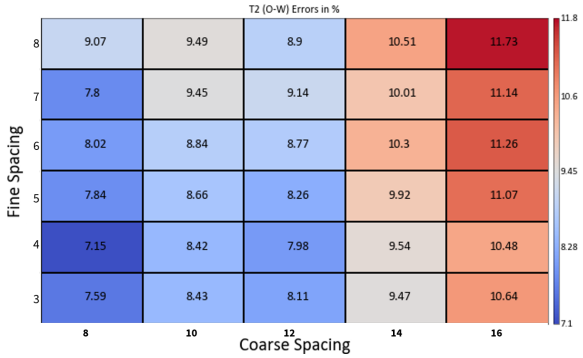

(c) Total estimation errors matrix

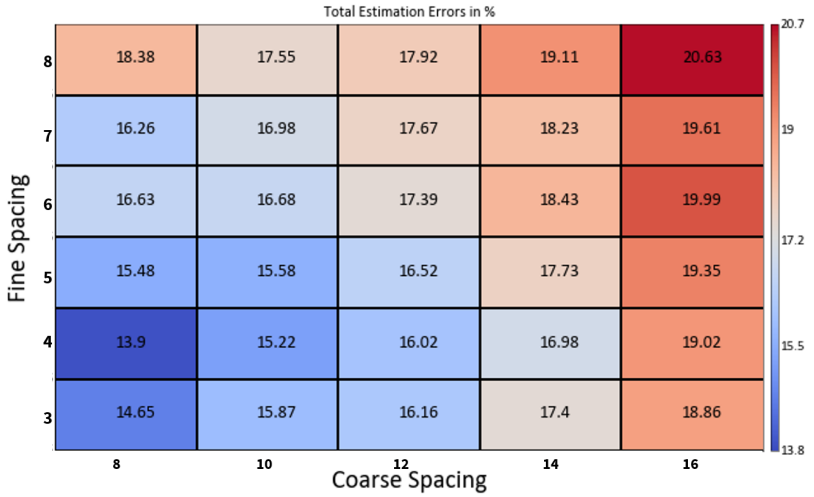

Figure 3.5: Estimation errors across all DHS combinations.

Figure 3.5 shows the relationship between combined spacings and estimation error type. While dilution has a stronger relation with FS, ore loss is more dependent on CS increase. TEE, as a result, displays a trend very well linked to the combination of both DHS.

Figure 3.6 shows the distribution of profits achieved by each DHS combinations. The line plot to the left shows the average profits earned by each combination of DHS as the thick gray line. The plot to the right contains the same information as a contour-lined matrix of DHS.

(a) FP results by combined DHS as individual realizations and average.

(b) FP results as contour-lines by CS on X-axis and FS on Y-axis.

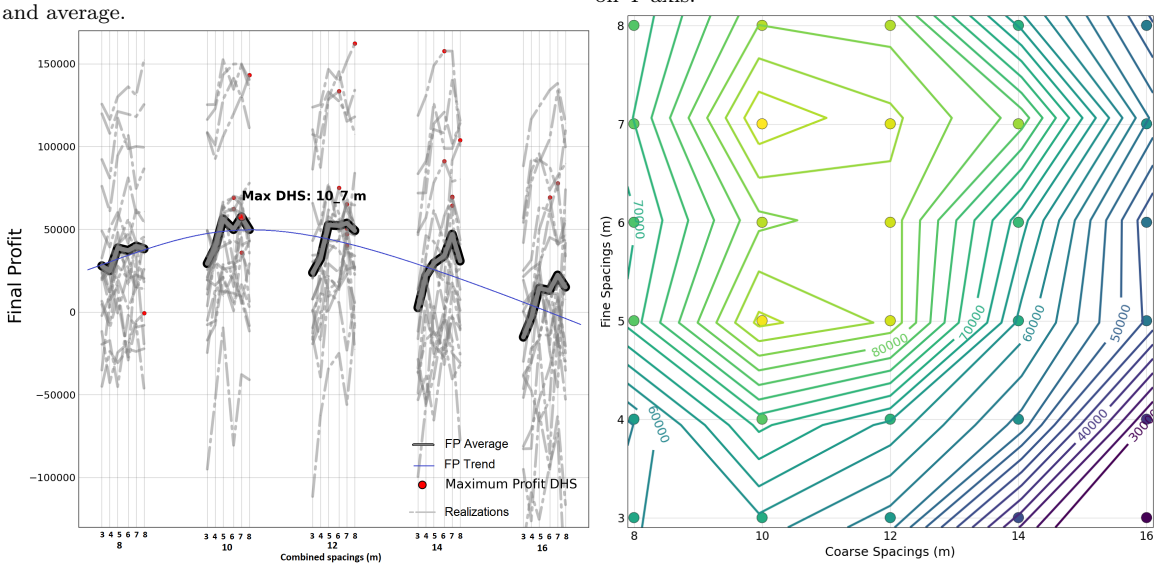

Figure 3.6: Final profit results informed in two forms: (left) line plots and (right) contour plots.

The thick gray line on the left-side of Figure 3.6 informs averaged FP results. FP trend (blue line) draws a smooth parabolic function across CS, despite the erratic behavior of individual DHS values. As FS decreases within each CS group, FP reduces too. While the maximum FP is at CS: 10m and FS:7m, the combination of 10m with 5m is very high-performing too. CS: 8m presents declining FP values, indicating that from that DHS to shorter, the FP function has passed its optimal turning point.

3.3.2 Comparison between methods

The relationship between TEE, FP, and the number of drill-holes of the two DHS methods is investigated. Figure 3.7 compare those metrics results between the two DHS methods. Figure 3.7a informs the negative correlation between TEE and the number of drill-holes. For the same CS, the reduction of FS is usually too costly for reaching lower TEE values profitably. Figure 3.7b conveys how TEE relates to FP. As expected, the greatest FP results occur for intermediate TEE rates. The DHS that accomplishes the most efficient combination of low TEE and low drilling count is likely to have the highest FP.

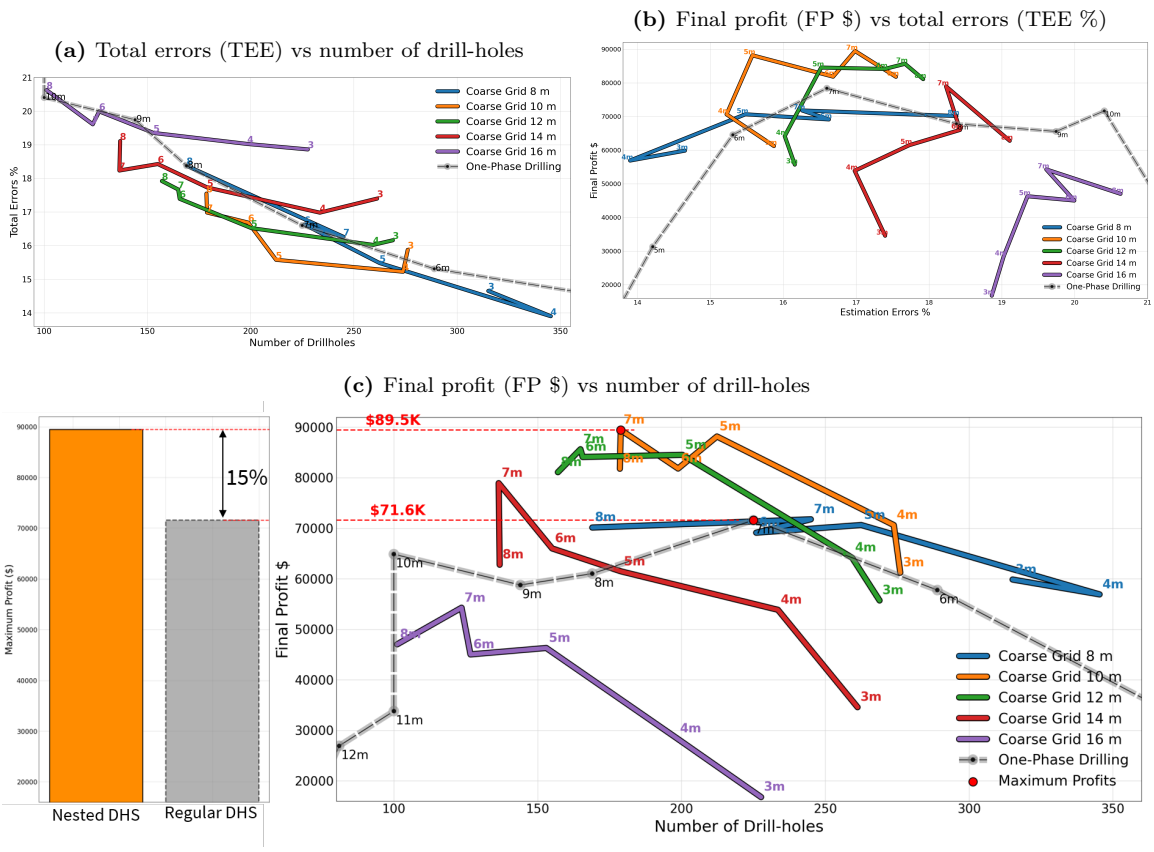

Figure 3.7: Plots relating number of data, TEE, FP between both DHS methods: regular and nested

Figure 3.7c shows FP averages for all combinations of nested DHS and the regular DHS results from Chapter 2 (dashed line). The horizontal red-dashed lines highlight the maximums for each method, where the nested DHS method improves FP by 15%. The nested DHS maximum profit is achieved with the combined DHS of CS: 10m and FS: 7m, composed of 179 drill-holes and having reached 16.7% of TEE. Whereas the regular DHS maximum profit occurred for a DHS of 7m, made of 225 drill-holes and having obtained a TEE of 16.59%. In conclusion, both maximum profits achieve similar TEE rates but the nested method performed it with 25% (51 drill-holes) less drilling than the regular method.

3.3.3 Discussions

Actual spacing

When merging two regular-spaced drillings (CS and FS), the resultant DHS is an irregular grid, as shown in Figure 3.8. Shorter DHS occurs around the prior estimated O-W limits (black lines). Increasing sampling density in the O-W zones is achieved, while avoiding redundant samples outside of the buffer zone.

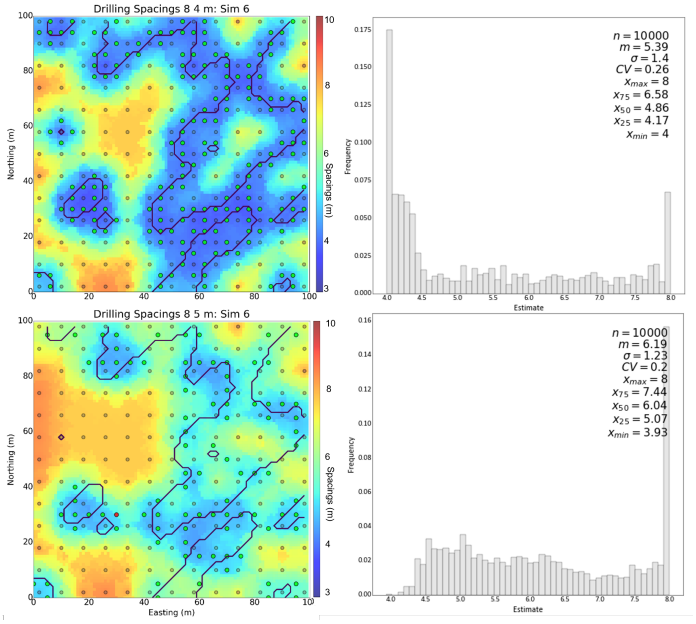

Figure 3.8: Final combined DHS map and histograms for CS= 8m and FS = 4m and 5m in realization #6. Black lines are prior estimated O-W limits.

Sampling density within O-W zones can become smaller than FS, as in the bottom of Figure 3.8. DHS histograms show high frequencies at the tested CS and FS. Values range from cleaning tolerance ($\boldsymbol{t}$=4m) up to CS distance.

Number of drilling data

One goal of the nested DHS is to reduce required drilling. Hence, it is expected to achieve higher FP and lower TEE with less drilling than regular DHS. Figure 3.9 compares the average number of drill-holes used in both methodologies.

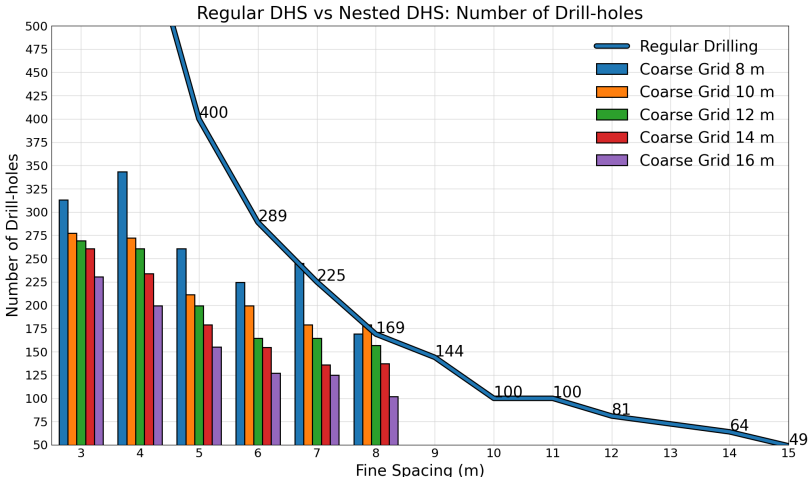

Figure 3.9: Regular vs nested DHS: Number of drill-holes

The number of regular drill-holes is a quadratic function of the area's size divided by DHS as

shown by Equation 3.3:

$$n_{dh} = (\frac{l_{\text{area}}}{DHS} + 1)^2 \tag{3.3}$$

, where n_{dh} = number of drill-holes, l_{area}= size of the GC area (m). The function of regular DHS counts is represented by the blue line in Figure 3.9 above. The number of drill-holes is generally lower for the nested DHS since just parts of the area (the O-W buffered zones) are sampled in the GC phase. For example, the number of drill-holes required to sample the area with an FS of 4m is much smaller than regular drilling at 4m (Figure 3.9). Denser DHS is only found at the critical O-W zones. This savings in the number of drill-holes benefit FP if the placement of drill-holes effectively reduces miss-classification errors of blocks.

Effectiveness of FS placement

Figure 3.10 examines the placement of FS along the estimated O-W boundaries in refining the estimate. One of the realizations is taken as an example.

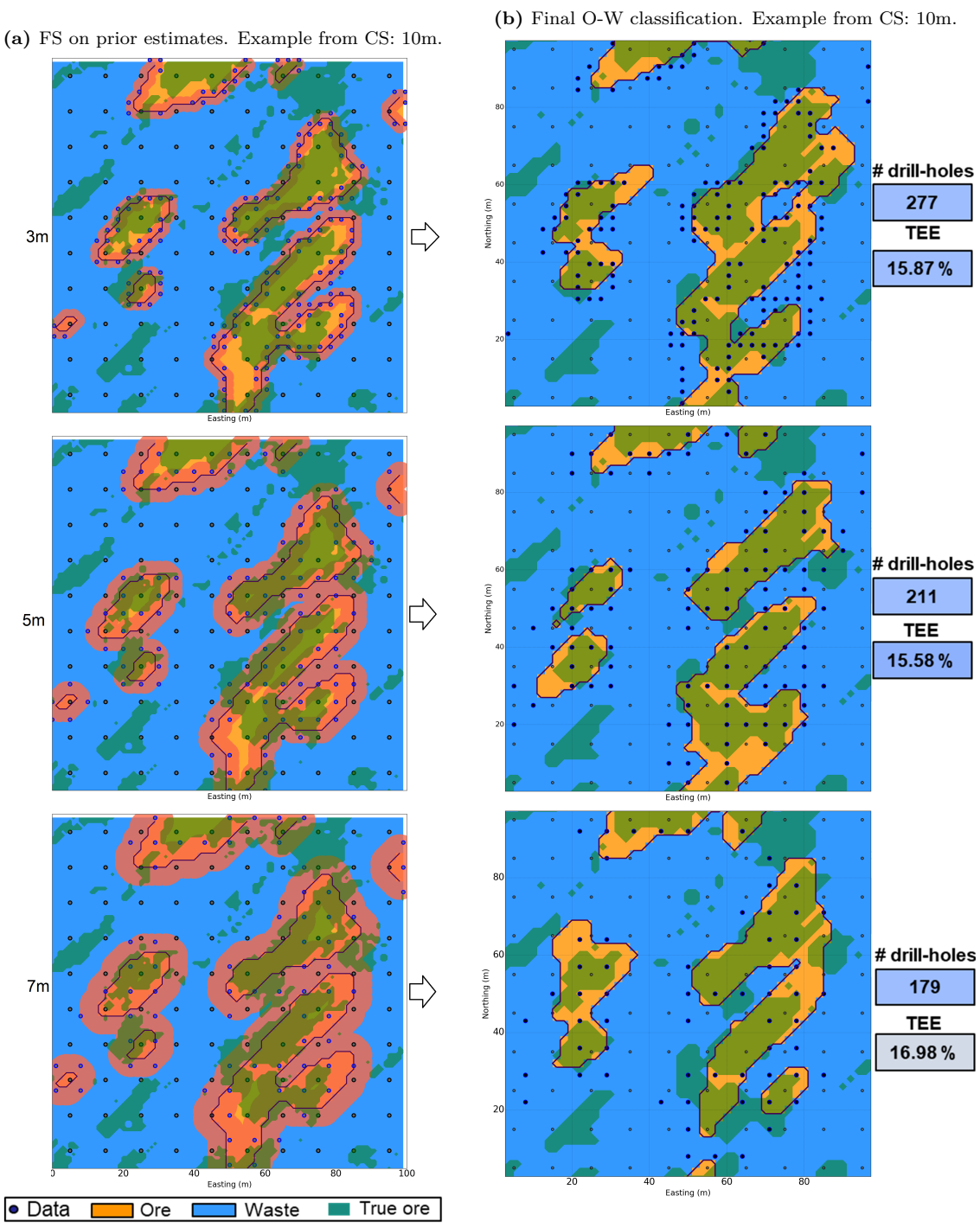

Figure 3.10: FS locations on the left side on top of prior estimated O-W classes, and the resultant final classes on the right, in relation to the shaded underlying true ore.

The effectiveness of the final DHS configuration relies on the CS estimate being able to identify good O-W boundaries and on FS being reasonable and sufficient in refining those zones. Figure 3.10 shows three resultant FS sampling and final estimations for a CS of 10m. Combined DHS of 10-3m adds excessive FS for little improvement on TEE, while DHS of 10-5m lies in the middle. DHS of

10-7m uses only 64% of the drilling to achieve a TEE just 1.1% higher, being the most effective. That effectiveness drives profit increase.

The nested DHS options plotted in Figure 3.7c shows some erraticity in its FP results. This effect of having erratic and unstable profit results across different DHS options could be derived from not having properly optimized which DHS options to use as options. Methods like binary search, Golden section or simply using only multiplicative options could be tested as future research work.

Drilling cost proportion

Optimization of DHS is relevant when drilling costs constitute a significant source of costs. The nested DHS methodology adds drilling efficiency by concomitantly optimizing two stages of drilling. The FP improvement is directly linked to the overall value of the drilling cost. In the example, Figure 3.11 shows drilling cost proportion of total expenses ranges from 6% up to 16%.

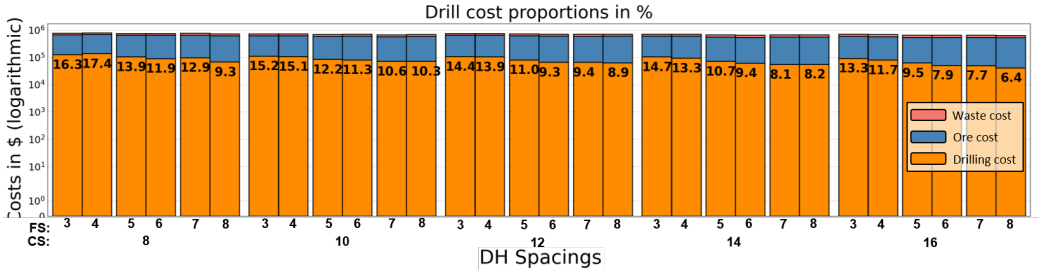

Figure 3.11: Drilling cost proportions per combined DHS.

The maximum FP gain by combined DHS of 10m-7m of 15% is in line with the magnitude of the average drilling cost proportion. Thus, the gain of applying such DHS methodologies to other cases could be assessed by calculating the average drilling cost contribution on the specific project.

Nested DHS optimization practicality

The nested DHS optimization is not about having two phases of GC drilling. The CS phase represents the prior drilling campaign, usually to convert mineral resources into reserves. It is the delineation of reserves' drilling phase. The simultaneous optimization of two drilling phases allows for the final one (GC) to be restricted to O-W boundaries. However, for the GC phase to be effective, the O-W boundaries must be reliable, which in turn usually depends on having denser grids at the reserve conversion drilling. This means investing more time and budget in the prior phase of drilling and saving on the GC phase. This trade-off is shown to be more profitable on the constraints of a theoretical example application. In reality, implementing a nested DHS optimization should consider operational and mine planning aspects that are out of this research's scope.

3.4 Conclusions

The nested DHS methodology can improve profit compared to regular DHS. The profit increase depends significantly on the proportion of drilling costs over the total operation costs. Many combined DHS options overcame regular DHS profitability in the example application, underpinning that providing enough and varied possibilities of CS and FS to be concomitantly optimized is an essential aspect of the O-W DHS framework.

Chapter 4

Systematic Assessment of Factors in DHS Optimization for Profit

4.1 Introduction

Determining the optimal DHS for final estimates is a big concern in mining operations. Embedded in this thesis is the concept that optimization of DHS for final estimates should aim for profit. The DHS is optimal given certain conditions and specificities, as listed in Section 1.1. DHS studies are specific and demand a cost-benefit analysis, which informs whether potential additional drilling is beneficial to decreasing model uncertainty beyond its cost or not (Rossi & Deutsch, 2013). Now, beyond finding an optimal DHS for a certain deposit or operation, this Chapter intends to broadly capture how optimization of DHS would vary across a wide range of possible mining scenarios. This is achieved through variation of input values for each mining factor like mining selectivity, ore spatial continuity, ore price, and others. A DHS optimization is run for each scenario on the same synthetic GC example from Chapter 2. Each scenario has a factor's value changed one at a time.

It is expected that seeing DHS optimization through a broader view can help understand the mechanisms that drive DHS optimization. The findings can serve as a learning reference for real DHS applications in the mining industry. After understanding how each factor affects DHS decisions, profit sensitivity to DHS variations is also tracked, for it is not a stable relationship.

4.2 Methodology

The DHS optimization for profit are systematically tested across a set of elements: **geology, mining selectivity, spatial continuity, nugget effect, ore price, ore proportion, and sampling error**. The values of each element are systematically changed, one at a time, to assess their effect on the decision of optimal DHS targeted at profit. The base case is the same dataset and DHS options from Chapter 2 (Section 2.3): unconditional simulation on a high-resolution grid with cell sizes of 0.1m x 0.1m dimensions in an area of 100m x 100m serve as underlying truths of the synthetic GC area. The economic and operational parameters are also the same as the previous examples (Table 2.1). The sensitivity analysis is done so that two different styles of geology along with two mining selectivity dimensions are priorly defined and changes in other factors are tested upon. Therefore, four possible scenarios of geology and mining selectivity constitute the basis for the DHS analyses.

4.2.1 The basic scenarios - geology and mining selectivity

- **Geology**

Two distributions are set up to represent different geological variables (Figure 4.1). One is named *abrupt* and consists of two discrete classes: ore and waste. Both classes have only one grade, so the boundaries between categories are always sharp, with no in-between values; hence, the name *abrupt*. The other distribution, called *disseminated*, is log-normal and positively skewed, resembling a precious metal's distribution of grades, with a long tail of extreme values (Figure 4.1).

- **Mining selectivity**

On top of the two geological configurations, two scales of mining selectivity are designed to further incorporate into the study of assessing DHS across different situations in the mining industry. While the distribution relates to the intrinsic characteristics of the deposit, the latter refers to operational specifications. Notwithstanding, both are considered major influencers of the optimal DHS, as the study shows. The scales are:

- 4 m x 4m: Most selective mining method.
- 10m x 10m: Least selective mining method.

The combination of the different geologies and mining selectivities are visually presented below:

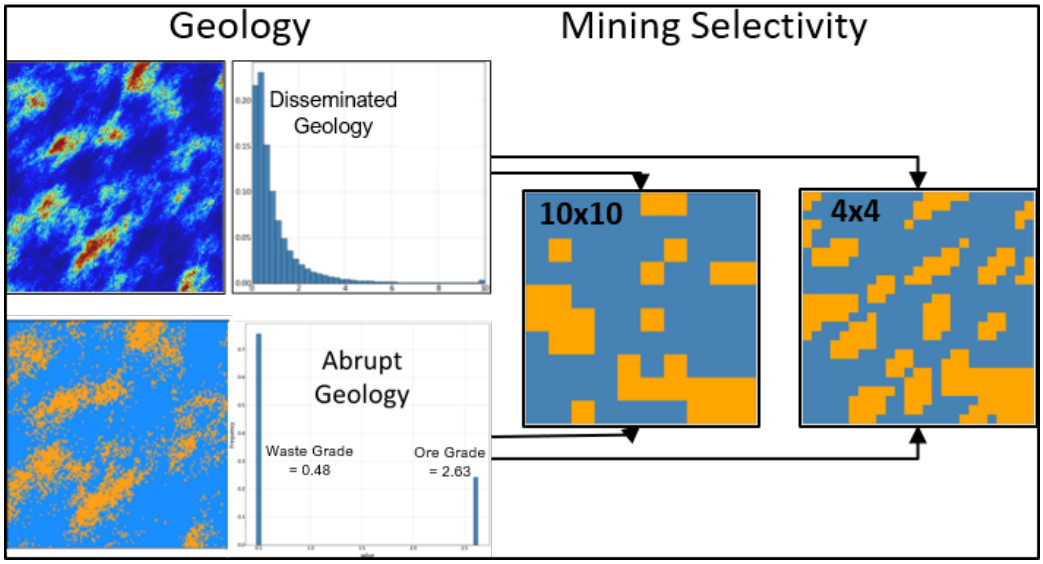

Figure 4.1: Geology and mining selectivity scenarios composing the basis for the DHS systematic assessment.

The two distinct geological distributions added by the two mining selectivity scales make up four main scenarios for our sensitivity study, where different aspects will be chosen and varied one by one on top of these fixed geology-selectivity base cases.

4.2.2 Elements to be assessed

Subsequently, optimal DHS analyses are carried out on all four combinations while systematically varying one element at a time. The elements chosen to be tested in this study are:

- **Variogram range of the deposit (spatial continuity)**: The spatial continuity is changed to generate unconditional simulations with varying variogram ranges. The extent of spatial continuity of a variable is assumed to be important for the decision of DHS, although the assumptions on how it works are usually intuitive.
- **Nugget effect of the deposit**: The variability of a deposit at a very short distance strongly affects how much drilling is needed to generate a profitable final estimate. Aiming to shed light on how optimal DHS is affected by increasing short-scale intrinsic variability, the nugget effect is also systematically tested.
- **Ore price**: The relative financial differences between the cost of drilling, the ore price, and the costs of mining and processing significantly impact the outcomes of optimal DHS aimed at profit. Such relationships of costs and prices are case-specific, but the assessment of ore price is included and tested thoroughly, given its significant influence.
- **Ore proportion**: The abundance of ore within the mining limits affects the decision of optimal drilling. Varying levels of ore proportion require different amounts of drilling to be properly represented in estimations.
- **Sampling errors**: Inaccurate and biased sampling mechanisms harm mining operations' profitability. Sampling issues are intimately connected to geostatistics (François-Bongarçon, 2004). The investigation of how and to what extent sampling errors affect the optimal DHS for profit is tested.

A summary of the value ranges tested per factor is displayed in Table 4.1.

Aspect	Minimum	Maximum	# of values	Base value
Spatial continuity (m)	2	50	9	25
Nugget effect (%)	0	80	5	20
Ore price ($)	2	200	10	16.66
Ore proportion (%)	6	80	7	24
Sampling errors (%)	0	75	4	0
Mining selectivity (m x m)	4	10	2	-
Geology	-	-	2	-
Total scenarios possible	-	-	50,400	-

Table 4.1: Summary of spectrums of variation applied per feature

The procedure of changing one value of a factor at a time is practical, organized, and interpretable. Most elements are unbounded with many possibilities. The study focuses on a pre-determined range of values (Table 4.1) to extract some reasonable interpretations from the results.

4.2.3 Grade - recovery curve

Metallurgical recovery is key in transforming grades into financial values. One way of expressing varying levels of mineral recovery is through a function with ore grade, even though grade alone does not always inform all the constraints that control plant recoveries. A robust recovery function in relation to grade has been incorporated, named as *Exponential model (EM)* recovery curve. The EM curve formula is expressed below, followed by its plot. It is an improved version of the previous uniform distribution of recoveries between ore and waste used in the Chapter 1 example (Table 2.1).

$$\text{EM Recovery}(g) = r_c * (1 - c/g), \text{if } g < c : \text{Recovery}(g) = 0 \tag{4.1}$$

, where g is the block's grade, c is the grade value below which recovery is null and r_c is the top recovery mark.

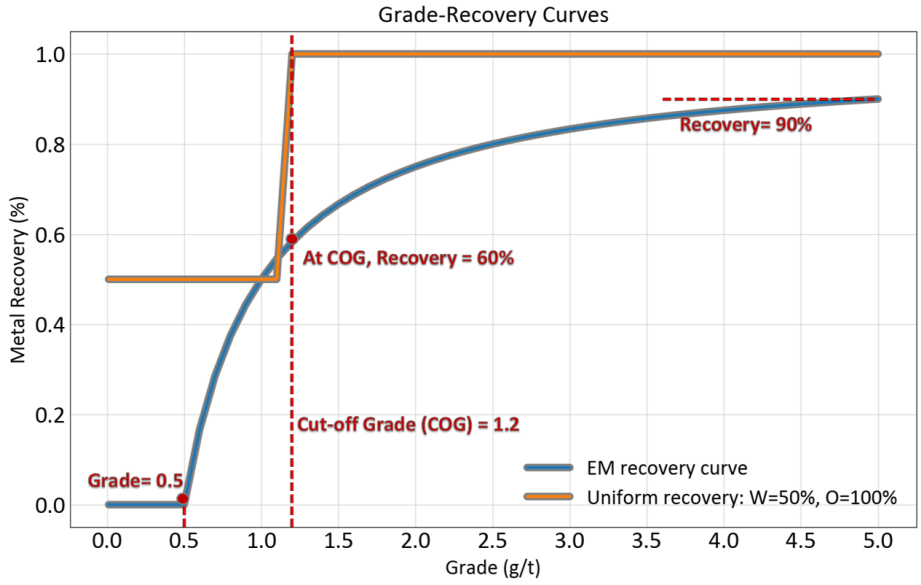

Figure 4.2: EM's model for the grade-recovery curve (blue) in comparison to the previous uniform curve (orange).

The EM is a non-linear grade-recovery curve, where up to grade $c = 0.5g/t$, recovery is zero and bounded at the top by recovery$(g = \infty) = 90\%$. It assumes a progressive recovery response to grade. The recovery at the cut-off grade (COG) is 60%. In this setup, high values of ore have better recovery rates, and marginal waste has a penalty response in metallurgical recovery. Very low-grade material performs poorly in the plant, returning zero profit given its null recovery response.

4.2.4 Mineable limits: dig-limits vs. re-block methods

One required step in DHS optimization studies is determining the actual mineable limits after having the final estimates. Only rarely are final high-resolution estimations mined as such. The O-W boundaries are adapted to the constraints of mining. Constraints are usually operational, related to equipment, space, time, and productivity restrictions. In our theoretical example, two main algorithms are compared to determine the actual mineable limits of final estimates:

- Dig-limits (DL - *igc_dl* (Vasylchuk & Deutsch, 2018)), the algorithm optimizes realistic excavation boundaries achieving up to 98% of maximum attainable expected profit.
- Re-block (*blkavg.exe*): Averaging of blocks to a bigger scale.

These methods are tested and compared against each other while performing optimal DHS for the same dataset.

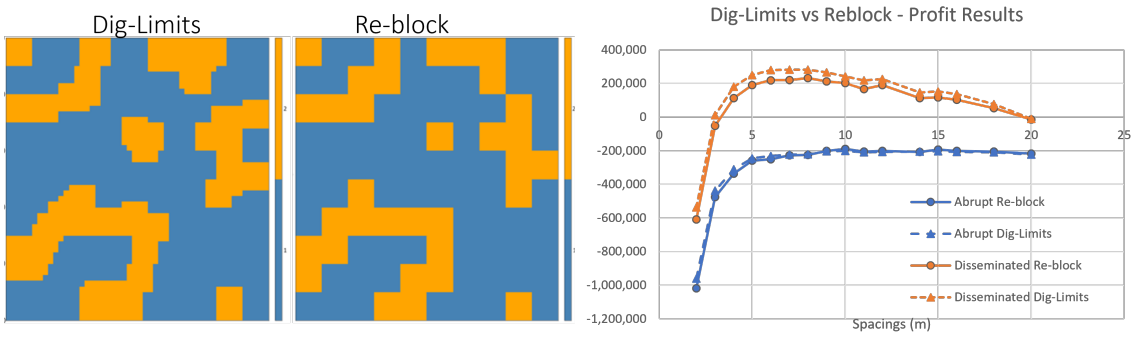

Figure 4.3: Dig-limits vs. re-block methods: comparison of mineable outputs (left-side) and the DHS profit curves between methods on the right-side.

As shown by the profit curves in Figure 4.3, the DL algorithm can achieve higher expected profits through its robust methodology of floating frames to continually calculate and replace expected profits. The edged mineable outcomes reinforce the concept of floating frames. Even though re-block does not systematically provide the highest attainable expected profit, the relative difference in profit values is deemed not significant. And most important, the shape of profits across DHS is equal between methods. Additionally, re-block has much greater computational efficiency: it processes the same data more than 20 times faster than DL.

For the systematic assessment of factors, absolute profit value is not the most important outcome. The optimal DHS curve shape is most relevant. Re-block algorithm attains the same FP curves, preserving the same optimal choice. Due to those aspects, the study will be carried out using re-block. More realizations can be considered to stabilize DHS results.

4.2.5 Metric for profit variation

A metric is proposed to summarize profit variability within DHS. Determining optimal DHS is only relevant if profit varies with DHS changes. As the systematic assessment shows, some combinations of factors lead to greater profit variation across DHS than others. Thus, in order to understanding profit sensitivity across multiple scenarios, a metric is developed. It is named Average Profit Variation (APV). APV informs whether changing DHS will substantially affect profit or not. It is the average percent variation on the seven higher FP results (out of the 16 regular DHS tested). The equation for APV is presented below:

$$\overline{APV} = \frac{1}{7}(\sum_{i=1}^{7} 1 - \frac{PV_i}{\text{max Profit}}) \text{ , for the greatest 7 profit values.} \tag{4.2}$$

, where $PV =$ Profit value.

In the results, the APV for each scenario of DHS analysis is plotted along the optimal DHS, which shows how variable profitability might be across different DHS options. It is an effective measure to detect scenarios where optimal DHS is critical for profitability.

4.3 Results per element

Each element has DHS optimization scenarios run across the entire range of values specified in Table 4.1. Each range is applied to the four combinations of geology and mining selectivity (Figure 4.1). The results are specific to this example.

4.3.1 Spatial continuity

The spatial continuity of a deposit affects the decision of optimal DHS. For each simulated scenario, a DHS-optimized decision is processed. The expression 'variogram range' on the graphs below is relative to the spatial continuity of the simulated deposit.

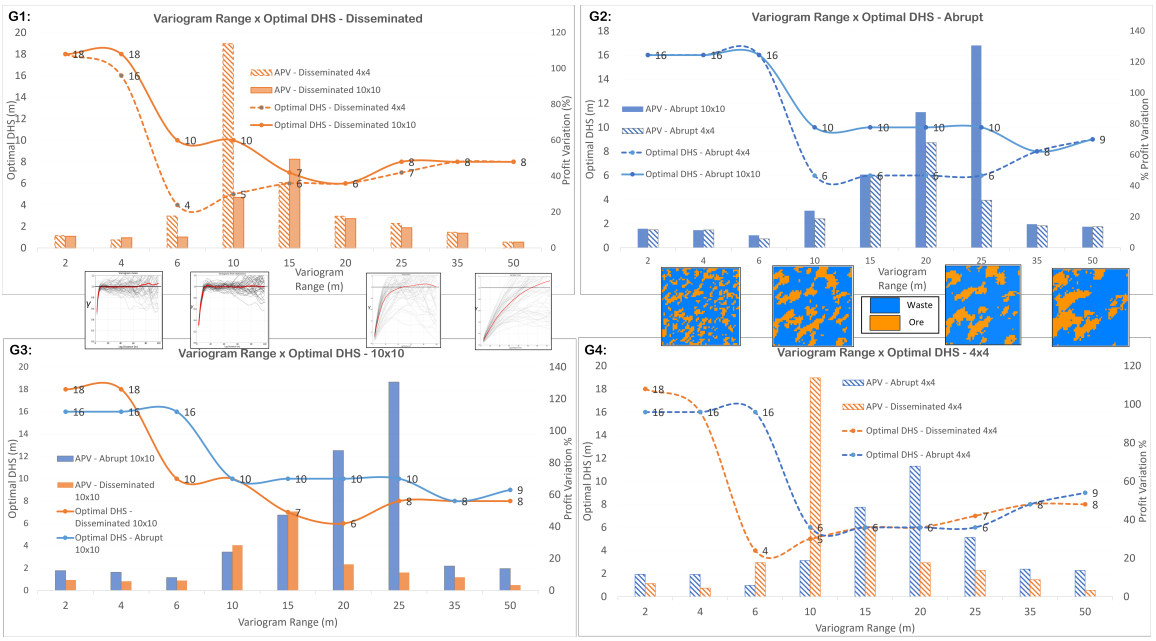

Figure 4.4: DHS results for varying ranges of spatial continuity - G1: disseminated graph, G2: abrupt graph, G3: 10x10 selectivity, G4: 4x4 selectivity.

The graphs in Figure 4.4 convey a lot of information. Regarding the overall effect of spatial continuity on optimal DHS decision, it is noticed that shorter DHS occurs for intermediate values of continuity, never on extremes. On extreme ranges, either short or large, DHS tends to increase. Especially for short-ranged deposits, DHS optimization goes toward drilling as few as possible in a sudden manner. The effects of geology and mining selectivity on optimal DHS are highlighted below.

- Effect of geology: In most continuity scenarios, the disseminated deposit style leads to shorter DHS than the abrupt style. That is not the case for very short continuity, where optimal DHS for the disseminated goes wider than for abrupt cases. In some other intervals of continuity, both geology types optimize at the same DHS. In general, disseminated geology represents a more complex geological distribution that calls for more drilling to deliver value.

- Effect of mining selectivity: More selective mining generally requires shorter drilling, but especially for some spatial continuity values between extremes. There is a well-marked minimum of DHS for every scenario, usually neighboring a very high APV value. On the very ends of spatial continuity (very short or too continuous), mining selectivity's role in determining the optimal DHS is significantly reduced.

Lastly, as regards profit sensitivity to DHS, depending on the geology, the spatial continuity, and the mining selectivity, the profit variations across different DHS can change substantially or not. In other words, different DHS can alter profits significantly, depending on the conditions mentioned

above. The sensitivity of profit across DHS is represented in our graphs as vertical bars with APV values. They inform how sensitive FP is across different DHS options. In general, APVs decrease on extremes of spatial continuity and peak at some point for intermediate values of continuity. Usually the peak is close to the scenario with minimum optimal DHS.

4.3.2 Nugget effect

The nugget effect of a mineral deposit expresses the variability at a very short distance. It is the pooling of microstructures and various error sources, not distinguishable at the sampling support, which is not punctual (Chiles & Delfiner, 2012). Nuggety ore deposits are common in the mining industry, especially for precious metals. The following assessment tries to capture the influence of varying nugget effect rates $C(0)\% : [0, 20, 40, 60, 80]$. Figure 4.5 communicates the results of the nugget effect assessment.

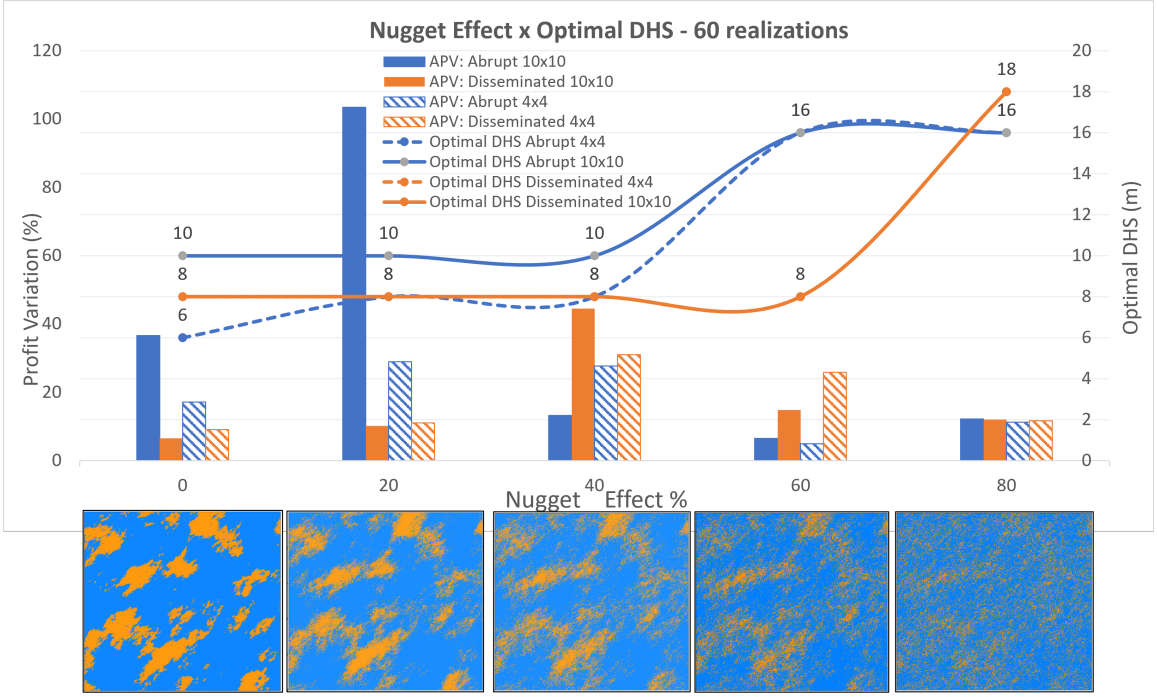

Figure 4.5: DHS results for nugget effect variations of the simulated deposit - lines: disseminated (orange), lines: abrupt (blue); line style: 10x10 selectivity (continuous), 4x4 selectivity (dashed).

The absence of short-scale variability in the deposit up to medium-variability (40%) meant no changes in optimal DHS for profit, except for one slight change in the selective abrupt case. No short-scale variability does not mean having to drill less, although different geologies demand unalike DHS. Increasing levels of the nugget effect lead optimal DHS to also increase due to the inefficiency of the drilling data to capture the shorter-scale variability. At the end of 80% of variability, the optimal DHS outcomes are almost as wide as they can be,because the scale of variability is too short for any DHS to help. Profit sensitivity to DHS changes is higher for intermediate to low rates of

nugget effect.

4.3.3 Ore price

Optimizing DHS for profit is an analysis of revenue minus costs. While infinite combinations of ore prices and cost sources could be considered, the issue can also be kept simple to assess only the most essential financial components: drilling cost, ore price, and cost of mining and processing. The following financial values were established in the application example as Figure 4.6 shows.

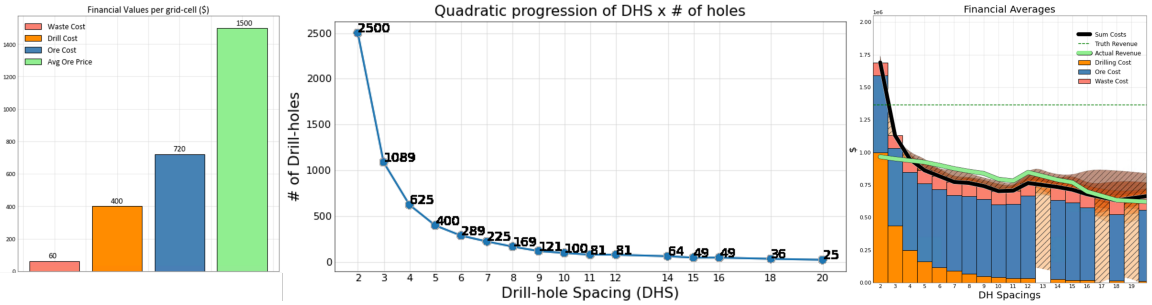

Figure 4.6: Individual financial values per grid-cell (left); Quadratic relation between DHS and number of drilling data (center); and an example plot of final financial compositions per DHS of a certain scenario (right).

The magnitudes of value between main costs and ore price for a mining cell of average ore grade (2.63) marginally pay for all the costs, leaving 19% as profit. A block with a cut-off grade (1.2) pays only for the ore cost, leaving the extra cost of drilling and waste as negative expenses to be paid by blocks of greater grade. Furthermore, costs are a quadratic function of DHS inverse because it is a 1D representation of a 2D grid of drill-holes, which means that any reduction in DHS results in quadratic consequences in drilling costs. Thus, as DHS reduces, the leading player for profit is drilling cost itself with its exponential increase while ore and waste costs do not alter much.

This financial behavior of components is essential to predict and understand optimal DHS outcomes. A greater ore price or a lower drilling price per unit might bring the same consequence: allowing more drills to be executed. For now, ore price is the only variable chosen to be varied in the light of directness, also because it is enough to outline the role of financial values in a DHS study.

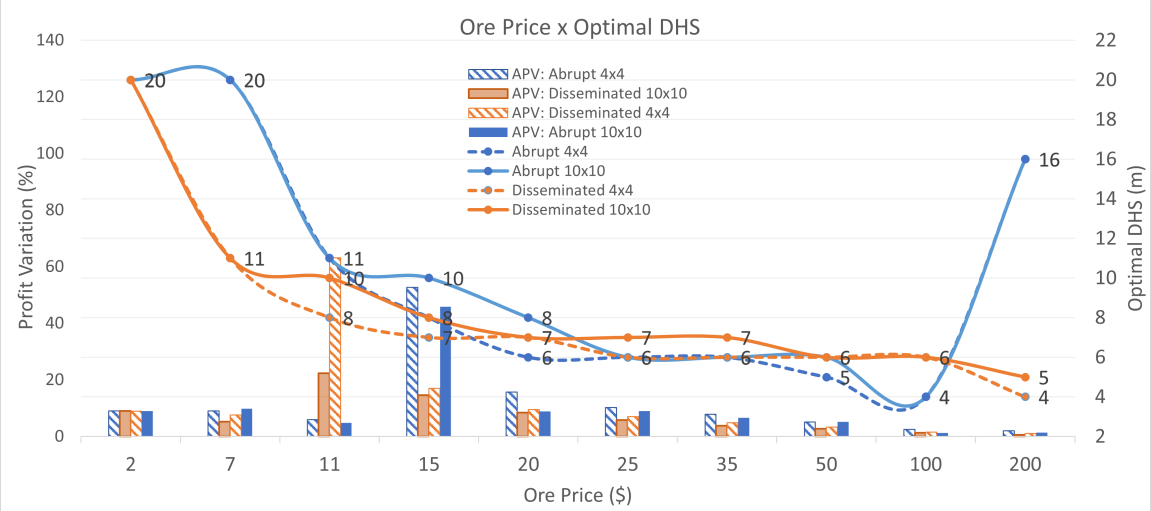

Figure 4.7: DHS results for systematic variations on ore price - line's color: disseminated (orange), abrupt (blue); line style: 10x10 selectivity (continuous), 4x4 selectivity (dashed); bars: APV.

The systematic variation of ore price generates interesting DHS results. The optimal DHS answer along the ore price axis has the shape of a wide valley. When applied to the extreme ranges of variability to both ends of ore price, the optimal DHS tends to increase to the widest available spacing. Although the valley shape is valid for all geology and selectivity scenarios, there are some distinctions between them.

As ore price decreases, all scenarios evolve from an intermediate DHS to the widest DHS available (20 m). As ore value is lost, the profitability of blocks with marginal grades is also progressively lost. That means they start being mined as waste instead of being sent to the plant, until all blocks are wasted due to the insignificant ore value. Then, drilling becomes unnecessary.

Inversely, as the ore price increases, the optimal DHS first decreases. Ore becomes increasingly valuable to pay for additional drilling that brings a financial return, maximizing ore extraction and minimizing dilution, which means substantial financial loss. However, as the price of ore keeps rising to large values, the DHS outcomes of the abrupt geology first reach its minimum spacing to then suddenly lift to a very wide DHS, where minimal drilling achieves the greatest return. For more complex geology as the disseminated, even excessively high ore prices lead to very short optimal DHS. The critical aspect probably lies on the very high values carried by the few extreme grades of the upper tail of the distribution. Those few blocks carry a lot of metal content and, thus, possess enormous financial value. Correctly mining those blocks sustains the very short DHS because processing the whole GC area as ore is still more costly than drilling and reducing excessive dilution.

Regarding selectivity, differences in DHS between both selectivities are usually present in scenarios where profit sensitivity is higher. Furthermore, more selective-mining scenarios demand shorter DHS than the less-selective ones. In other words, DHS follows selectivity in terms of dimensions.

4.3.4 Ore proportion

The ore proportion variation was done by applying transformations to the distribution of grade values while keeping the ore price fixed. Those transformations allow the financial margin of mining a block of a particular grade to remain stable throughout the assessment. Otherwise, the testing between ore price and ore proportion would risk being very similar. In the first case, the amount of ore does not change, although the financial margin of mining ore varies. The financial margin is stable in the latter, whereas the abundance of ore within the area changes.

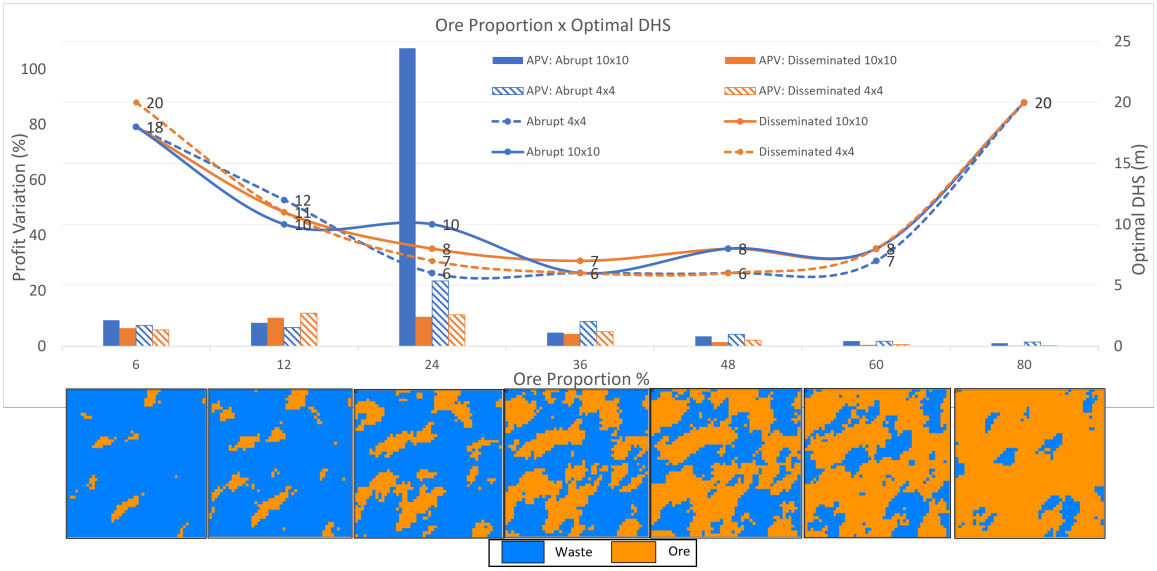

Figure 4.8: DHS results for systematic variations on ore proportion - Lines: disseminated (orange), abrupt (blue); continuous line: 10x10 selectivity, dashed line: 4x4 selectivity.

As the abundance of ore in the GC area reduces, the optimal DHS increases, meaning it is too costly to drill more to find a very strict amount of ore, which does not pay for the costs. As the ore proportion increases, the optimal DHS draws a parabola-shaped curve, where for mid-proportions of ore, shorter DHS is required. If the proportion of ore is excessively high, the DHS goes to the maximum since rather to mine it all as ore and have no useless expenses on drilling. No significant contrasts exist between geology types and mining selectivity when ore proportion is varied. The usual pattern is maintained that lower selectivity usually calls for slightly lower DHS.

4.3.5 Sampling errors

Sampling errors in mining diminish the profitability of operations in many ways. However, the question the following assessment seeks to answer is whether sampling errors affect the decision of optimal DHS in the GC stage. Three types of sampling errors are considered and applied to the sampled data: unbiased, positively-biased, and negatively-biased. The results are informed by Figure 4.9 next.

(a) DHS results for unbiased sampling errors.

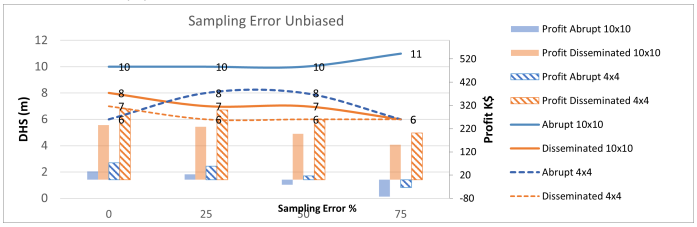

(b) DHS results for positively-biased sampling errors

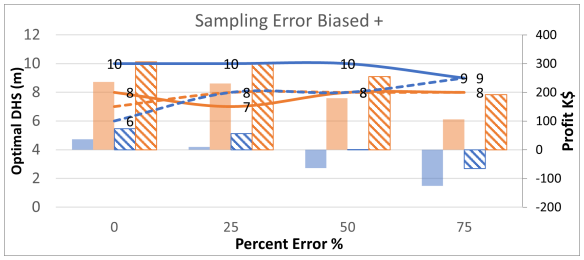

(c) DHS results for negatively-biased sampling errors

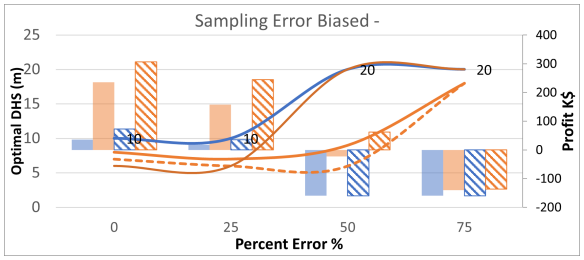

Figure 4.9: DHS results for systematic variations on sampling errors - line color: disseminated (orange), abrupt (blue); line style: 10x10 selectivity (continuous), 4x4 selectivity (dashed).

As shown in Figure 4.9, sampling errors are not likely to cause significant changes in optimal DHS decisions, given that most variations are minor. Out of the three possible errors, the unbiased ones are the less harmful to profit and the less prone to alter DHS decisions. Although minor, distinct variation patterns in DHS outcomes are seen: the disseminated type shortens DHS as unbiased errors increase while the abrupt type behaves oppositely.

The positively-biased errors are not significantly damaging to profit and do not change DHS decisions as much as the negatively-biased errors. For the abrupt case, negatively-biased errors of very high magnitude (50%) might lead to the widest DHS available (which means the samples do no help) because all samples will inform waste regardless. For the disseminated case, sampling errors seem to be more forgiving: increased negatively-biased errors might be mitigated by shorter DHS. Even though for more significant errors, the tendency is DHS to increase to avoid costs for no-value added by samples.

4.4 Discussions

4.4.1 Maximum profit and other maximums

The optimization of profit through DHS does not mean that other important mining elements are maximized as well. Elements such as ore tonnage, feed grade, dilution, and TEE could go along and be optimized with profit maximization for some cases, but not necessarily. In Figure 4.10, the results from one scenario in the systematic study are explored: 25m of spatial continuity (the scheme's base-case). Each of those elements' outputs is displayed along DHS options. Highlighted is the value that maximizes profit and the actual outcome for that element.

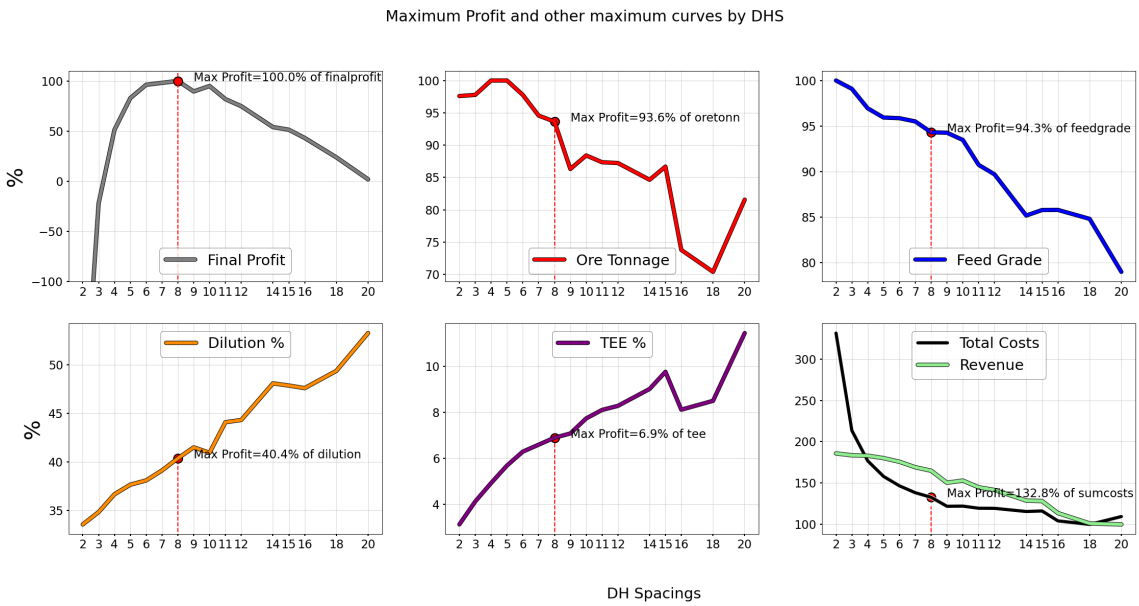

Figure 4.10: Maximums within curves of profit and other common mining elements: ore tonnage, feed grade, dilution, TEE and total costs.

Figure 4.10 exhibits the curves of standardized average values achieved across DHS for six different aspects in one of the scenarios (specifically: disseminated geology, 10x10m selectivity, 25m of spatial continuity). Clearly, optimization does not happen concomitantly between outputs. While maximum profit is reached by DHS of 8m, ore tonnage peaks at DHS of 4m. Feed grade, TEE, and dilution are all optimized at the shortest DHS of 2m, which is far from financially optimal. From that perspective, it is sustainable that having profit as the primary metric for optimization is justifiable due to it incorporating all the others, assuring a safe economic decision.

4.4.2 DHS sensitivity to elements - partial dependencies analysis

The optimal DHS and profit are consequences of the combined effect between elements like spatial continuity, mining selectivity, and others. However, is it possible to quantify each element's influence on optimal DHS decisions? An attempt at individual relevance quantification is elaborated using the Coefficient of Variation (CV) of the optimal DHS outcomes grouped per element. The mathematical formulation for reaching each element's influence (dependency) on DHS follows next:

$$\text{Dependency} = \frac{CV}{\%I} \tag{4.3}$$

where CV equals $CV = \frac{\sigma}{\mu}$ and $\%I = \%$ input range.

So, for each group of runs, divided per element, CV is calculated to be then divided by the % input range tested in that element. A total of 188 DHS optimization runs have been computed for the study. Standardizing CV values by the % input range is deemed mandatory, so DHS variations are brought to the scale of how much has been varied for that element. For example, the nugget

effect has been tested up to 80%, while spatial continuity only until 50% (50m range within a 100m-long area). Thus, treating DHS outcomes variability on the same basis for both elements would be unreasonable.

The above-mentioned calculations led to the following tabled results:

Table 4.2: Summary of numeric values sustaining the partial dependencies analysis of each element.

Element	Min input	Max input	Min possible	Max possible	% Input range	Average DHS	CV	# of runs	CV/% input
Mining selectivity (m)	4	10	4	20	38%	9.67	0.43	94	1.14
Geology	-	-	-	-	50% *	9.67	0.45	94	0.91
Spatial continuity (m)	2	50	0	100	49%	10.14	0.42	36	0.87
Ore price ($)	2	200	2	300	66%	8.9	0.51	56	0.76
Ore proportion (%)	6	80	6	100	79%	11.2	0.48	28	0.61
Sampling errors (%)	0	75	0	100	75%	9.27	0.44	48	0.58
Nugget effect (%)	0	80	0	100	80%	9.85	0.40	20	0.50

*: Given the subjectivity of geological distributions' nature, a percentual of 50% input possibilities have been assumed.

The $\frac{CV}{\%I}$ is then considered a fair statistical representation of the element's relevance to influence DHS. This statistical metric is then referred to as dependency. The Table 4.2 is aimed at showing how dependency is calculated for each element. The values of CV show very stable results between 0.4 and 0.5 for all elements, which reinforces that variability across all groups is not very disparate. The standardization of CV by % input range is quite determinant for precising the element's relevance. Hence, it is not by chance that exactly the element with the smallest % input range is the one with the greatest relevance: mining selectivity.

The dependencies values are plotted in a tornado chart (Figure 4.11) to facilitate sorted visualization of relevances per element:

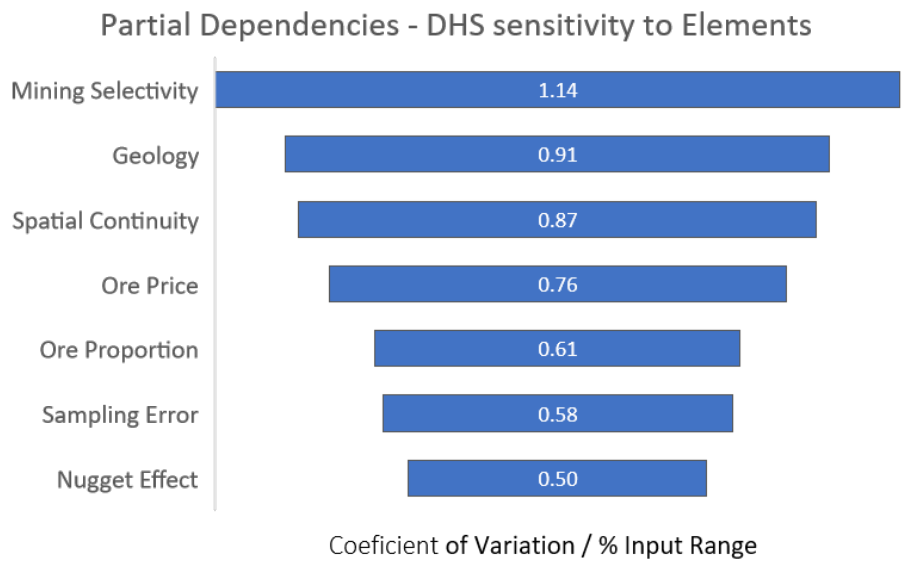

Figure 4.11: Sorted partial dependencies of DHS to elements, informed through the standardized CV of runs for each of them.

The tornado chart in Figure 4.11 shows that dependencies are quite close in magnitude, meaning that, although there are differences in DHS sensitivity, they are not discrepant. By putting aside subtle variations from the chart, two main groups can be distinguished with respect to DHS's sensitivity to them.

- Greatest influencers of DHS: Mining selectivity, geology, and spatial continuity. Those three elements stand out as the ones to which DHS is most sensitive.
- Least influencers of DHS: Ore proportion, sampling error, and nugget effect. In fact, the variations applied to those elements are mostly not seen in reality, such as 50% of sampling errors or 80% of the nugget effect.

Ore price lies between both groups, which has an intermediate influence on optimal DHS decisions for profit. Thus, ore price is controlled by the economy's dynamics, which is subject to unpredictable changes.

4.4.3 Profit sensitivity to DHS

Studying optimal DHS changes over many scenarios naturally raises a second question: *'How important the optimal DHS is for profitability?'*. Alternatively, put in other words, *'how sensitive is profit to the DHS?'*. To what extent changes in DHS affect profits is investigated. For some situations, changing DHS considerably affects profit, and for others, the change of DHS means little variation in financial results. The metric APV has been designed to support the understanding of

profit sensitivity to DHS. It informs profit values oscillation across the most relevant DHS options. A high APV means changing DHS for that scenario will imply significant profit changes.

By choosing specific scenarios of distinct APVs within the assessment graphs and looking into its profit curves, the profit sensitivity to DHS can be actually visualized. The profit sensitivity to DHS is shown in Figure 4.12:

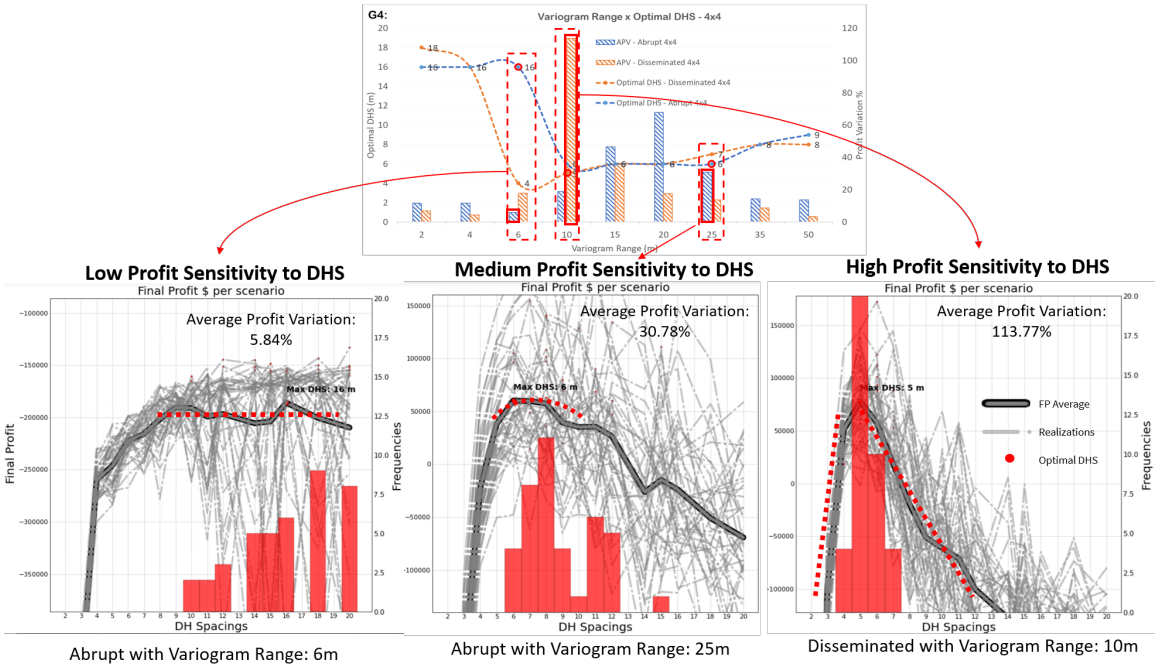

Figure 4.12: Scenarios of divergent profit sensitivity to DHS, within the spatial continuity assessment.

Using the spatial continuity assessment as an example, three contrasting scenarios of profit sensitivity to DHS are chosen, and their profit curves are shown in Figure 4.12. The curves visually explain the sensitivity itself. The profit graphs on the bottom show the average profit line (thick gray line) along with red bars of frequencies that each specific DHS reached a maximum profit across the forty realizations.

When APV is low, the profit curves are flatter, suggesting that varying DHS will not alter profit much. Whereas for high APVs, the profit curves are steep, where aside from one or two options of DHS, all the others will greatly diminish profit results. Thus, finding the optimal DHS is especially critical for profit in scenarios of high APVs. Even though what drives profit sensitivity to DHS is still obscure at this research stage.

4.4.4 Drivers of profit sensitivity to DHS

The profit sensitivity to DHS is variable, as seen in Figure 4.12. To understand what factors primarily drive profit sensitivity to DHS, the entire dataset of DHS optimizations is analyzed in terms of input's correlations to the output of interest: *APV*. The higher the correlation between

the input variable and APV, the higher its influence on profit sensitivity is deemed. The dataset of optimal DHS runs is plotted in figure 4.13 below as horizontal bars, with inputs (yellow bars) and output (blue bars).

(a) All databases of DHS optimizations lined-up, conveying most of the elements (yellow) and outputs (blue).

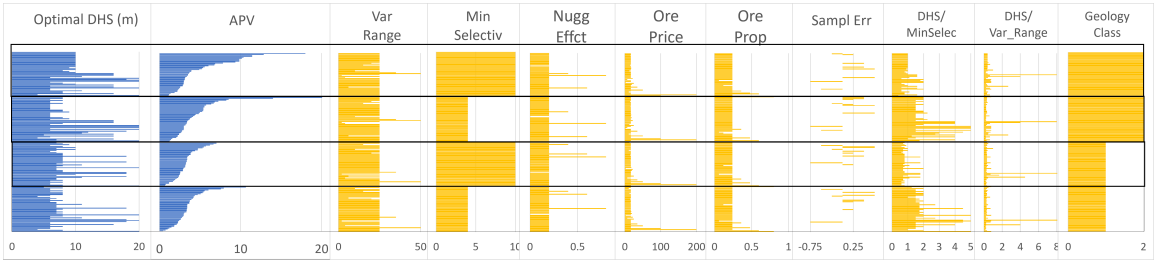

(b) All database of DHS optimizations lined-up, sorted by descending profit sensitivity.

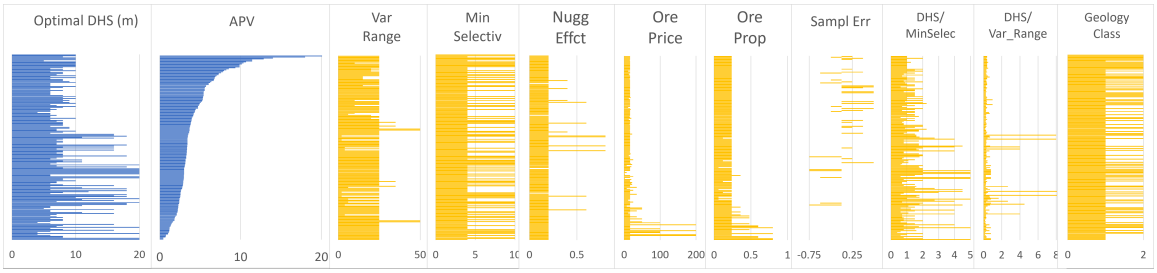

Figure 4.13: All DHS runs on y axis and the values of inputs (yellow) and outputs (blue) sorted by geology and mining selectivity (top) and by APV (bottom).

Thought-provoking trends can be perceived from the series of combined values shown above. Figure 4.13a is jointly sorted by geology and mining selectivity, the leading factors of the DHS study. In it, for every sub-set of the four combinations between geology-mining selectivity, we have a full spectrum of APVs. On all those sub-sets, intermediate values of ore price and ore proportion are associated with high-profit sensitivity. Looking at figure 4.13b on the bottom, where the same data is sorted descendingly by APV, it is easier to detect the inverse tendency between optimal DHS and APV. Wider DHS solutions usually mean less profit sensitivity to DHS decisions. Additionaly, larger sampling errors lead to higher APV. Also, lower ratios of *DHS* /mining selectivity are linked to greater sensitivity. Even more, the abrupt geology is more connected to higher profit sensitivity.

Those interpretations can be confirmed by the correlation between elements and APV, as seen in Figure 4.14:

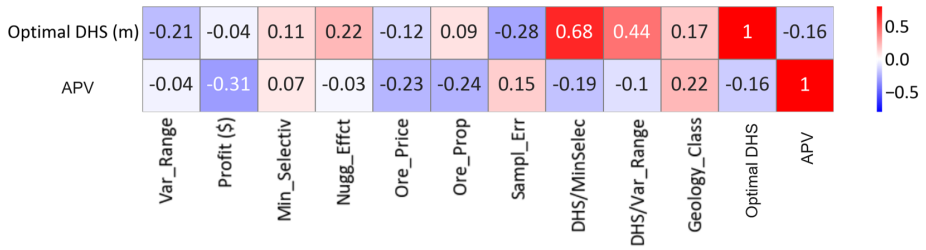

Figure 4.14: Correlation values between optimal DHS and APV with elements of input.

Figure 4.14 show the correlation values from the outputs APV and optimal DHS with several inputs. The correlation values are not high, although patterns from Figure 4.13 are confirmed, such as negative correlations of APV with ore proportion, ore price, and optimal DHS. Whereas positive correlations of APV with abrupt geology and sampling errors.

4.4.5 Univariate variations in a multi-dimensional space

Table 4.1 counts the number of values assessed per element, resulting in 50,400 unique scenarios possibly being tested for optimal DHS. Our current research has produced 188 optimal DHS assessments out of 50,400. Drawing general conclusions based on the current number of runs may be dangerous. A base case of values has been established, and the elements were changed one at a time to verify the optimal DHS changes. Further testing of elements variations with that dataset or with others might reinforce or not the patterns observed in this study.

Chapter 5

Case Study - Applying the DHS Optimizations to a Real Cu-Mo deposit

5.1 Introduction

The two DHS optimization methods for profit in GC context (regular and nested) are applied to blast-hole (BH) samples from a real copper-molybdenum deposit. SGS realizations conditional to the dense BH data are used to represent the unknown true version of the deposit. The geostatistical approach to jointly model the bivariate case study uses equivalent grades of copper (Cu). The required operational and economic parameters to run the optimizations for profit are based on the deposit's most recent public disclosure of mineral resources and reserves. The results from each method, which are aimed at dedicated drilling systems, are compared in different forms, findings are discussed, and pros and cons are assessed. The nested DHS methodology can increase profitability, yet the magnitude of earnings depends largely on the drilling cost relative to the deposit's operational costs and geological characteristics.

5.2 The dataset

The data consists of blast-hole (BH) samples from a copper-molybdenum deposit. The data available comprehends 7,752 samples 15m long, distributed within four different portions of the open-pit mine. Each data group has between three and six benches sampled (Figure 5.1). The samples have two variables of interest to be considered in this work: molybdenum (Mo, in ppm units) and total copper (Cu, in %).

The dataset's geological setting is here not exposed in order to remain confidential. However, mineralization controls and the geological context of the dataset have been explored and taken into account. Geological understanding usually assists in many ways throughout a geostatistical study, like domaining, determining preferential continuity directions in variography, and determining which modeling strategies to adopt.

5.2.1 Exploratory data analysis

The BH data spacing, Mo and Cu grade's uni- and bi-variate statistics are explored. Perspective 3-D views and vertical cross-section of BHs are shown in Figure 5.1.

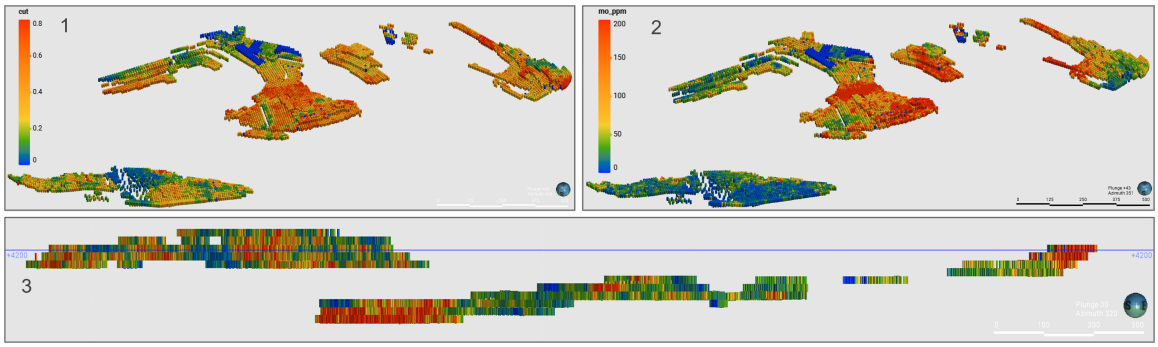

Figure 5.1: BH data spatial configuration in three different views: 1) Perspective of Cu; 2) Perspective of Mo grades, 3) and vertical view, showing the number of benches per group.

Spatial distributions of Cu and Mo are similar but not always coincident in the sampled data (Figure 5.1), where high and low values' concentrations of each element are occasionally not following the other's pattern. The available BH data is fragmented in space and disconnected from each other in four main cohesive groups. The BH data is then spatially divided into those four groups based on their contiguous configuration within the pit (Figure 5.2).

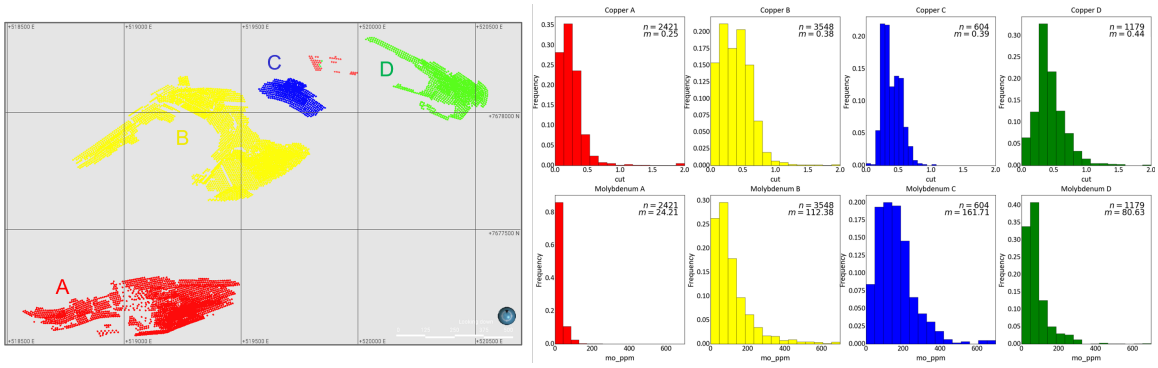

(a) Plan view of BH groups (left side); histograms of distributions of Mo and Cu per group (right side).

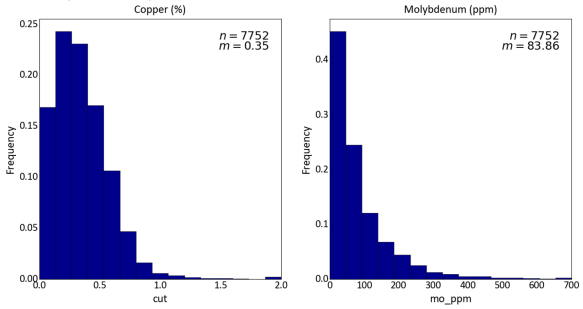

(b) Histogram of BH samples for both variables accounting for all groups together: Mo and Cu.

Figure 5.2: Visual division of BH groups and their histograms for both variables.

Variables Mo and Cu exhibit positively skewed distributions of grades, having Mo a longer tail of high values. Group A possesses notably smaller concentration values than the other groups for both elements. The bivariate statistic between both variables of interest is investigated (Figure 5.3). The correlation coefficient ρ measures the linear relationship between variables, while ρ_s measures

the rank correlation coefficient, which is less sensitive to extreme pairs and more suitable to detect monotonic relationships (Isaaks & Srivastava, 1989).

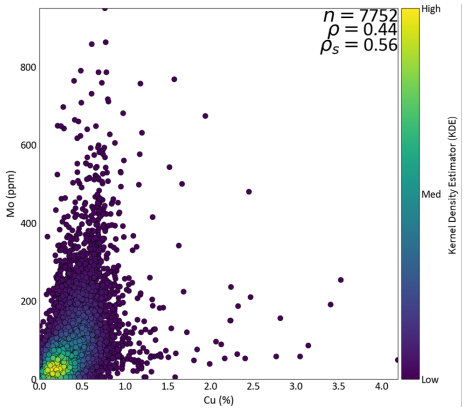

Figure 5.3: Scatter-plot displaying correlation between Mo and Cu grades in BH samples.

The bivariate relationship of Mo and Cu is monotonic, having ρ a lower value than ρ_s, indicating a linear component, although with significant dispersion of values. As shown by the correlation, Mo and Cu mineralizations share similar patterns to some extent, even though their spatial behavior is not always coincident since anomalous concentrations also occur separately, as seen in the map from Figure 5.1 and in the scatterplot from Figure 5.3. The reason for their spatial dissimilarities could be related to subtle different spatial continuity directions (Figure 5.5) or driven by different host rocks or alteration types.

A histogram of the existing data spacing for each group helps inform the presence of clustered sampling (which would require declustering for representative distributions) and assists in determining optimal lag for calculating the variogram's experimental points. The BH's configuration is regularly spaced, as shown by Figure 5.4 below.

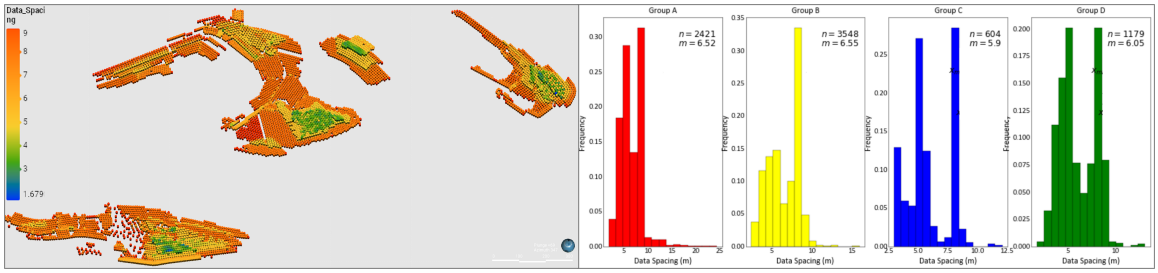

Figure 5.4: Spacing between BHs plotted as map (left-side) and histograms per group.

BH spacings are quite constant across all the groups on the horizontal plane, averaging around 6.5 meters (considering the three nearest samples). The sampling interval with the highest frequency is approximately 8m (histograms from Figure 5.4). Top benches display shorter spacing, especially due to overlapping samples along the vertical direction (probably owing to undercuts).

5.2.2 Joint modeling technique

The decision of which multivariate modeling technique to adopt to simulate and estimate the deposit depends on factors such as financial values and spatial continuity orientations. In relation to financial values, the selling prices and metallurgical recoveries considered for the study are based on recent public disclosures:

$$Cu \text{ Price: } s_{cu} = 3.0\$/lb, \text{ Recovery: } r_{cu} = 85\%$$

and

$$Mo \text{ Price: } s_{mo} = 10.0\$/lb, \text{ Recovery: } r_{mo} = 74\%$$

which implies that at average grades, the financial value of each element is:

$$\text{Revenue}_{cu} = g_{cu} * r_{cu} * s_{cu} = 0.30\%(*22.04) * 0.85 * 3.0lb/t = 16.86\$/t$$

$$\text{Revenue}_{mo} = g_{mo} * r_{mo} * s_{mo} = 83.86ppm(*10^{-3} * 22.04) * 0.74 * 10.0lb/t = 1.36\$/t$$

Thus, Cu constitutes the main element of interest, speaking for **92%** of the revenue on average, and Mo holds **8%**. This major financial value of Cu in relation to Mo can be referred as hierarchical due to Mo's minor secondary value significance. The element's individual spatial continuities are verified and exhibited in Figure 5.5.

(a) BH variogram maps for Cu. Maximum continuity directions are highlighted as black arrows.

(b) BH variogram maps for Mo. Maximum continuity directions are highlighted as black arrows.

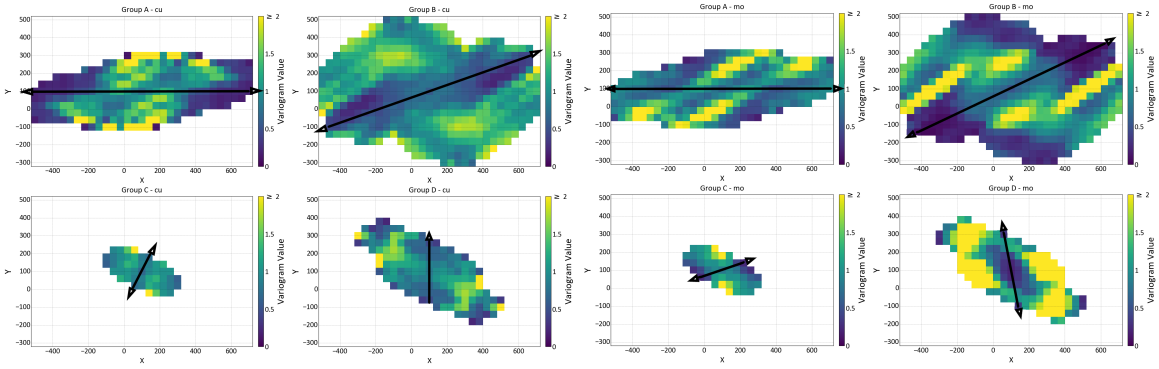

(c) BH Experimental points and variogram model of Cu.

(d) BH Experimental points and variogram model of Mo.

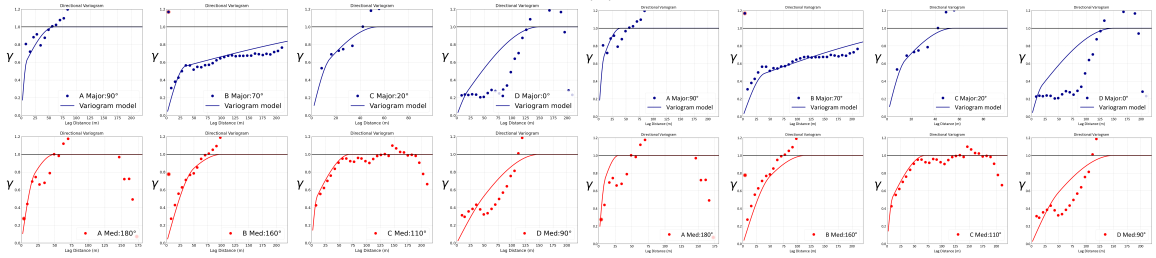

Figure 5.5: Variogram maps, experimental points and models for Cu and Mo from BH data.

The variogram maps and the modeled variograms for each group are similar. Subtle changes in experimental points and preferential direction of anisotropy are identifiable. Main continuities

are oriented towards east, north, or northeast, having great consistency between directions of both elements for the same group of BH. Experimental points show clear structures, with few or no indications of noise, that is, sampling errors.

Aside from group B, anisotropy is not strong in any of the groups, which is more continuous along the northeastern direction. Therefore, beyond having good correlation and hierarchical order of financial significance, both elements also share similar spatial continuity. Given that evidence, the grades will be combined as *equivalent grades* of Cu, as established by the equation:

$$G_{cu_{eq}} = g_{cu} + \frac{(s_{mo} * g_{mo} * r_{mo})}{s_{cu} * r_{cu}} \tag{5.1}$$

where g_{cu}, s_{cu}, r_{cu} respectively refer to Cu's grade, selling price, and metallurgical recovery; and s_{mo}, g_{mo}, r_{mo} mean Mo's price, grade and recovery, respectively.

Equivalent grade modeling requires allowance from a geostatistical perspective (similar spatial continuities and reasonable correlation) but are also motivated by financial reasons (strong hierarchical order of values). As seen, Cu and Mo possess similar spatial continuities and strong hierarchical financial values to encourage equivalent grade adoption. In the resultant cu_{eq} variable, the Cu component has a much stronger influence on the final variable, whereas Mo should only control more of the variable response in areas of anomalous high Mo. The spatial and statistical distribution of the resultant variable of interest cu_{eq} to be modeled is seen in Figure 5.6:

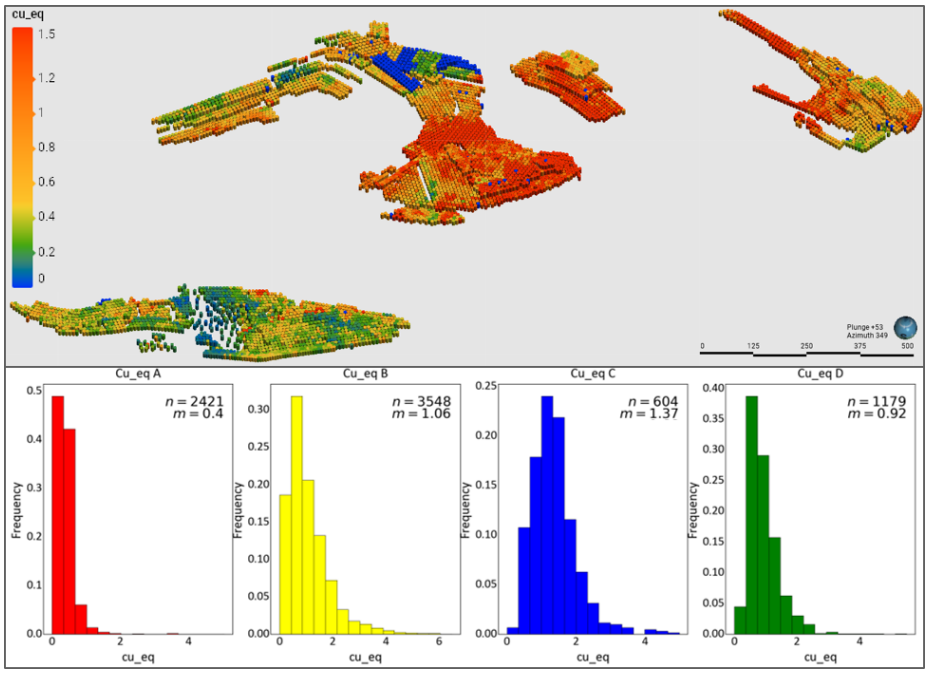

Figure 5.6: Visualization and statistical distribution of copper equivalent grades per group.

The spatial distribution of cu_{eq} resembles Cu, apart from the values being greater and the cu_{eq} distribution honoring the high-grade zones of molybdenum distinctively,e.g., in group C where Mo is high (Figure 5.6). The average grades seen in histograms from Figure 5.6 are substantially higher

than Cu (see histogram from Figure 5.2b).

5.2.3 Economic and operational parameters

The TF utilized in the Cu-Mo DHS optimization is the same as in previous chapters (see Equation 2.1). To optimize DHS for the Cu-Mo deposit, all economic and operational parameters have been retrieved from that operation's most recent public disclosure. The cost and operational parameters employed in the study case are revealed in Table 5.1:

Table 5.1: Table of operational and financial parameters based on the deposit's latest public mineral disclosure, to be used for the Cu-Mo DHS optimization.

Parameters required	**Value**	**Units**
Operational costs and values		
- Drilling cost	750	$/drill-hole
- Ore mining and processing cost	18.72	$/ton
- Mining cut depth	15	meters
- SMU dimensions	20x20x15	m
- Waste mining cost	3.37	$/ton
- Average density	2.48	g/cm³
- Copper recovery	85	%
- Molybdenum recovery	74	%
Economic values		
- cu_{eq} cut-off grade	0.33	%
- Copper selling price	3.0	$/lb
- Molybdenum selling price	10.0	$/lb

The economic and operational parameters do not change across both DHS methodologies. The metallurgical recoveries are assumed constant for any grade beyond or equal to the cut-off grade. For the case of misclassified ore-as-waste, that is, dilution sent to the plant, a penalty of -50% of recovery is applied since dilution is often expected to have poorer plant recovery due to many possible reasons.

5.3 Regular DHS optimization

The regular DHS methodology (aimed at optimizing regularly-spaced drilling) is applied to the BH dataset, using cu_{eq} as the variable of interest. The DHS workflow employed is the one described in Section 2.2. Next, the application of each step from the workflow is described.

5.3.1 Variography

The cu_{eq} grades have their spatial continuity assessed regarding preferential direction and ranges. The resulting variogram models serve as the spatial continuity models to run the BH data's conditional simulations.

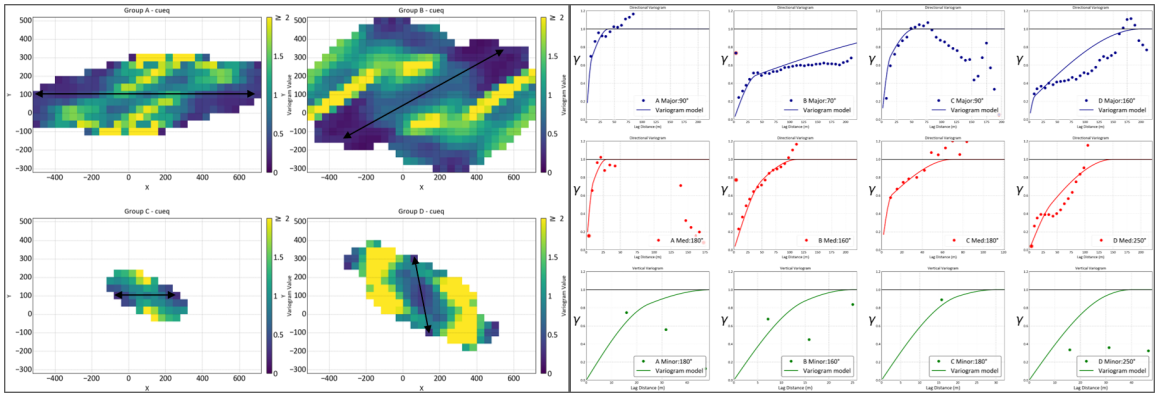

Figure 5.7: cu_{eq} grade's variogram maps, experimental points, and models to be used as the spatial continuity model for conditional simulations. Black arrows represent the maximum continuity directions.

The variogram models obtained are like the individual variable models. The anisotropy is usually weak (except for group B), as the variogram models have ratios close to 1:1 in most cases, and the ranges are relatively short, between 30m to 150m (aside from group B as well). The variogram model of group A is shown in the form of variogram equations (Equation 5.2) as an example, followed by a summary table (Table 5.2) containing all variogram model parameters across the four BH groups.

$$\begin{aligned}
\gamma_{max_A}(h) &= 0.0 + 0.5Sph_1(10m) + 0.5Sph_2(40\ m) \\
\gamma_{med_A}(h) &= 0.0 + 0.5Sph_1(10m) + 0.5Sph_2(30\ m) \\
\gamma_{vert_A}(h) &= 0.0 + 0.5Sph_1 1(25m) + 0.5Sph_2(50\ m)
\end{aligned} \tag{5.2}$$

Table 5.2: Variogram model summary per BH groups

Directions	Azimuth °	Nugget effect (%)	Str1 sill (%)	Str1 range (m)	Str2 sill (%)	Str2 range (m)
Group A						
- Maximum	90	0	0.5	10	0.5	40
- Medium	180	0	0.5	10	0.5	30
- Minimum	-90	0	0.5	25	0.5	50
Group B						
- Maximum direction	70	0	0.4	40	0.6	400
- Medium direction	160	0	0.4	50	0.6	115
- Minimum direction	-90	0	0.4	15	0.6	25
Group C						
- Maximum direction	90	0	0.5	15	0.5	55
- Medium direction	180	0	0.5	10	0.5	70
- Minimum direction	-90	0	0.5	20	0.5	30
Group D						
- Maximum direction	160	0	0.2	10	0.8	200
- Medium direction	250	0	0.2	40	0.8	150
- Minimum direction	-90	0	0.2	30	0.8	40

*Str= Structure; All structures are *spherical*.

As contained in Table 5.2, group B has much greater spatial continuity and strong anisotropy between maximum and medium directions than the other groups. Group B also carries the greatest area and number of BHs. The restricted spatial availability of BH of the other groups might contribute to limited spatial continuity.

5.3.2 Conditional simulations

One SGS realization is created per group conditional to the BH data, using cu_{eq} as the variable of interest. The decision of a single realization per group of data is based on some reasons:

- The high-density conditioning data at short-spacing (average spacing of 6m).
- The high number of data per group.
- Several benches per group serve a similar purpose as multiple realizations.

A dense and large dataset, available along several benches, might compensate for the need for many realizations to produce stable results. Realizations have a cell size of 2mx2mx15m, leading to large simulated models. The results from simulation are displayed in Figure 5.8, in the form of maps and histograms.

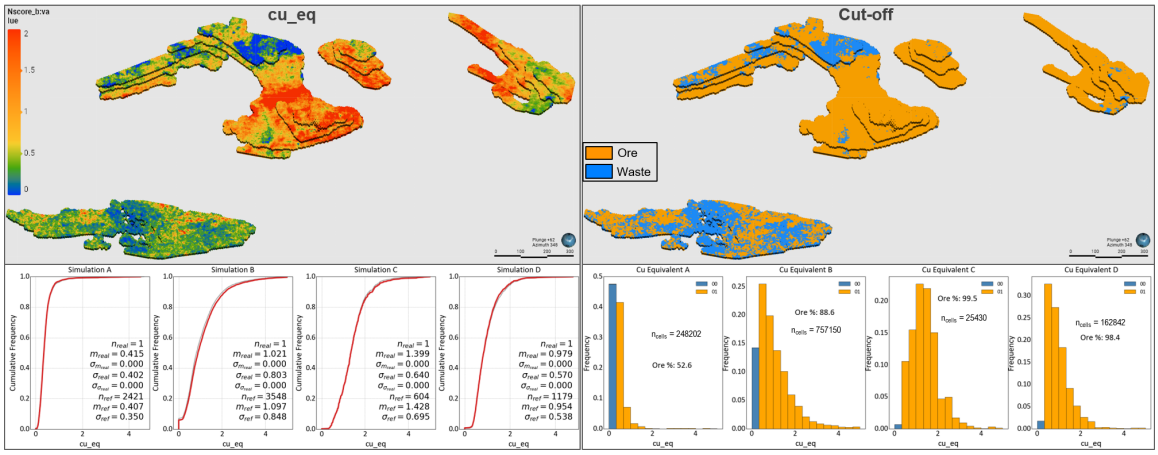

(a) Conditional simulations maps: cu_{eq} grades on top-left, O-W classes on top-right. Histogram validations on bottom-left, histogram with proportions on bottom-right.

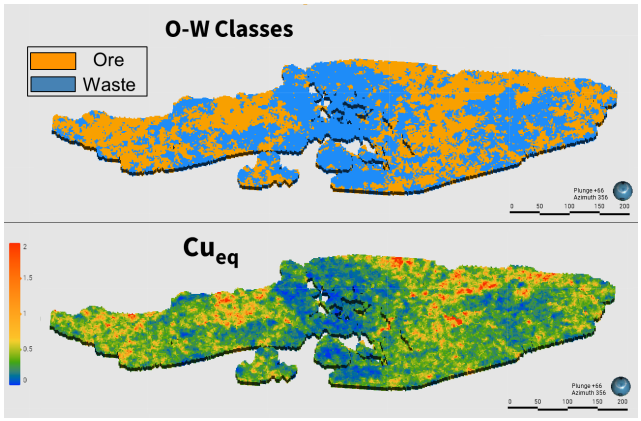

(b) Detailed view of simulated data group A: more scattered grades and lower ore proportion.

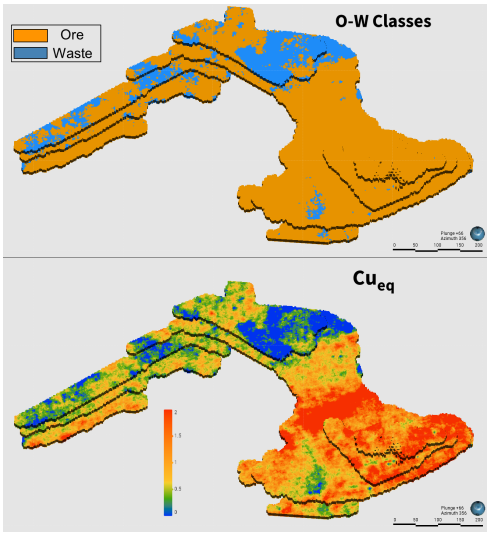

(c) Detailed view of simulated data group B: high continuity of grades and higher ore proportion.

Figure 5.8: Conditional simulations maps from cu_{eq} as grades and O-W classes, and histograms of CDFs and proportions.

The simulations adhere well to the conditioning data as informed by the validation cumulative histograms from Figure 5.8. The proportions of O-W per group are calculated using the cut-off grade ($cog_{cu_{eq}} = 0.3331$) and displayed along the histograms. Groups C and D of BHs are composed only of ore, while group A has approximately half of each, and group B has about 88% ore.

As in Section 4.3.4, the extremes (either excessive or absent) of ore proportion lead DHS optimizations for profit to minimize drilling since it is usually impossible to have the small pockets correctly estimated at reasonable costs. Therefore, for this case study, the DHS optimizations are performed only on groups A and B, considered the key areas for the DHS study. Groups C and D might not contribute to meaningful results of optimal DHS, given their absolute ore occurrence.

5.3.3 Re-sampling

The regular sampling consists of ten options, which are established as follows:

$$\textbf{Regular Samplings (m)} = [5, 8, 10, 12, 15, 18, 20, 22, 25, 30]. \tag{5.3}$$

The drilling option represents final GC drilling, and a wider range of options is provided to have an FP curve well delineated where both ends are expected to perform worse than the intermediate spacings. An example of every option of regular sampling is seen next:

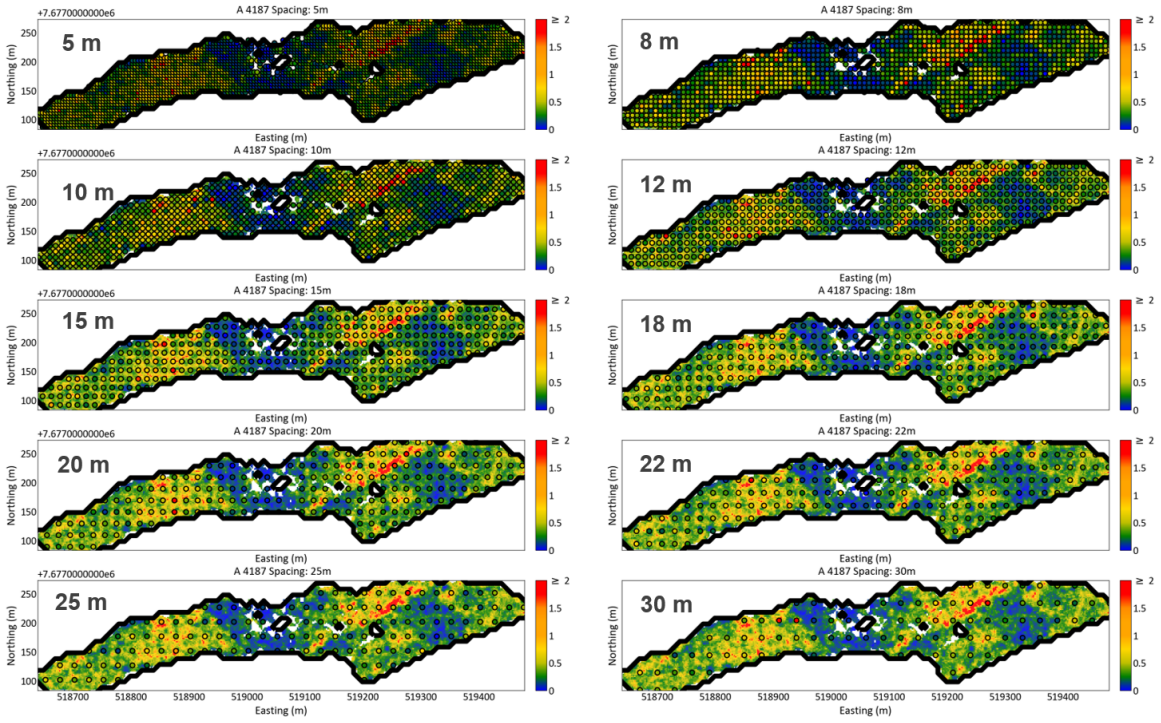

Figure 5.9: Example of regular sampling spacings collected from one of the benches, serving as an illustrative aid of the process.

The total number of sampled data in the first sampling is 10 spacings$*$18 benches = 180 datasets. Thus, it is required to fit a hundred and eighty variogram models to estimate the same number of grids. Given the high number, the autofitting variograms function will be utilized.

5.3.4 Auto-fit variography

The 180 datasets have variogram models auto-fit to their respective experimental points. Automated adjustments are made necessary in some spatial models, mainly on a few excessively continuous ranges, which are reduced to twice the range of the first structure. Models fit to the data can be observed in Figure 5.10.

(a) Main direction experimental variogram points and autofit models from BH groups A.

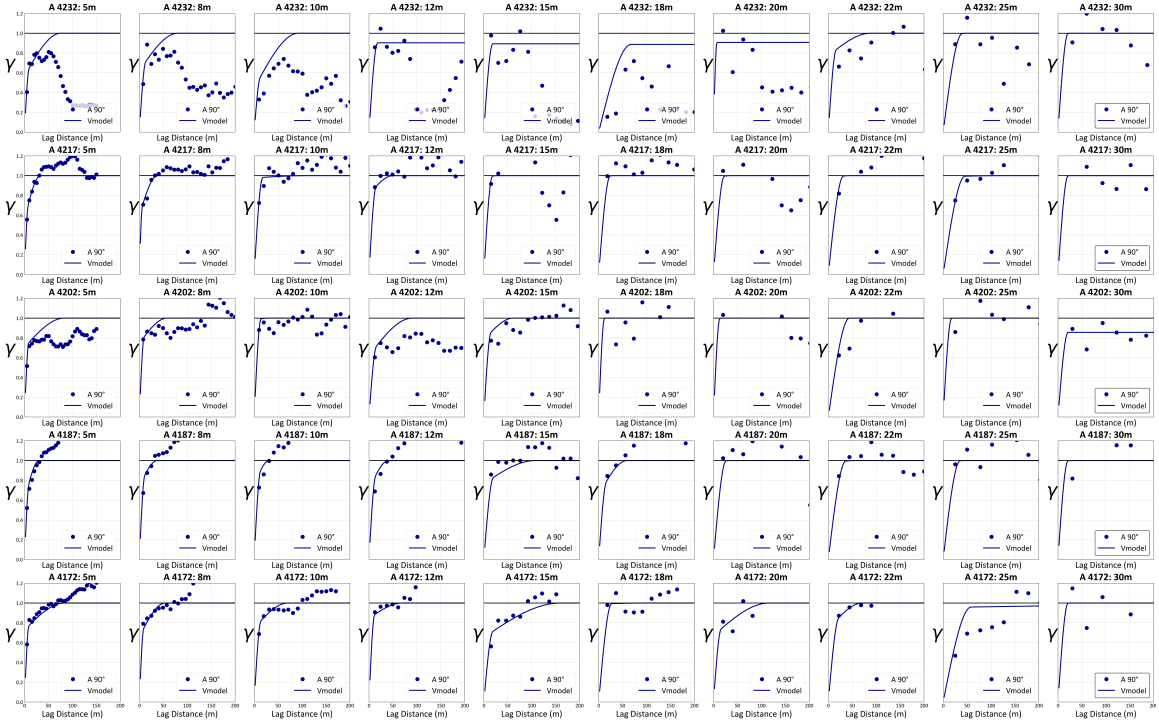

(b) Main direction experimental variogram points and autofit models - BH groups B.

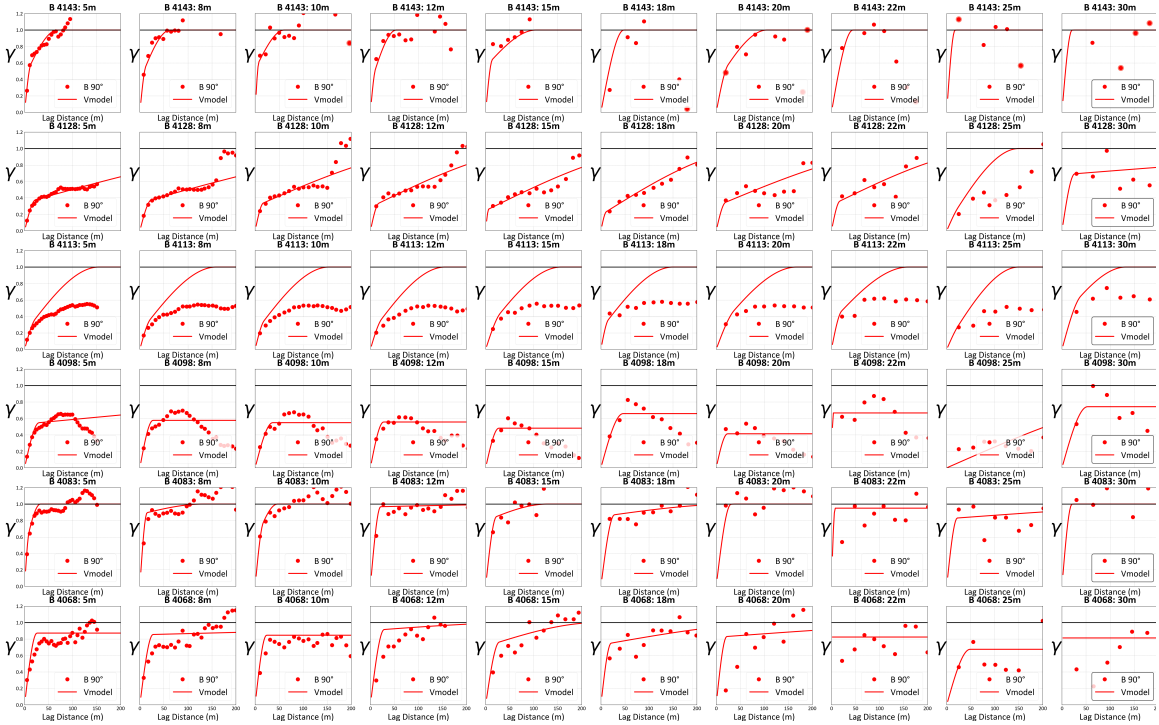

Figure 5.10: Main direction experimental variogram points and autofit models - BH groups A (top) and B (bottom). Benches vary along Y axis and regular DHS along X axis.

The continuities of variogram models do not exhibit any clear systematic trend as DHS varies. For data sets with well-behaved experimental points, most models fitted well. However, for a few

noisy experimental points, fitting is worse. Fittings have been post-processed to adjust extreme models. The auto-fit variograms are used as the models of spatial continuity in the OK estimations, which will produce the final estimated maps per DHS. Diversely from previous examples, different variogram models are calculated for each re-sampled DHS, allowing DHS optimizations to be affected by differing levels of information on spatial continuity.

5.3.5 Estimations

Each of the eighteen benches is estimated with OK ten times: one per DHS being assessed. The estimated maps for one example area are displayed in Figure 5.11 across every DHS as continuous cu_{eq} grades and as O-W classes.

(a) OK Estimated maps of bench A 4202 across all regular DHS.

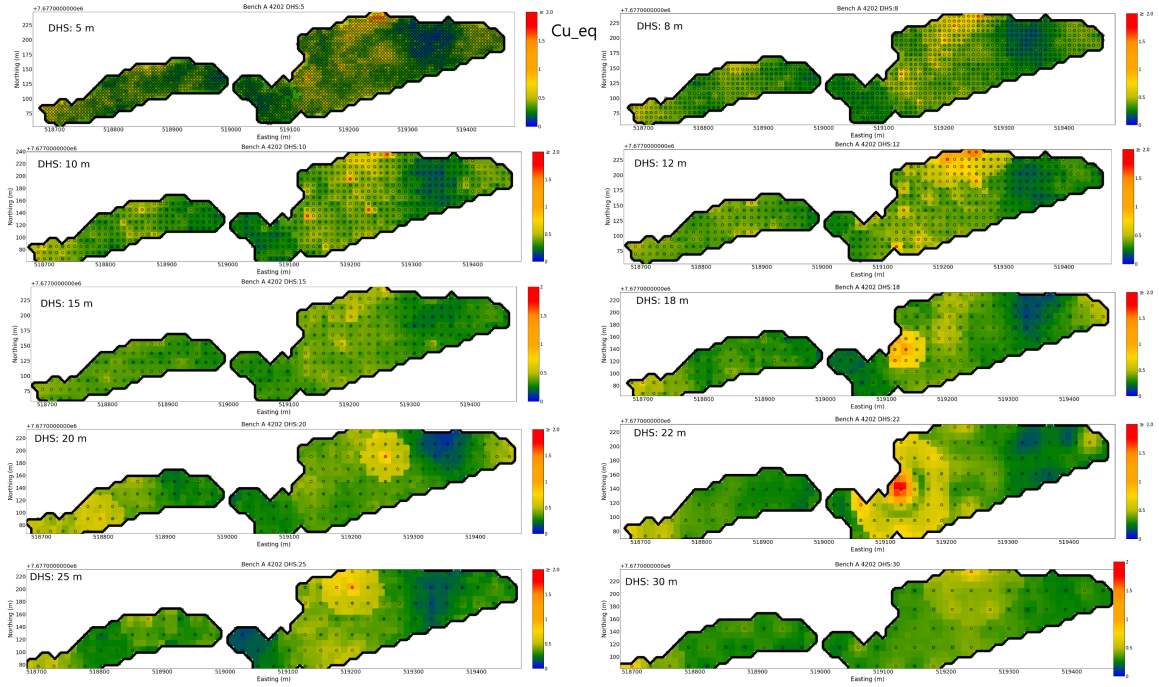

(b) O-W maps on grid-cells of 10mx10m on bench A 4202 across all regular DHS.

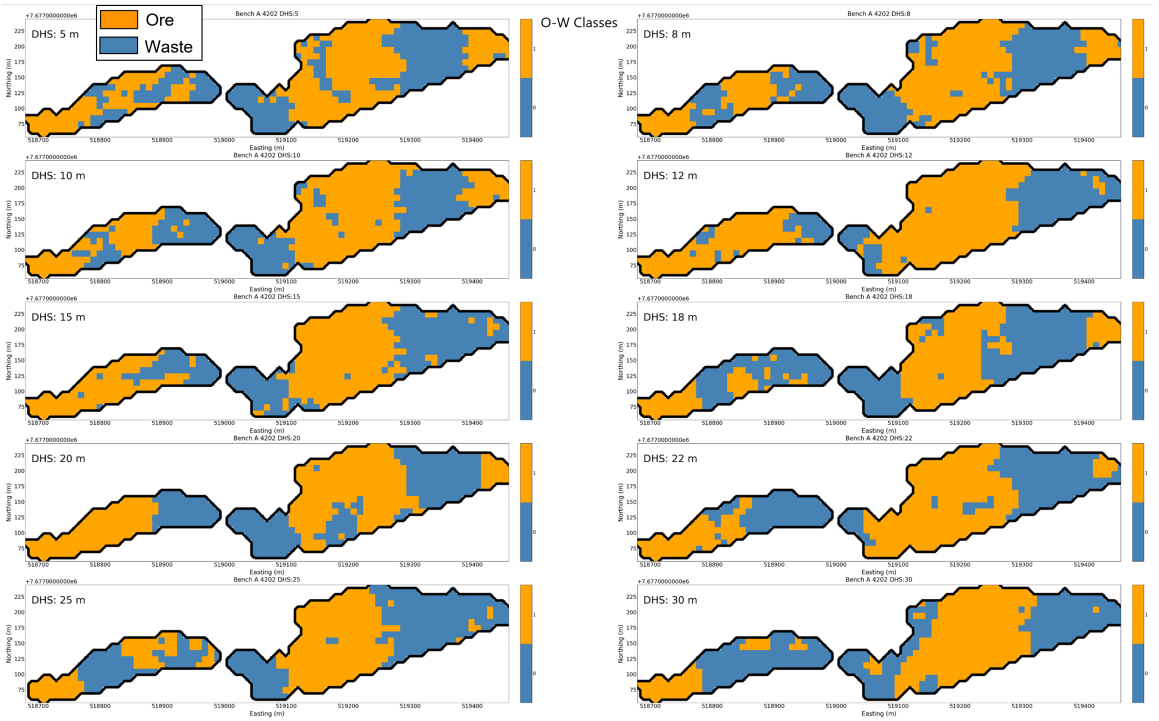

Figure 5.11: Estimated and O-W maps of bench A 4202 across all regular DHS being assessed.

The sequence of maps from Figure 5.11 shows that as the level of sampled data decreases, so does the resolution of grade estimates. The pattern in O-W distribution follows the estimated grades, where shorter DHS leads to more detailed O-W contours.

5.3.6 Mineable limits transformations and misclassification errors

Estimated products are processed to mineable limits by re-blocking of grid-cells into SMU scale, which is 20m x 20m x 15m for this example, as shown in Table 5.1. The metric TEE for estimation performance is also calculated for every scenario.

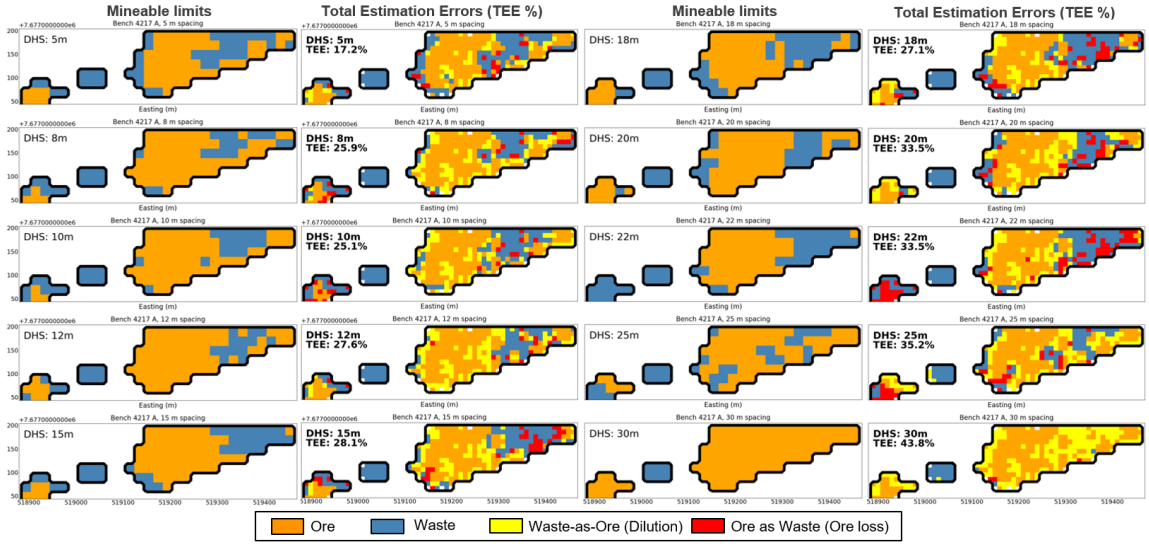

Figure 5.12: Mineable limits and misclassification errors maps across all spacings - example from bench A 4217.

For the set of classified maps plotted in Figure 5.12, TEE gradually increases together with DHS. This pattern was seen and discussed in the previous Chapters (see Figure 2.8 and Figure 3.5), also confirmed by the averages of all estimated scenarios (Figure 5.13a).

(a) Regular DHS vs TEE - a monotonic trend.

(b) Profit against TEE - a quadratic trend.

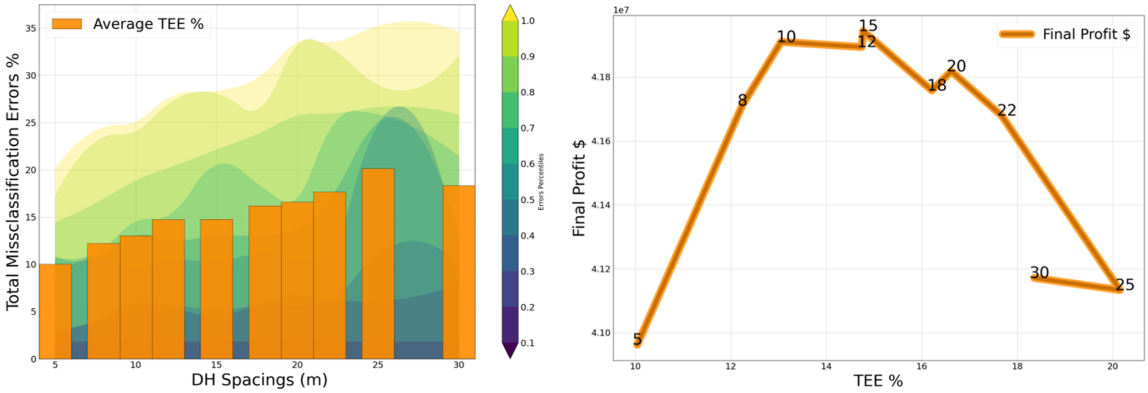

Figure 5.13: Trends between FP, TEE and regular spacing for the BH data's DHS optimization.

Figure 5.13a exhibits clear and expected positive monotonic relationship between TEE and DHS, where variables grow together but at an oscillating rate. On the other hand, FP's quadratic trend with TEE is exhibited in Figure 5.13b, peaking at an intermediate DHS of 15m. Those two trends within the case study results corroborate the synthetic data results from Chapters 2 and 3.

5.3.7 FP results

The FP results derived from the DHS optimizations are informed in Figure 5.14 in two ways: split by groups of BHs, since there are significant changes, and jointly between groups A and B.

(a) Final profit curves per BH groups. **(b)** Joint final profit curve of BH groups A and B.

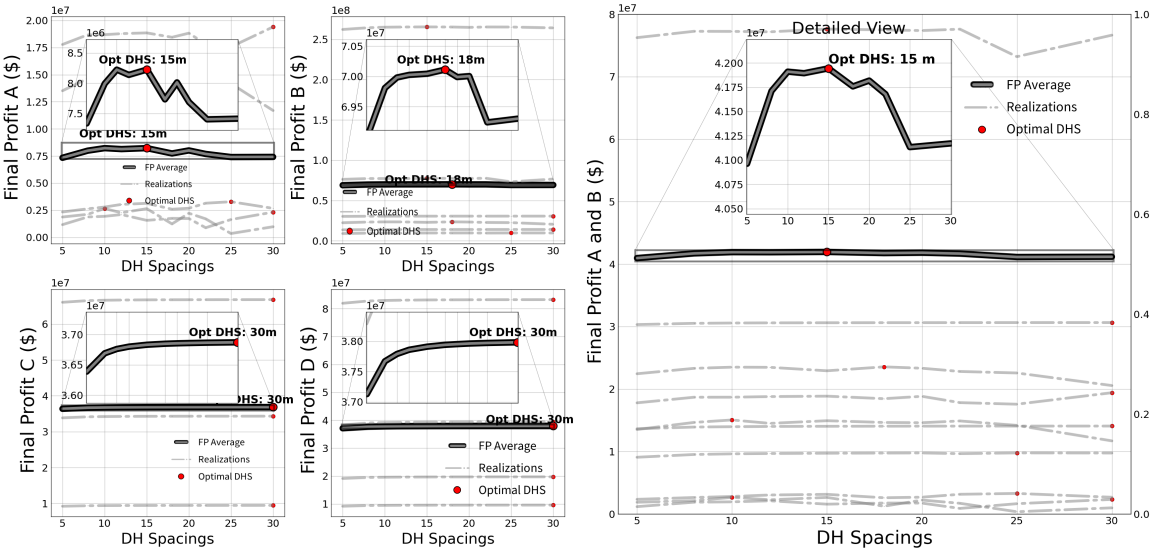

Figure 5.14: Final profit curves from regular DHS optimization on the BH data.

Maximum FP is found at different DHS options across the BH groups. Areas C and D, which contain exclusively ore, are optimized at the widest spacing tested (30m), while areas A and B are optimized similarly on intermediate DHS options. Areas A and B, which are deemed more suitable for DHS study (given their O-W proportions), have their results added up as a joint optimal DHS output, which would be DHS: 15m.

5.4 Nested DHS optimization

The nested DHS optimization targeted at O-W boundaries, described in Section 3.2, is applied to the Cu-Mo BH data, following the framework contained in Figure 3.1.

5.4.1 Buffering and re-sampling O-W boundaries

After having prior estimated models originated from the first phase of drilling (CS), the O-W boundaries from each model is buffered to generate the preferential O-W zones to accommodate the final samplings. Figure 5.15 shows an example of prior estimated GC areas being labeled as O-W classes.

(a) Prior estimations from CS=12m as Cu_{eq} grades.

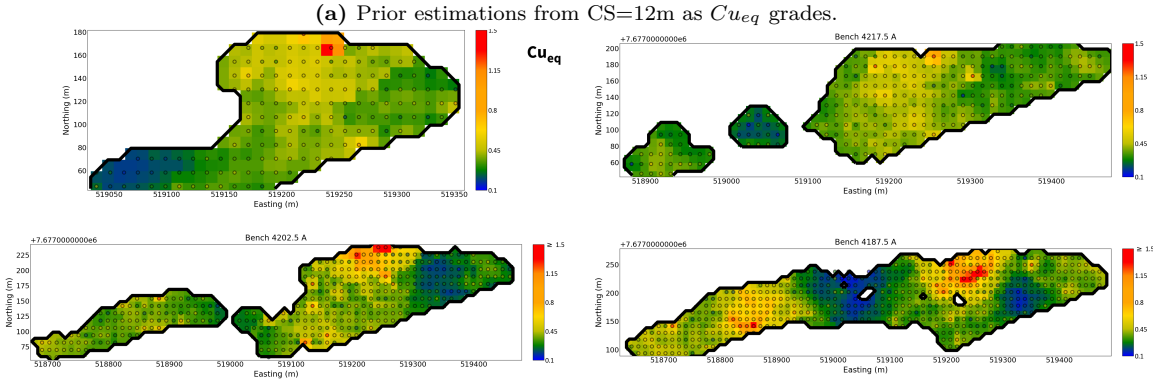

(b) Prior estimations from CS=12m as O-W classes, highlighting the O-W vertices which control the buffering of preferential zones for FS.

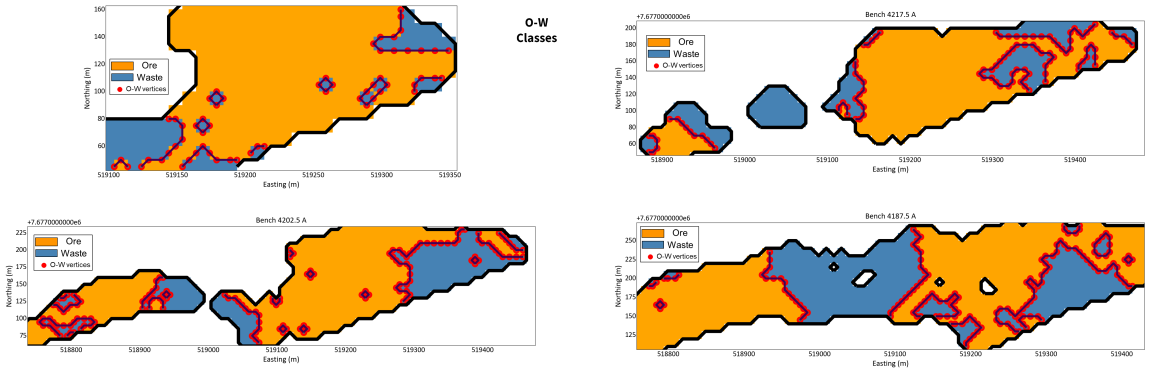

Figure 5.15: Prior estimations from CS=12m as *cu* grades (top) and as O-W classes (bottom) at benches from group A.

Figure 5.15 shows the prior estimated maps for CS: 12 m, where the O-W vertices are located and buffered into O-W zones. The buffer distance for this study has been set as equal to the FS to be sampled. The sampling spacings to be applied to the BH dataset are:

$$\textbf{Coarse Spacings - CS (m)} = [10, 12, 15, 18, 20, 22, 25]. \tag{5.4}$$

and

$$\textbf{Fine Spacings - FS (m)} = [6, 8, 10, 12, 15]. \tag{5.5}$$

The cleaning tolerance considered for eliminating redundant samples between CS and FS is $t = 4m$. FS are collected within the O-W zones, as shown in Figure 5.16.

(a) O-W buffering to generate target sampling zones in GC stage.

(b) Fine samplings in O-W zones.

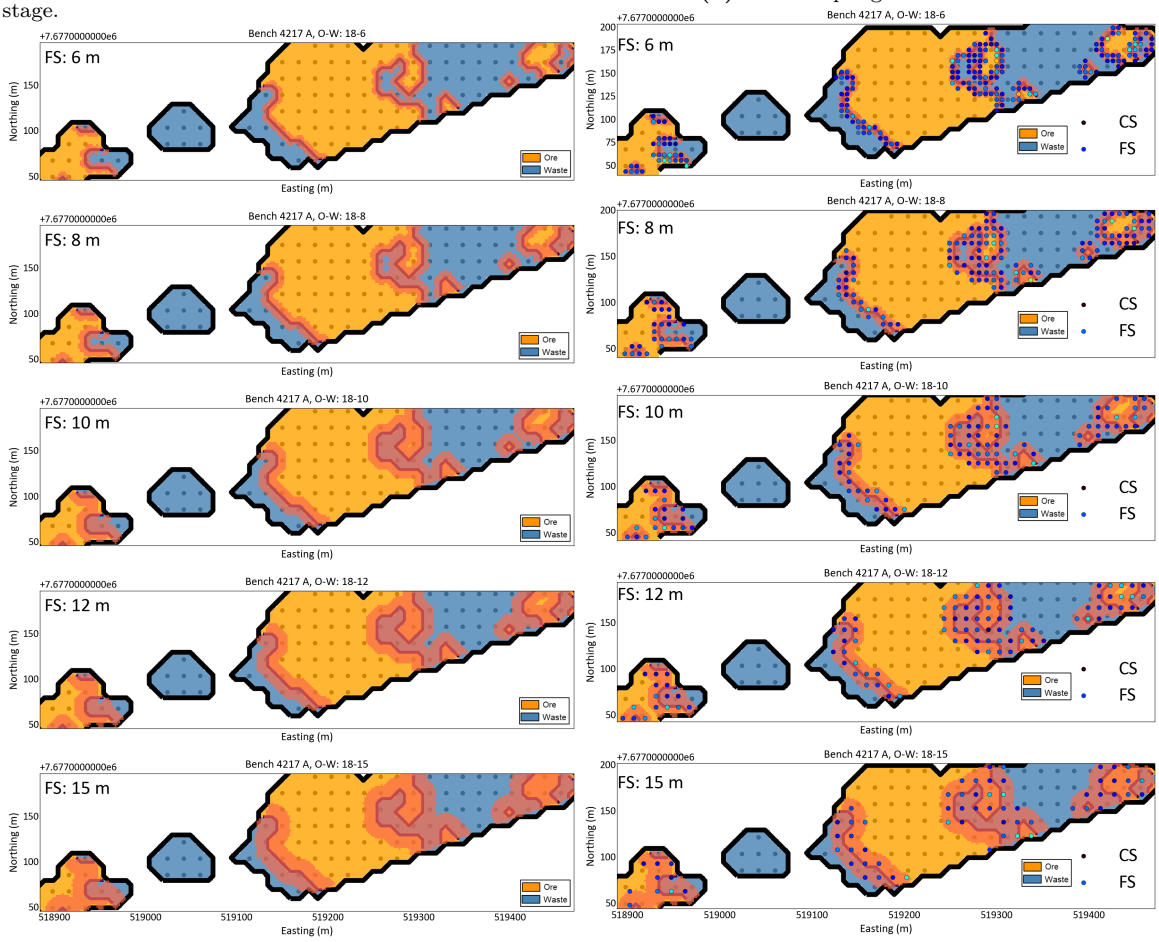

Figure 5.16: O-W buffers to accommodate FS (left-side) and actual FS after cleaning performed (right-side). Bench A 4217 CS: 18m.

The five options of FS are sampled from every scenario, as illustrated in Figure 5.16, where FS values increase from top to bottom. The final datasets for performing final OK estimations are merged between CS and FS, after cleaning of close samples is executed.

5.4.2 Final estimations, mineable limits, and TEE

Final OK models are estimated assuming the same autofit variogram models from BH of the regular DHS (Section 5.3.4). The final models are processed to SMU sizes of 20m x 20m x 15m, which then are deemed mineable given the selectivity level of the project. The resultant TEE is calculated on the final mineable limits. Figure 5.17 exhibits the final estimated models, mineable limits, and TEE maps from one of the benches along all scenarios of CS options (increasing from top to bottom).

(a) Final estimations in original O-W boundaries, labeled as TEE.

(b) Mineable limits at the scale of SMU= 20m x 20m.

(c) TEE at the SMU scale of the final GC models.

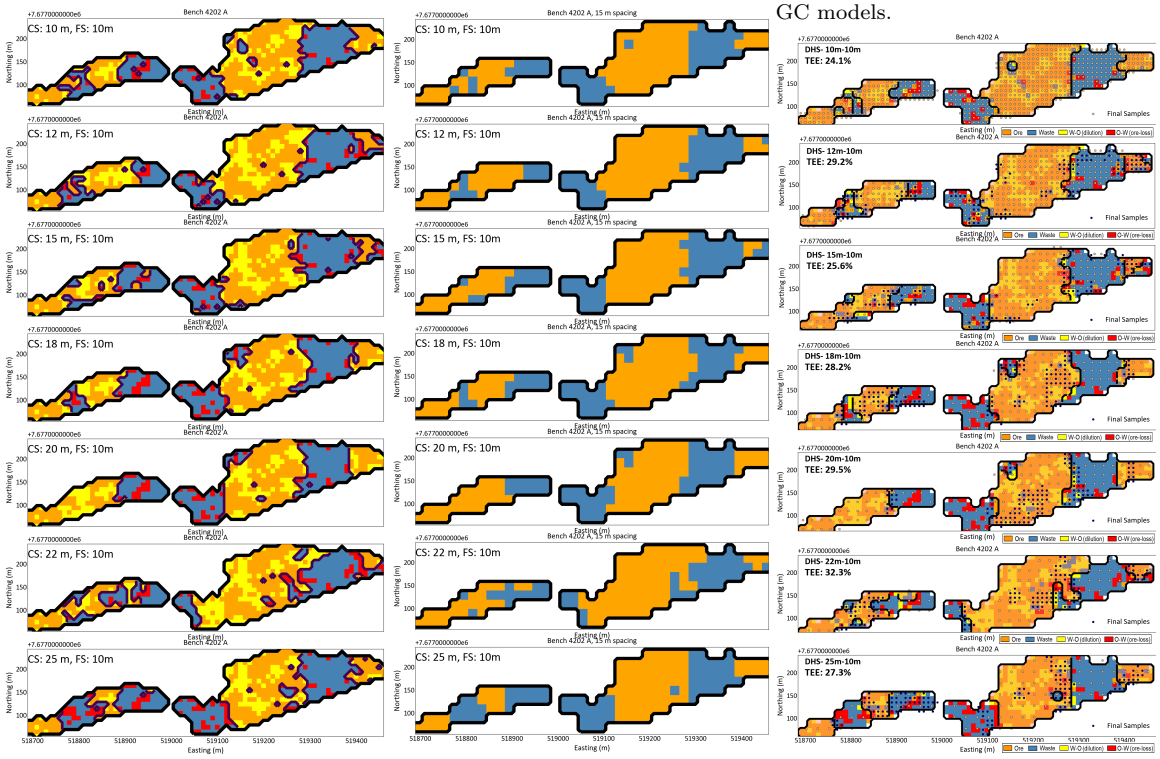

Figure 5.17: Final estimations: 10m at original O-W boundaries, reprocessed to SMU and TEE associates to both. Increasing CS from top to bottom.

Figure 5.17 illustrates the scenario of bench A 4202 of final estimates evolving to mineable limits and TEE associated to those limits. The trend of increasing TEE with the increase of CS is noticed, although when limited to an individual scenario, the pattern is not always present (wider CS estimations having lower TEE). The FS visible on the maps from Figure 5.17c disclose an interesting effect, where their misclassification persist even with a dense FS pattern on top of some blocks. Reasons for the misclassification include the variability of grades sampled, the smoothness of kriging, irregularly spaced data in a moving neighborhood within kriging systems, and varying variogram models (Wackernagel, 2003). In relation to TEE, the results on TEE across the combinations of CS and FS within key BH groups A and B are explored in Figure 5.18.

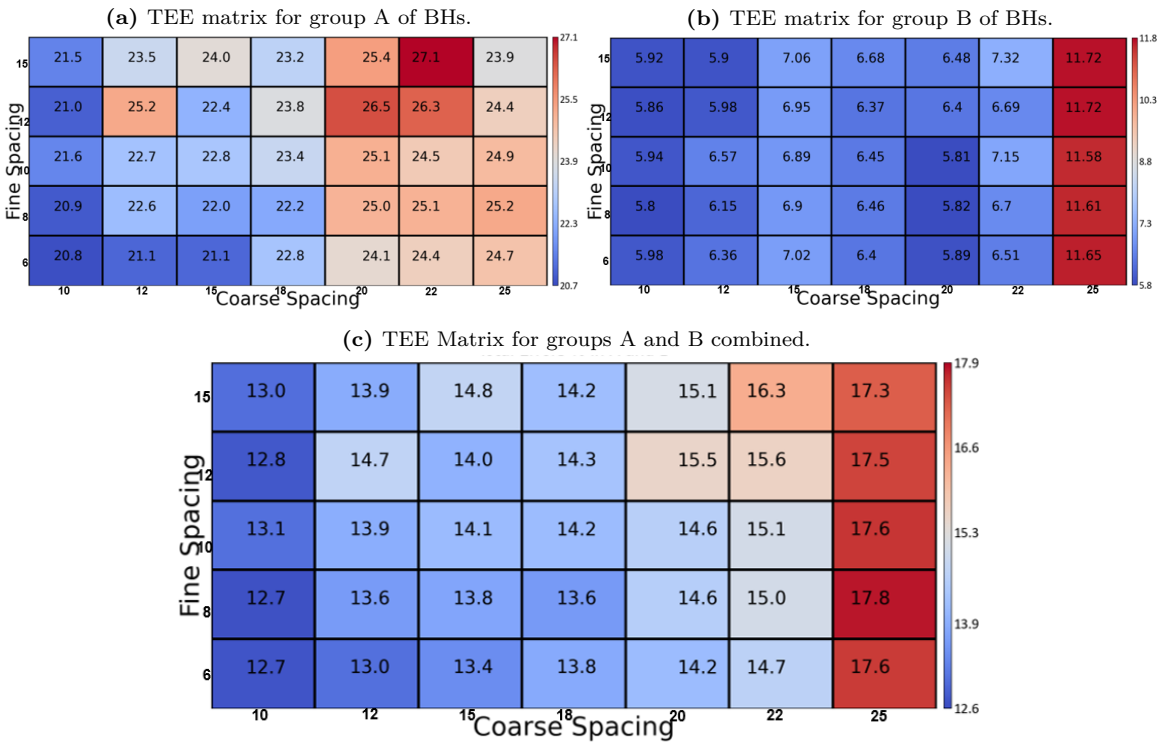

Figure 5.18: TEE matrix for all combined DHS options for groups A and B separately and together.

Area A presents much greater misclassification rates than area B, as variable cu_{eq} has a much lower spatial continuity in this area. When looking at the combination of both groups of BHs, the TEE values ranges from 12% up to 17%, and the monotonic trend between DHS and TEE is clearly visible.

5.4.3 FP results

DHS optimization results for profit are informed in two different forms as a way to enhance understanding: as matrixes (Figure 5.19) and as linear plots (Figure 5.20). FP results are shown jointly and separately for groups A and B.

(a) FP matrix for group A of BHs.

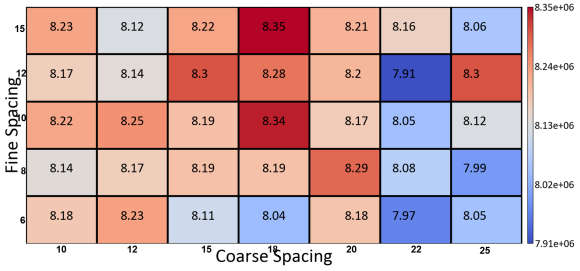

(b) FP matrix for group B of BHs.

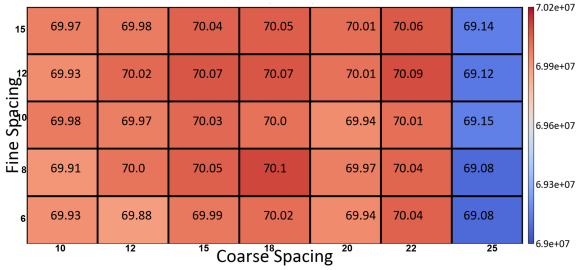

(c) FP matrix for group A and B together.

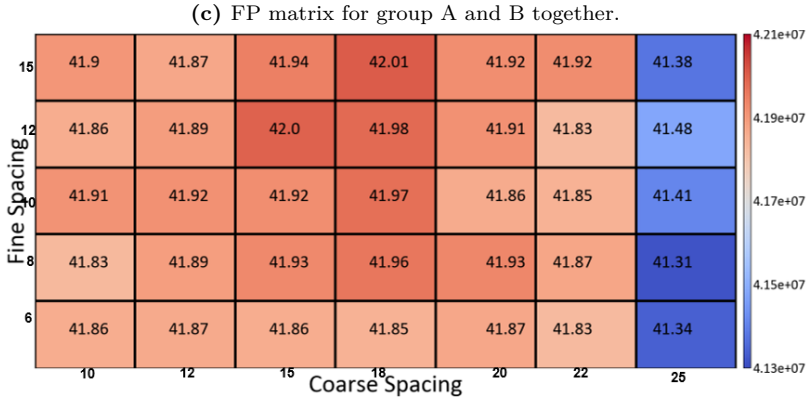

Figure 5.19: Matrixes of FP results along every combination of DHS.

Given the available ore, FP absolute values are much higher for area B than for area A. Because of that, FP variations are greater across DHS in A than in B. For group A, two optimum DHS options deliver almost equivalent FP results: *18m-15m* and *18m-10m*. Correspondingly, for group B, also two DHS options attain similar FP results:*18m-8m* closely followed by *22m-12m*. The average FP values when joining groups A and B result in the final optimal DHS decision of *18m-15m*. Group B has much greater weight than group A when averaging FP because of its higher FP returns. The same FP results are also informed as linear plots in Figure 5.20.

(a) FP for group A of BHs.

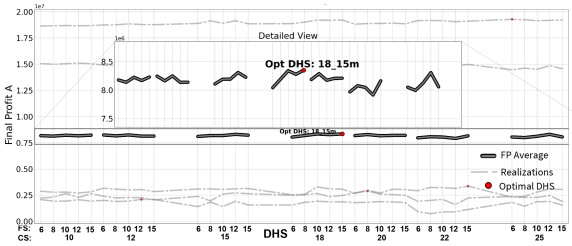

(b) FP for group B of BHs.

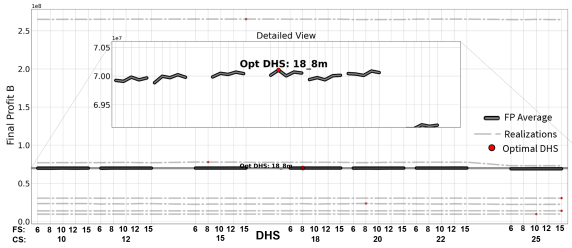

(c) Joint FP for groups A and B.

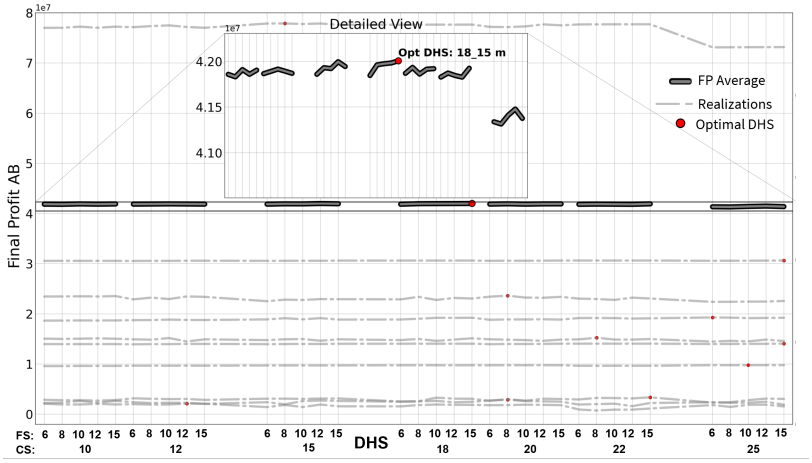

Figure 5.20: FP results per combinations of DHS of groups A, B separately and together.

When looking jointly at groups A and B from Figure 5.20, the individual realizations present very large gaps of FP values between them due to size and grade variations across benches. Group B of BH data has greater area and higher grades when compared to group A. Optimal DHS of *18m-15m* for both groups delivers an average value of $42 million, where the average ore tonnage of a bench of both groups is approximately $1.48Mt$. This represents a large area that probably comprises several GC areas within its limits. Examples of the optimal DHS configuration are visible in Figure 5.21.

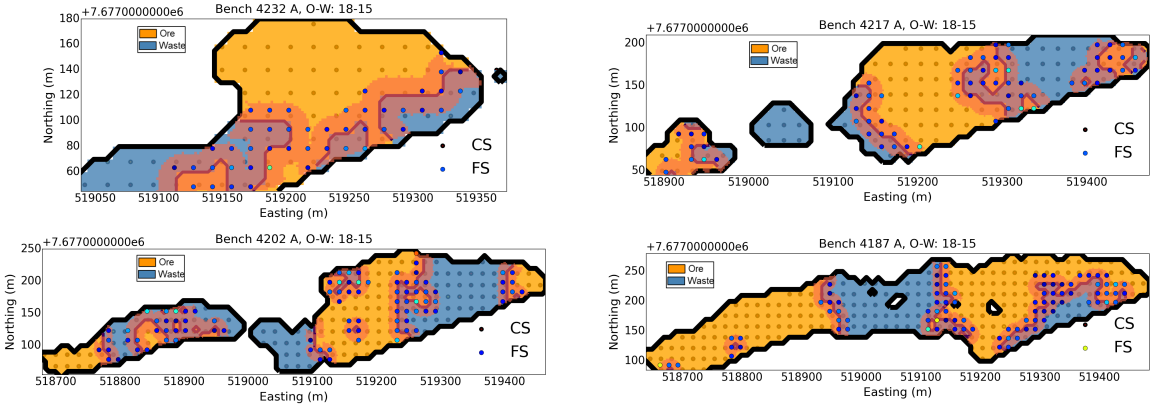

Figure 5.21: Optimal DHS of 18m-15m configuration in benches from group A.

Optimal DHS:18m-15m constitutes a combination of two relatively wide and very similar spacings:

18m and 15, which produces a good sampling pattern due to the cleaning tolerance $t = 4m$. The joint optimal DHS solution is not disparate from the optimal DHS per group, and could be adopted as a way to unify a single DHS solution for both areas.

5.5 Comparison of results

Drilling count

The nested DHS method saves on drilling count when comparing its FS to regular DHS. Figure 5.22 informs the average number of drilling between methods for the BH data, grouped by CS.

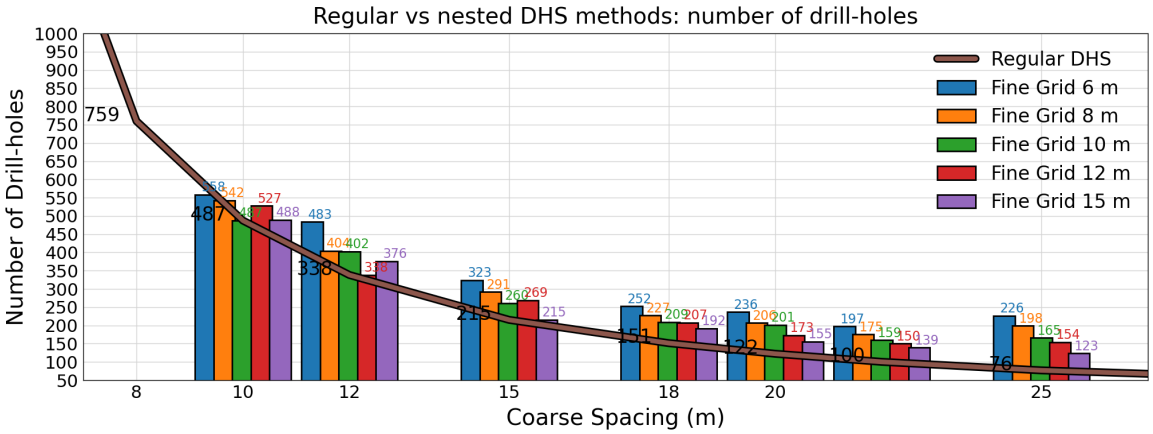

Figure 5.22: Average drilling count per DHS option. Comparison of DHS methodologies.

The grouping of combined DHS along the same CS in Figure 5.22 illustrates how much drilling is added by the FS stage from the nested DHS. As CS gets wider, the proportion of samples added by FS increases. Nevertheless, overall effectiveness is lost. As the results suggest, the optimal proportions of drilling for CS and FS for this case study are around two-thirds and one-third, respectively. For example, at the optimal DHS of 18m-15m and 18m-10m, FS represents 28 and 35% of drill-holes proportion, respectively.

The FP-optimized results are compared between regular and nested DHS methodologies. Figure 5.23 exhibits both methods' profit curves.

(a) FP curves (groups A and B) from both DHS optimization methods. Maximums are zoomed in.

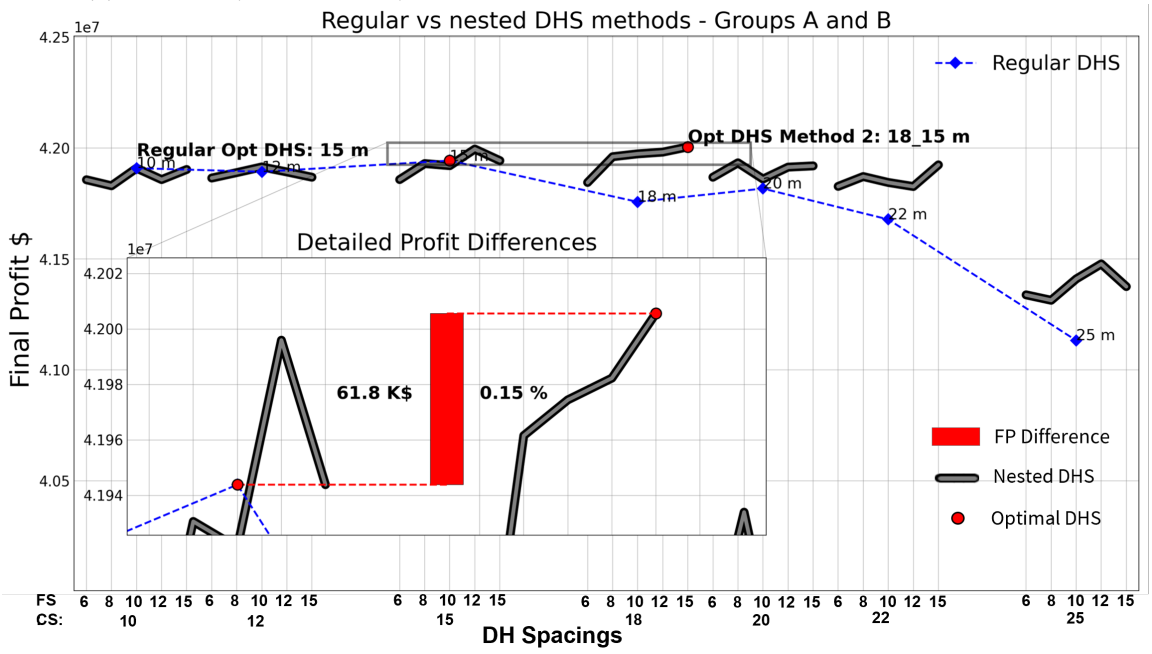

(b) FP curves (only group A) from both DHS optimization methods. Maximums are zoomed in.

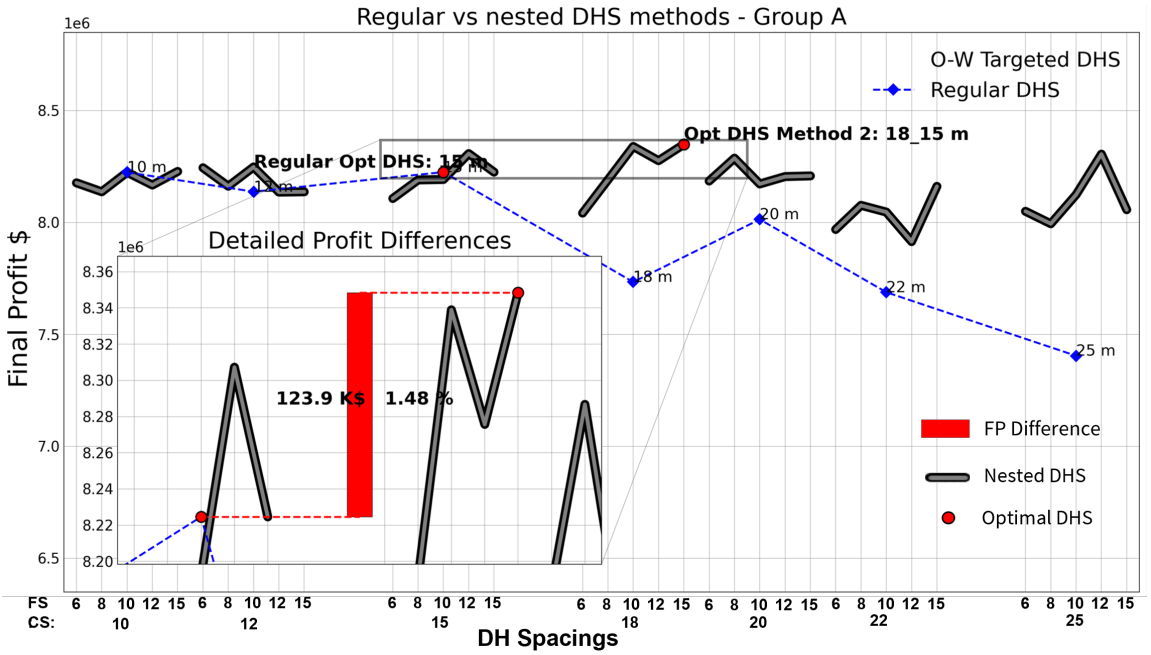

Figure 5.23: Comparison of profit curves between DHS optimization methods within groups A and B together, and group A alone.

The full set of DHS combinations (thick gray line) can overcome regular DHS profitability (dashed blue line) along many combined DHS, as visible in Figure 5.23a. However, the actual improvement in profit amidst both maximums is small (0.15%). In absolute value, profit increase means $ **61.8 K**. It is a low increase, considering that the average bench value is of the order of $ 40 M.

Nevertheless, due to area B's size and homogeneous nature, the results of comparative profits

only within group A have enlarged differences. In area A, O-W targeted DHS methodology delivers gains 1.48% higher, accounting for + $ **123.9 K** on average. Performance between both DHS optimizations is further explored, including other relevant metrics, such as TEE and drilling count, and how they relate to FP and DHS.

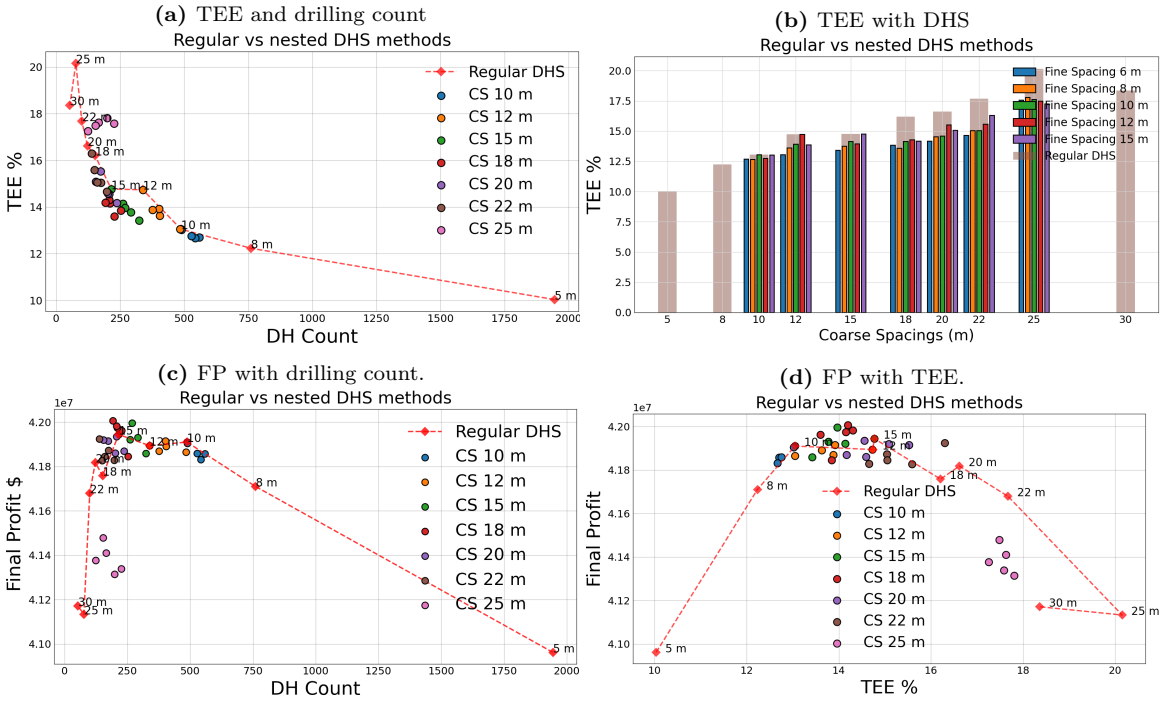

Figure 5.24: Comparison of DHS methods using different metrics.

Figure 5.24a inspects how TEE relates to the number of drill-holes. The effectiveness of the sampling configuration is higher when similar DH counts achieve lower TEE. DHS combinations that place toward the plot's lower left corner are more effective because it means a low TEE for a low drilling count. Figure 5.24b relates TEE to DHS rather than drill-hole numbers, which are monotonically related to drilling costs.

In Figure 5.24c, the highest point means the best result among the DHS optimizations. Moreover, it elucidates that many drilling patterns are ineffective by either drilling too much without bringing value or by saving on drilling but at a high cost on estimation quality. However, when using TEE against FP, it is more apparent that maximum FP is not achieved by very low TEE (Figure 5.24d), but instead through the best combination of drilling count and estimation results. Balance is critical between drilling cost and estimation quality. The effectivity of sampling placement drives most of the result's differences.

5.6 Discussions

5.6.1 Ore proportion effect

The effect of ore proportion on DHS optimization (Section 4.3.4) ,when abundant or absent, is leading DHS to its widest extremes because drilling more adds no value in improving correct destination. When ore proportion is intermediate, DHS is optimized at very short DHS because additional drilling does bring value by reducing TEE. Herefore, areas C and D, which contain only ore, have been disregarded as useful for DHS studies. However, in a mining context of multiple ore destinations based on grade thresholds (e.g., low-, intermediate, high-grade materials), or where precise grade estimates are crucial, optimal DHS will likely remain short even in contexts of high ore proportion.

5.6.2 Relevance of drilling cost

Financial gains with DHS optimizations are closely linked to the magnitude of drilling costs. If drilling costs are high, so can be the economic benefit of the DHS optimization.

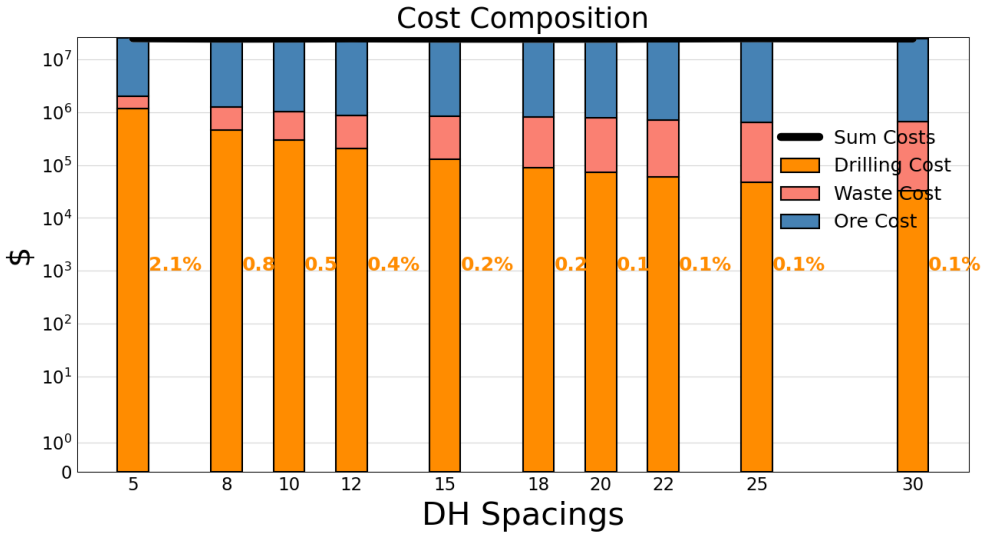

Figure 5.25: Percentual drilling cost contribution to total costs per DHS. Y axis is in logarithmic scale.

As shown in Figure 5.25, the selected drilling cost is relatively small when compared to total expenses, ranging from 0.1% at the widest spacings up to 2.1% for the shortest. At the optimum DHS of 15m, drilling cost accounts for only 0.2% of total costs. Seen that way, the final FP increase of 0.12% corresponds to the costs of drilling on the optimization. The DHS optimization is able to save 60% of the total drilling expenses. Drilling cost is set at \$50/m or \$750/drill-hole for the case study.

A sensitivity analysis is undertaken based on the evidence that DHS optimization's gains are directly linked to drilling cost. Drilling cost is varied up to ten times its original value of \$ 50/m.

The absolute financial gain with nested DHS against the regular one is informed by the graph in Figure 5.26.

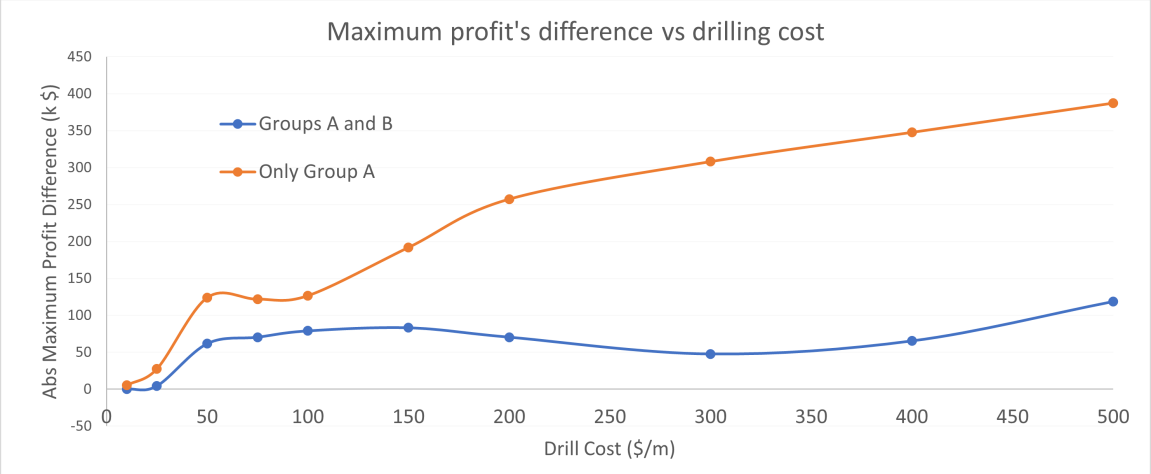

Figure 5.26: Drilling cost sensitivity analysis.

Earnings from applying the nested DHS method increase consistently as drilling costs. The practical benefit of such a DHS method is dependent on drilling costs. In area A, the earnings are more sensitive to changes in drilling cost than when accounting for area B. The rate for profit increase is lower, although also monotonically increasing, for areas together, as the slopes of lines in Figure 5.26 show. This analysis offers the understanding that a greater benefit of applying concomitant DHS optimization is achieved in projects with higher drilling expenses.

5.6.3 Optimal combined DHS

The most effective combined DHS results from merging two relatively wide spacings (18m and 15m), which drastically reduces the number of drill-hole counts while still being effective due to the cleaning process allowing samples proximity until 4 m apart. The combined spacings between such wide CS and FS produce shorter spacings than the numbers suggest. This system allows different spacings to be set together, enabling irregular patterns. Of all combinations, the most profitable DHS does not excessively sample the O-W region while reducing misclassified blocks substantially.

Figure 5.27: Actual data spacings of combined prior and final samplings - Example of CS=18m on bench A 4202.

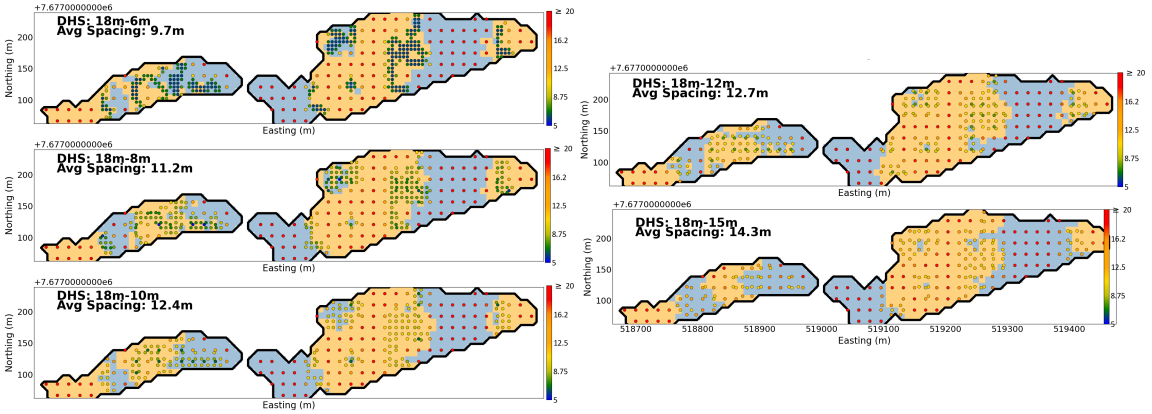

Figure 5.27 exposes the actual data spacing across CS=18m, including the most profitable DHS of 18m-15m. The colors of samples indicate the shorter spacing across O-W boundaries, which end up being frequently shorter than the FS applied. The average spacing is also plotted, conveying values even smaller than the FS itself, as is the case for DHS 18m-15m, which average spacing is 14.3m. In the zones where FS is applied, spacing achieved is around 10m.

5.6.4 Domaining

No type of domaining has been considered to run the DHS optimization, other than the BH grouping (A, B, C, and D), which has been established by simple contiguous positioning of samples. No qualitative variable has been considered to group, yet the BH dataset has lithological and other variables available. DHS optimizations can be carried out by domains possibly prompting different optimal DHS, which in turn could be adopted separately or merged into an unique optimal DHS through a determined criteria.

5.6.5 Validity of results

DHS optimizations for profit depend on many financial and operational parameters, and any DHS optimization on profit is only valid for that specific set of values chosen. The sensitivity of optimal DHS upon changing any parameter's value is potentially very high, as Chapter 4. Hence, the DHS optimum results in this Chapter are only valid for the set of parameters chosen throughout the study.

5.7 Conclusions

The two DHS optimizations are successfully applied to the Cu-Mo BH data. When compared, the nested DHS generated increased profits for different combinations of DHS, especially for BH group

A, where ore proportion is close to half, spatial continuity is short, and grades are mostly marginally above the cut-off grade. In area B, where ore proportion is around three-quarters, spatial continuity is high and grades are greater, profit increase is smaller. Optimal DHS is slightly wider for area A than for area B. The relevance of drilling cost on overall total costs plays a vital role in whether or not the DHS optimization is suitable to deliver more significant earnings.

The DHS optimizations are made for dedicated drilling systems, which are different from the method currently used by the mining operation of the case study. An eventual trade-off study between a dedicated drilling method and BH would only be justifiable in the presence of errors in the latter. The variograms from the BHs indicate no nugget effect and well-behaved experimental points. Thus, significant errors should not be expected for the BH samples of that operation, which reinforces the suitability of BH as a GC sampling tool in that context. The nested DHS method is designed to be automated and to enhance profit. However, the actual implementation of such a technique should be carefully assessed, taking into account technical, mine planning, and operational factors. The nested DHS implies anticipating a good part of the drilling to the phase prior to GC, which significantly changes budgets, timing, and mine planning aspects.

Chapter 6

Conclusions

The Drill-hole spacing (DHS) optimizations in grade-control (GC) aim to solve the most profitable DHS solution for dedicated drilling systems at final estimates. Optimizing profit means incorporating every relevant aspect of the process into the transfer function (TF), enabling DHS optimizations to be customizable and adapted to any mining project's context. As a final estimate, the research attempted to clarify that profit is the metric which can encompass all the others, assuring the greatest outcomes in mining.

6.1 Main contributions

The main contributions of this Thesis are considered to be:

1. The establishment of a detailed methodology for generating DHS optimizations for profit in GC. The entire process of generating optimal DHS was described in detail, highlighting important technical considerations involved in each step.

2. The development of a nested DHS methodology that enhances profitability through targeting O-W zones from a previous reliable estimation. The nested method addresses the decisive concept of sampling effectiveness to amplify profitability. The typical regular DHS is challenged and transformed to be limited only along areas which need denser sampling. The key aspects of the method are 1) to optimize two drilling phases together, 2) to assume that the O-W boundaries are the critical areas for further sampling, and 3) to combine two regular drillings and allow cleaning tolerance to be short. The nested DHS method is simple to be executed, fully automated, and, as proved by the examples, increases profit, although the magnitude of gains depends on a few factors.

3. The understanding of how different factors affect DHS and the varying levels of profit sensitivity to DHS according to those factors. The systematic assessment enabled a greater understanding of how DHS optimizations for profit operates and what combination of factors drives most of the DHS changes. Several insights are possible through carefully analyzing the graphs from Chapter 4. Finally, appreciating under what circumstances profit is sensitive to DHS is valuable for practitioners of DHS optimizations in varied contexts. Many metrics were explored and indicate what combinations of factors make DHS likely to affect profit significantly.

6.2 Limitations and future work

The assessment of several factors' influence on DHS outcomes was limited to univariate changes, and therefore only a portion of the multivariate space has been sampled. Future work on DHS could explore bivariate or even multivariate changes in factors' values for a deeper look at the engines of optimization for profit.

Multivariate modeling is a common challenge also for DHS optimizations. The case study from Chapter 5 used equivalent grades to merge the two relevant variables. However, no analysis evaluated the impact that different multivariate modeling techniques could have on optimal DHS decisions. The comparison of different multivariate methods is another possibility to explore in DHS's further research.

The representation of more complex geological features such as veins, folds, and faults has not been incorporated in the simulation of underlying truths of the deposits. The effect of more complex geological features on optimal DHS compared to simpler ones could be encompassed through techniques for continuous variables. One possible technique to employ is SGS with locally varying anisotropies (LVA) (Boisvert & Deutsch, 2011) to generate more geologically realistic reference models.

In the same line of SGS with LVA, categorical modeling previous to continuous variable estimation/simulation has also not been considered in the DHS examples. Geostatistical methods able to portray realistic geologic features such as Hierarchical Truncated PluriGaussian (HTPG) (Silva & Deutsch, 2019; Velasquez Sanchez, 2023) or Multiple Point Statistics (MPS) simulation (Strebelle, 2002) could be considered for modeling categories to posterior continuous simulation. The employment of such approaches involves challenges like merging multiple categorical models with subsequent continuous variables simulations and having access to training exhaustive images. The accumulation of multiple nested simulations from categories into continuous might be computationally demanding. On the other hand, HTPG and MPS modeling might produce geologically realistic models with more curvilinear features that two-point statistics cannot characterize (Pyrcz & Deutsch, 2014). The realistic simulated model is the motivation to potentially improve DHS optimizations rather than being based on reference models limited to honoring global data statistics and two-point variogram, given that most of resource model's uncertainty resides in geological interpretation (Journel, 2018).

Additionally, the present work only accounted for DHS examples with a single determining threshold between ore and waste rather than multiple classes of ore. The consideration of multiple destinations of ore based on distinct grade thresholds might significantly alter the optimal DHS responses. That is likely to happen because VoI is inherently added to drilling that distinguishes those grade intervals. Multiple destinations constitute another option to be eventually explored in upcoming research on DHS optimizations.

DHS optimizations can be approached as a Machine Learning (ML) task in future research on

the topic. ML methods such as Convolutional neural networks (CNN) could be trained by inputing many combinations of values between the factors not only univariately (as done in the sensitivity analysis from Chapter 4) but also multivariate changes. The multivariate space involving such DHS optimizations is big given that it involves geology, mining and economic parameters. Training a ML model to be tested in outputing optimal DHS decisions for other datasets sounds like an interesting reasearch path, although quite challenging especially due to the big number of variables involved.

The choice of which nested DHS options should be used can possibly be improved, given that FP results from that DHS method in both application cases are a bit erratic (Figure 3.7c and Figure 5.24). The improvement in those FP results could be achieved through a heuristic method to optimize the best choices of combined DHS prior to running DHS optimizations. The current study DHS options were based only on the author's judgement without assistance of any methodology.

References

Abzalov, M. (2016). *Applied mining geology* (Vol. 12). Springer.

Afonseca, B., & Silva, V. (2022). Defining optimal drill-hole spacing: A novel integrated analysis from exploration to ore control. *Journal of the Southern African Institute of Mining and Metallurgy*, *122*(6), 305–315.

Barnett, R., Lyster, S., Pinto, F., MacCormack, K., & Deutsch, C. (2018). Principles of data spacing and uncertainty in geomodeling. *Bulletin of Canadian Petroleum Geology*, *66*(3), 575–594.

Boisvert, J., & Deutsch, C. (2011). Programs for kriging and sequential gaussian simulation with locally varying anisotropy using non-euclidean distances. *Computers & Geosciences*, *37*(4), 495–510.

Boucher, A., Dimitrakopoulos, R., & Vargas-Guzman, J. (2005). Joint simulations, optimal drillhole spacing and the role of the stockpile. *Geostatistics Banff 2004*, 35–44.

Caers, J., Scheidt, C., Yin, Z., Wang, L., Mukerji, T., & House, K. (2022). Efficacy of information in mineral exploration drilling. *Natural Resources Research*, *31*(3), 1157–1173.

Chiles, J.-P., & Delfiner, P. (2012). *Geostatistics: modeling spatial uncertainty* (Vol. 713). John Wiley & Sons.

Clark, I., et al. (1979). *Practical geostatistics* (Vol. 3). Applied Science Publishers London.

CSA. (2011). *National Instrument 43-101 Standards of Disclosure for Mineral Projects,* (Tech. Rep.). Toronto, ON: Canadian Securities Administrators (CSA). Retrieved from `https://www.osc.ca/en/securities-law/instruments-rules-policies/4/43-101`

Deutsch. (2018). All realizations all the time. *Handbook of mathematical geosciences: fifty years of IAMG*, 131–142.

Deutsch, & Journel, A. (1997). *Gslib geostatistical software library and user's guide*. New York, second edition. 369 pages.: Oxford University Press,.

Deutsch, J., & Deutsch, C. (2015). Introduction to choosing a kriging plan. *Geostatistics Lessons*. Retrieved from `https://geostatisticslessons.com/lessons/introkrigingplan`

Dimitrakopoulos, R., & Godoy, M. (2014). Grade control based on economic ore/waste classification functions and stochastic simulations: examples, comparisons and applications. *Mining Technology*, *123*(2), 90–106.

François-Bongarçon, D. (2004). Theory of sampling and geostatistics: an intimate link. *Chemometrics and intelligent laboratory systems*, *74*(1), 143–148.

Goovaerts, P. (1997). *Geostatistics for natural resources evaluation*. New York: Oxford University Press.

Hall, T., Scheidt, C., Wang, L., Yin, Z., Mukerji, T., & Caers, J. (2022). Sequential value of information for subsurface exploration drilling. *Natural Resources Research*, *31*(5), 2413–2434.

Harding, B. (2021). *Drillhole spacing determination with value of information* (Master's Thesis). University of Alberta, Edmonton, AB.

Isaaks, E. (2005). The kriging oxymoron: a conditionally unbiased and accurate predictor. *Geostatistics Banff 2004*, 363–374.

Isaaks, E., & Srivastava, R. (1989). *An introduction to applied geostatistics*. Oxford University Press.

Journel, A. (2018). Roadblocks to the evaluation of ore reserves—the simulation overpass and putting more geology into numerical models of deposits. *Advances in applied strategic mine planning*, 47–55.

Journel, A., & Huijbregts, C. (1976). *Mining geostatistics*. United Kingdom.

Kentwell, D. (2022). Empirical geostatistics #1 – kriging slope of regression: sensitivities and impacts on estimation, classification and final selection. *International Mining Geology Conference, AUSIMM, Brisbane, Australia and Online*.

Koppe, V., Costa, J., Peroni, R., & Koppe, J. (2011). Choosing between two kind of sampling patterns using geostatistical simulation: regularly spaced or at high uncertainty locations? *Natural Resources Research*, *20*(2), 131–142.

Matheron, G. (1963). Principles of geostatistics. *Economic geology*, *58*(8), 1246–1266.

Ortiz, J., Magri, E., & Líbano, R. (2012). Improving financial returns from mining through geostatistical simulation and the optimized advance drilling grid at el tesoro copper mine. *Journal of the Southern African Institute of Mining and Metallurgy*, *112*(1), 15–22.

Pinto, F. (2016). *Advances in data spacing and uncertainty* (Master's Thesis). University of Alberta, Edmonton, AB. ()

Pinto, F., & Deutsch, C. (2014). *Thoughts on Data Spacing, Uncertainty and the Value of Information* (CCG Annual Report 2014). Edmonton AB: University of Alberta. Retrieved from `http://www.ccgalberta.com`

Pyrcz, M., & Deutsch, C. (2014). *Geostatistical reservoir modeling*. Oxford University Press, USA.

Rossi, M., & Deutsch, C. (2013). *Mineral resource estimation*. Springer Science & Business Media.

Santibanez-Leal, F., Ortiz, J., & Silva, J. (2020). Ore-waste discrimination with adaptive sampling strategy. *Natural Resources Research*, *29*, 3079–3102.

Silva, D., & Boisvert, J. (2013). *Infill Drilling Optimization for Maximizing Resource Tonnage* (CCG Annual Report 2013). Edmonton AB: University of Alberta. Retrieved from `http://www.ccgalberta.com`

Silva, D., & Boisvert, J. (2014). *A Case Study on 3D Infill Drilling Optimization* (CCG Annual Report 2014). Edmonton AB: University of Alberta. Retrieved from `http://www.ccgalberta.com`

Silva, D., & Deutsch, C. (2019). Multivariate categorical modeling with hierarchical truncated pluri-gaussian simulation. *Mathematical Geosciences*, *51*(5), 527–552.

Strebelle, S. (2002). Conditional simulation of complex geological structures using multiple-point statistics. *Mathematical geology*, *34*, 1–21.

Usero, G., Misk, S., & Saldanha, A. (2019). An approach for drilling pattern simulation. In *Mining goes digital* (pp. 59–66). CRC Press.

Vargas, A. (2017). Optimizing grade-control drillhole spacing with conditional simulation. *Minería y Geología*, *33*(1), 1–12.

Vasylchuk, Y., & Deutsch, C. (2018). *Optimization of Surface Mining Dig Limits with Realistic Selectivity* (CCG Annual Report 2018). Edmonton AB: University of Alberta. Retrieved from `http://www.ccgalberta.com`

Velasquez Sanchez, H. (2023). *Truncation trees in hierarchical truncated plurigaussian simulation* (Master's Thesis). University of Alberta, Edmonton, AB.

Verly, G. (2005). Grade control classification of ore and waste: a critical review of estimation and simulation based procedures. *Mathematical geology*, *37*(5), 451–475.

Wackernagel, H. (2003). *Multivariate geostatistics: an introduction with applications*. Springer Science & Business Media.